AD-A115 513 AIR FORCE INST OF TECH WRIGHT-PATTERSON AFB OH SCHOO--ETC F/G 20/9
CATHODE SHEATH EFFECTS IN EXTERNALLY-IONIZED GAS DISCHARGES.(U)
DEC 81 M R HALLADA
UNCLASSIFIED AFIT/GEP/PH/81D-4 NL

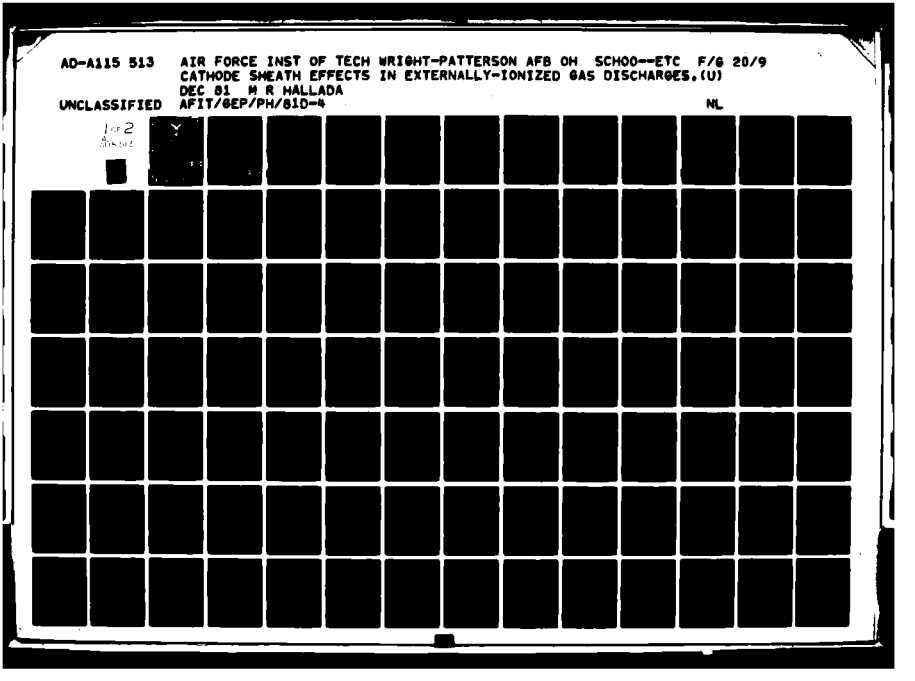

UNITED STATES AIR FORCE

AIR UNIVERSITY

AIR FORCE INSTITUTE OF TECHNOLOGY

Wright-Patterson Air Force Base, Ohio

AFIT/GEP/81D-4

CATHODE SHEATH EFFECTS IN EXTERNALLY-IONIZED GAS DISCHARGES

AFIT/GEP/PH/81D-4 Marc R. Hallada
Capt. USAF

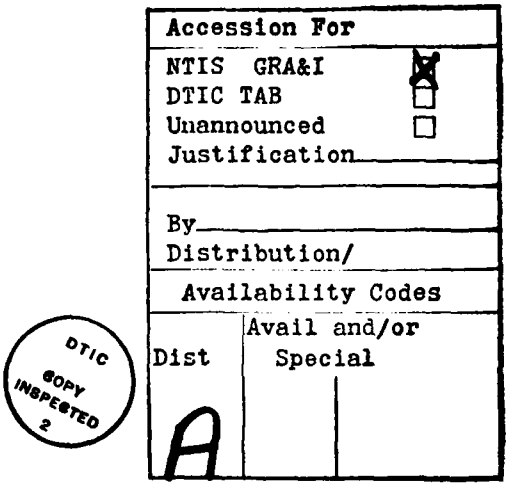
Accession For
NTIS GRA&I
DTIC TAB
Unannounced
Justification
By
Distribution/
Availability Codes
Dist
Avail and/or
Special
A

DTIC
COPY
INSPECTED
2

AFIT/GEP/PH/81D-4

CATHODE SHEATH EFFECTS

IN

EXTERNALLY-IONIZED GAS DISCHARGES

THESIS

Presented to the Faculty of the School of Engineering

of the Air Force Institute of Technology

Air University

in Partial Fulfillment of the

Requirements for the Degree of

Master of Science

by

Marc R. Hallada, B.S.

Capt USAF

Graduate Engineering Physics

December 1981

Contents

Preface

An understanding of cathode sheath effects in gas discharges is necessary for the design of efficient high-energy plasma switches. Such switches are essential for the rapid switching of high-energy inductive energy stores. Experimental investigations of this type of switch are being conducted by Dr. Peter Bletzinger of the Aero Propulsion Laboratory, Energy Conversion Branch. The theoretical investigations of the present study were done in support of his work with such plasma switches.

A number of people provided guidance and encouragement to me during the course of this study. In particular, thanks are given to: Dr. Peter Bletzinger, who helped me realize that numbers and diagrams without physical insight are meaningless; Lt. Col. William Bailey, who insisted on consistent boundary conditions and also helped me find reality; Capt. Gary Duke, who provided empathy and consolation through his analytic investigation of a similar problem; Capt. Greg Schneider, who listened critically and spoke helpfully; and especially my wife Cheryl and children Christopher and Joshua, who helped me establish priorities and keep my perspective throughout the ordeal.

Marc R. Hallada

List of Figures

Page

List of Tables

List of Symbols

A	Attachment coefficient (1/cm)
A	Ampere
C	Coulomb
cm	Centimeter
d	Distance between electrodes (cm)
d_a	Thickness of anode sheath (cm)
d_c	Thickness of cathode sheath (cm)
D_e	Longitudinal diffusion coefficient of electrons (cm^2/sec)
D_i	Longitudinal diffusion coefficient of ions (cm^2/sec)
d_p	Length of plasma region (cm)
e^-	Electron
e	Electronic charge (1.6×10^{-19} Coulombs)
eV	Electron volt
E	Electric field strength (V/cm)
E_{as}	Electric field strength at anode sheath/plasma interface (V/cm)
E_{cs}	Electric field strength at cathode sheath/plasma interface (V/cm)
I	Current (Amps)
J	Total current density (A/cm^2)
j_e	Electron flux ($1/cm^2$/sec)
j_+	Positive ion flux ($1/cm^2$/sec)
k_e	Electron mobility (cm^2/V/sec)
k_i	Ion mobility (cm^2/V/sec)
k_+	Positive ion mobility (cm^2/V/sec)
kV	Kilovolt (1000 volts)
K	Boltzmann constant (1.38×10^{-16} erg/°K)
mA	Milliampere (.001 Ampere)

n_e	Number density of electrons ($1/cm^3$)
n_m	Number density of metastable neutrals ($1/cm^3$)
n_+	Number density of positive ions ($1/cm^3$)
N_o	Number density of neutrals ($1/cm^3$)
R	Resistance (ohms)
R_{im}	Metastable ionization rate coefficient (cm^3/sec)
R_r	Recombination rate coefficient (cm^3/sec)
S	Electron-ion pair production rate ($1/cm^3/sec$)
t	Time (sec)
Td	Townsend (1×10^{-17} V-cm^2)
T_e	Average electron temperature (eV)
T_i	Average ion temperature (eV)
V	Potential (volts)
V_i	Ionization Potential (eV)
v	Volt
V_A	Voltage drop across anode sheath (volts)
V_C	Voltage drop across cathode sheath (volts)
V_P	Voltage drop across positive column (volts)
V_T	Total voltage drop across discharge (volts)
V_0	Supply voltage (for gas discharge)
W_e	Electron drift velocity (cm/sec)
W_+	Positive ion drift velocity (cm/sec)
x	Longitudinal distance (cm)
α	Townsend ionization coefficient (1/cm)
γ	Secondary emission coefficient (electrons per incident ion)
ε_o	Permitivity of free space (8.85×10^{-14}C/V/cm)

η	Secondary emission coefficient (ions per incident electron)
μA	Microamp (10^{-6} Ampere)
ν_i	Rate of ionization (1/sec)
σ	Cross section (cm^2)
*	Excited species
-	Negative charge
+	Positive charge
°K	Degrees Kelvin

Abstract

Lowke's theoretical investigation[1] of gas discharges sustained by an external ionization source was extended. In addition to the processes of electron diffusion, electron-ion recombination, and ionization of the ground state considered by Lowke, electron-impact ionization of metastable states and secondary emission from the cathode were included in the present analysis. Current-voltage (I-V) characteristics were obtained for discharges in argon and methane. At current densities of $1A/cm^2$, Townsend ionization in the cathode sheath resulted in positive-ion number densities which significantly exceeded those in the positive column. I-V characteristics obtained revealed a sharp rise in the current at an "ignition" voltage. The slope of the high-current region of the characteristic increased for an increase in secondary emission. With the addition of metastable ionization, the ignition voltage and the entire I-V characteristic shifted to lower discharge voltages. Below the ignition voltage and at low external ionization source strengths, an unstable region of negative differential conductivity was observed.

[1] J. J. Lowke, D. K. Davies, J. Appl. Phys., 48(12), 499 (1977).

CATHODE SHEATH EFFECTS

IN

EXTERNALLY IONIZED GAS DISCHARGES

I. Introduction

Background

High-energy switches with short switching times and long operational lifetimes are essential in many areas of current scientific interest. In particular, the realization of both controlled fusion and directed energy weapons will require such switches. Although spark-gap type switches have been used for rapid switching, they cannot function at high repetition rates over an extended period of time. In addition, spark-gap switches cannot switch "off" high energies (Ref. 1:1). Such "off" switches are required for inductive energy storage schemes, which are very attractive in many high-energy applications. Inductive energy storage is much more compact (and thus more mobile) than capacitive energy storage. As a consequence, the Air Force is particularly interested in the development of high energy "off" switches for use in the power supplies of directed-energy weapon systems.

One of the most promising approaches to producing such "off" switches involves the use of an external electron beam to produce ionization within a gas discharge. The gas discharge's operating parameters are selected such that the electron-beam-produced ionization is essential to maintain the discharge. As a consequence, the external electron beam can be used to control the current flowing through a gas discharge. The discharge acts as a volumetric conductor only while the electron beam

irradiates the active region of the discharge (Ref. 1:2). A discharge which exhibits this type of behavior is known as an externally-sustained gas discharge.

Literature Review

Although external sources of ionizations have been widely used to control gas discharges, their application to the area of high-energy switching is relatively recent. A large portion of the work concerning external ionization has dealt with applications to high pressure discharges in gas lasers (Refs. 2:3:4). Consequently, early switching experiments made use of the electron guns and gas mixtures associated with gas discharge lasers. These high current density electron guns allowed gas mixtures with significant quantities of atomic or molecular species with large electron affinities to be used. These "attaching" species, in turn, produced very short switch rise and fall times. However, in these experiments, the energy expended by the electron beam was usually of the same magnitude as the energy switched (Ref. 5:1).

More recently, electron-beam-sustained switches with much higher gains (ratio of energy switched to switching energy) have been investigated, primarily experimentally, by several authors. Koval'chuk et.al. reported (1976) achieving gains as high as 100 by decreasing the electron beam current density (i.e. the external ionization source strength) in a nitrogen gas discharge (Ref. 6). In 1980, Bletzinger experimentally investigated several gas mixtures (Ar, Ar/O_2, and CH_4) at these lower electron beam current densities. He observed a discontinuous transition to a high conductance region as the discharge voltage was increased beyond a certain value. Bletzinger found methane to be one of the most promising switching gases (achieving gains as high as 1000), because of

its low "on-voltage" and high dielectric strength. He also discovered that methane's conductivity and current gain were increased by the addition of argon (Ref. 5). The discontinuous transitions in the current-voltage (I-V) characteristics obtained by Bletzinger were also observed by Averin et.al. in a concurrent investigation. Averin maintained that their experimental parameters allowed them to "trace out" this discontinuity, which they termed a region of "negative differential conductivity" (Ref. 7).

Several theoretical investigations of a general nature, dealing with electric gas discharges sustained by various sources of ionization, have also been conducted. A very thorough study of discharges with external ionization produced by photoionization of the gas was conducted by Wardlaw and Cohen in 1972. They analytically investigated the properties of such discharges as a function of applied electric field and ionization source strength. Although they included losses due to diffusion, they neglected recombination losses because their ionization source strengths were quite small and thus their charged particle densities were also very small (Ref. 8). Previously, in 1958, Ward calculated the properties of discharges sustained by photoelectric emission from the cathode. He found that at high current densities a maximum was produced in the positive-ion number density in the cathode sheath (Ref. 9). Although such positive space charges were previously observed in self-sustained discharges, Ward was the first to calculate such an effect in externally-sustained discharges.

This peak in the positive-ion number density was also observed in later theoretical investigations of discharges sustained by uniform sources of ionization. In addition to finding such a "peak," Zakharov

et.al. (Ref. 10) also calculated the "negative differential conductivity" region later seen in experiments by Averin, Bletzinger, and Koval'chuk (Refs. 7, 5, 6). Another computational investigation, by Lowke and Davies (Ref. 11), was reported in 1977. They also found the positive ion density maximum in the cathode sheath, although it only occurred for the highest current densities they considered. (Their currents were, in general, much lower than those considered by Zakharov.) The rise in current theoretically predicted by Lowke and Davies was not as rapid as that observed experimentally by Averin, Bletzinger, and Koval'chuk. However, Lowke and Davies' analysis did not account for two potentially important processes: secondary emission of electrons from ion bombardment of the cathode and ionization of metastables in the gas (Ref. 11). A very thorough theoretical analysis of externally-ionized gas discharges (including secondary emission from the cathode) was reported by Aleksandrov et.al. in 1978. They analytically modeled an externally-sustained discharge using asymptotic expansions in each of several longitudinal regions. Although their analysis did not consider diffusion, it did include electron-ion recombination, Townsend (impact) ionization, and secondary emission. Aleksandrov attempted to describe the causes of the observed rapid current rise by identifying the dominant physical processes in several regions near the cathode (Ref. 12:143). Both Aleksandrov and Lowke dealt with the effects of external ionization, recombination, and electron impact ionization. The present investigation extended the calculations done by Lowke and Davies to include the additional processes of secondary emission and metastable ionization.

Problem

The objective of this study was to investigate the properties of

an electric gas discharge which is maintained by a spatially uniform, external source of ionization. A one-dimensional model of a discharge between two parallel conducting electrodes, the anode and cathode, was adopted. Particular emphasis was placed upon the discharge properties in the vicinity of the cathode. In order to carry out this investigation, the system of differential equations describing the physical processes occurring in such a discharge was solved numerically and compared with experimental results and simplified analytic solutions.

Assumptions

A number of assumptions were made in order to make the numerical solution of this set of equations less complicated without significantly sacrificing reality. Additionally, it was hoped that these assumptions would ease subsequent attempts to gain physical insight into the meaning of these solutions. Two of the assumption dealt with the physical environment of the discharge, but the majority were concerned with limitations on the types and nature of the processes considered.

The externally-sustained gas discharge's transverse dimension (perpendicular to the anode-cathode axis) was taken to be large enough for a one-dimensional analysis to be appropriate. Planar electrodes perpendicular to this axis were the boundaries between which the discharge occurred. The region between the electrodes contained a source of positive ion and electron pairs which was assumed to be both spatially uniform and constant for all values of the electric field.

The majority of the assumptions made are concerned with the types of physical processes allowed to occur in the discharge. Initially, the interactions of only electrons, neutral atoms and molecules, and singly-charged positive ions were considered. Later, this assumption was

relaxed and the influence of metastable neutrals was included. Thus, the processes considered at each point in the investigation were limited by the types of particles available. Initially, the only kinetic processes allowed were Townsend (impact) ionization and electron-ion recombination. With the inclusion of metastable neutrals, the process of metastable ionization was added. Throughout the investigation, the diffusion of positive ions was neglected: because of the relatively low fields encountered, the ion mobilities were much less than those of electrons.

The final assumption, which affected nearly all of the processes mentioned and greatly simplified the calculations, was that the discharge was in equilibrium with the local sustaining electric field. This assumption permitted the use of tabulated values for equilibrium transport coefficients (local drift velocities and diffusion and ionization coefficients) obtained from drift tube measurements or calculated by solving the collisional Boltzmann equation. The validity of this assumption is particularly questionable in the electrode regions since the equilibrium coefficients are characterized by uniform electric fields and uniform neutral number density distributions, requirements which are certainly not satisfied near the electrodes. Additional assumptions were also made concerning the boundary conditions at the electrodes and at various points within the discharge. These boundary condition assumptions and the previously listed assumptions are explained in more detail as they are encountered in the development of the theory in the following chapter.

General Approach

Based upon the assumed quasi-equilibrium, the gas discharge was modeled by a set of four coupled first-order differential equations.

These equations are: the continuity equations for electrons and positive ions, the electron current density equation, and Poisson's equation. In certain regions of the discharge, this particular set of equations becomes "stiff," i.e. some terms are changing very rapidly while others are changing very slowly. To solve this stiff system of equations, a computer program called Gear, written by C. W. Gear (Ref. 25), was used. This program uses an implicit linear multistep method, termed a "backward differentiation formula" method. Using Gear, the charge and current densities, the electric field, and the voltage were calculated as functions of position within the inter-electrode gap. Compiling the results from a number of these calculations, current-voltage (I-V) discharge characteristics were produced for several source strengths, pressures, and secondary emission coefficients for argon and methane discharges. The computer code written to model these discharges was validated by comparing the calculated I-V curves and the spatial variation of the field and number densities within particular discharges with those calculated by Lowke and Davies (Ref. 11). In addition, the I-V curves calculated for argon were also compared with experimental I-V characteristics obtained by Leffert et.al. (Ref. 13). The computer code was then modified to include the effects of secondary emission of electrons from the cathode and ionization of gas atoms in metastable states. This modified code was used to assess the relative importance of these processes in various gas discharges. The results of these calculations were compared with experiments performed by Bletzinger (Ref. 5) and theoretical calculations by Zakharov et.al. (Ref. 10).

Sequence of Presentation

The physical processes considered in the computer calculations

performed are presented in the following chapter, entitled "Theory." The expressions used for the various reaction rates and coefficients for these processes are described and any approximations made are noted. More specific information is given in Appendix A. In addition, the classification and characteristics of gas discharges, in general, are also presented in this chapter.

The physics described in the theoretical chapter is transformed into a model of a gas discharge in chapter III, "Numerical Method." In this chapter, a system of differential equations which describes the interaction of the physical processes in a gas discharge is developed. The boundary conditions imposed on this set of equations are also described.

The solutions to these equations for a range of discharge parameters are presented in chapter IV, "Results." These results are presented in two forms, in "profiles" of the spatial variation within a discharge of the independent variables and in current-voltage (I-V) "characteristics" obtained by plotting the voltage drop across the discharge for a range of discharge currents. These I-V characteristics are compared to similar characteristics which were measured experimentally.

However, because the calculations and experiments do not completely agree, indicating that other physical processes may need to be considered, suggestions for further research are presented in the final chapter, "Conclusions and Recommendations." Also, a brief summary of the physical insights revealed by the calculations and their implications for gas discharge switch design are included in this final chapter.

II. Theory

A gas discharge may be defined as a gas with free charged particles which allow the gas to carry a current. Gas discharges can occur over a wide range of gas pressures and can carry currents ranging over more than twelve orders of magnitude: from one millionth of an amp to one million amps. Gas discharges may exist only transiently, as in sparks or lightning, or they may operate in the steady state, as in neon lights. In addition, the discharge's behavior is often greatly influenced by the nature of the electrical circuit of which it is a part. In all cases, however, since gases are normally insulators, charged particles must be produced in some way to carry the current in a discharge. In addition, an electric field must be provided to drive these charged particles in order for them to form a current.

Charge Carrier Kinetics

Cosmic and ultraviolet radiation, natural radioactivity, and thermal collisions among gas particles are responsible for producing a background level of charged particles (~1000 positive and negative ions per cm^3) in all gas samples under normal conditions (Ref. 15:47). The higher levels of ionization required for efficient current conduction may be produced by an external source of charged particles and/or by the imposition of an electric field on the gas. This electric field is usually produced by applying a voltage across two electrodes placed in the gas. The field exerts a force on the charged particles which is parallel to the field. The fluid equation of motion for one species of such particles is:

$$n\left[\frac{\delta \vec{p}}{\delta t} + (\vec{W}\cdot\nabla)\vec{p}\right] = \pm en\vec{E} - \vec{\nabla}P - mn\nu\vec{W} \qquad (1)$$

where $\vec{p}$ is the momentum, P is the pressure, m is the mass, n is the number density, $\vec{W}$ is the velocity, ν is the average collision frequency, and $\vec{E}$ is the electric field. In one dimension, in a steady state, and for negligible pressure gradients, this equation reduces to:

$$0 = \pm enE - \frac{dP}{dx} - mn\nu W \tag{2}$$

Using the ideal gas law, the drift velocity may be represented as

$$W = \left(\frac{\pm e}{m\nu}\right)E - \left(\frac{KT}{m\nu}\right)\frac{dn/dx}{n} \tag{3}$$

where T is the temperature and K is the Boltzmann constant. In this equation, the coefficient of the electric field is called the mobility and the coefficient of the number density gradient term is called the diffusion coefficient.

$$K \equiv \frac{\pm e}{m\nu} \tag{4}$$

$$D \equiv \frac{KT}{m\nu} \tag{5}$$

These two coefficients are connected by what is known as the Einstein relation:

$$K = \frac{\pm eD}{KT} \tag{6}$$

Also, in both coefficients, the collision frequency, ν, for a particle in a gas of neutral number density, N, is given by

$$\nu = N\langle v\sigma\rangle \tag{7}$$

where $\langle V\sigma\rangle$ is the average of the product of the particles' relative velocity and the collision cross-section. Thus, in the case of negligible diffusion, equation 3 may be expressed as

$$W = \frac{\pm e}{m\langle\sigma v\rangle}\left(\frac{E}{N}\right) \qquad (8)$$

Because of the direct relationship between number density and collision frequency, this type of functional dependence on the ratio (E/N) is very common in the study of gas discharges. (The units for E/N are volt-cm^2 or Townsend, where 1 Townsend (Td) = 1 x 10^{-17} volt-cm^2.)

The functional dependence of the mobility and the diffusion coefficient on the collision cross-section, which is generally a non-linear function of E/N, requires complicated analytic fits or tabulated data in order to be modeled correctly. Tabulated values for the drift velocity and diffusion coefficient for electrons in argon and methane were obtained from solutions of the collisional Boltzmann equation and experimental measurements. However, it was experimentally found that the mobility of positive ions could be described independent of the field strength (Ref. 11:4994). More detailed information on the actual values used for these "material functions" is contained in Appendix A.

The electrons and positive ions, whose behavior in a gas discharge is described using these material functions, must be produced in some manner for a current to flow in a gas, which is normally an insulator. How these charged particles are generated and lost in the gas discharges investigated in this study is the subject of the next section.

Fundamental Processes

To accurately model the behavior of a gas discharge, it is necessary to consider the detailed interactions of individual gas particles. In this analysis, "average" properties are used to describe particles of the same type. These average particles are assumed to interact with each other and with the electrodes in ways which lead to the loss or

production of charged particles. Those processes which are considered in the generation of charged particles include: impact (Townsend) ionization of neutral particles in the ground and metastable states and secondary emission of electrons from the cathode. Those processes considered in the loss of charged particles include: electron-ion recombination and electron diffusion.

Impact Ionization. A small voltage applied to two parallel electrodes immersed in a gas will cause the electrons and ions naturally present in the gas to flow to the oppositely-charged electrodes and thus produce a current. At a given applied voltage, an electric field is produced between the electrodes which accelerates the charged particles to the electrodes. At higher applied voltages, the strength of this electric field is increased, accelerating the charged particles, particularly the electrons (because of their greater mobility), even more. At voltages larger than a certain value, the electrons gain enough energy between collisions to ionize neutral particles with which they collide (see Table I). The electrons produced may also be accelerated by the electric field and collide with other particles, producing more ionizing collisions. At this point, the gas is said to have "broken down." In an attempt to theoretically describe the increase in current which results, Townsend introduced the quantity α, known as Townsend's first ionization coefficient. This coefficient is defined as the average number of ionizing collisions made by an electron in traveling one cm in the direction of the electric field. Thus, the change in the number density of electrons, dn_e, occurring in a distance dx is given by:

$$dn_e = n_e \alpha dx \qquad (9)$$

Table I

Kinetic Reactions

Excitation	
$A + e \rightarrow A^* + e \rightarrow A + e + h\nu$	
Ionization	
$A + e \rightarrow A^+ + 2_e$	Townsend (impact) ionization
$A^* + e \rightarrow A^+ + 2_e$	metastable ionization
Recombination	
$A^+ + B + e \rightarrow A + B$	three-body recombination
$AB^{+} + e \rightarrow A + B$	dissociative recombination
$A^+ + e \rightarrow A + h\nu$	radiative recombination
Attachment	
$A + e \rightarrow A^- + h\nu$	radiative attachment
$AB + e \rightarrow A^- + B$	dissociative attachment
$2A + e \rightarrow A^- + A$	three-body attachment

(if recombination and diffusion are neglected). It may be assumed that an electron will ionize a gas molecule if the energy it acquires between collisions equals or exceeds the ionization energy, eV_i, (V_i is the ionization potential) of the gas molecules:

$$eEx \geq eV_i \tag{10}$$

where x is the path length between collisions for an electron and E is the electric-field (Ref. 33:514). Also, the average number of ionizing collisions which will occur in a given path length is inversely proportional to the electron mean free path. Thus, Townsend's ionization coefficient may be expressed as the inverse of the mean free path, L, times some function, F, of the energy gained by an electron (Ref. 33:515).

$$\alpha = \frac{F(Ex)}{L} \tag{11}$$

However, as mencioned earlier, only those electrons whose path lengths between collisions exceed x will have energies large enough to ionize gas molecules. The fraction of these electrons with free path lengths exceeding x is obtained from kinetic theory and is given by

$$f(x) = e^{-x/L} \qquad \text{(Ref. 33:515)} \tag{12}$$

Thus, the number of electron mean free paths which exceed x in a given unit length is just

$$\left|\frac{df(x)}{dx}\right| = \frac{1}{L} e^{-x/L} \qquad \text{(Ref. 33:515)} \tag{13}$$

This expression, then, may be used to represent Townsend's ionization coefficient. Recalling that the mean free path is inversely proportional to the gas pressure, and using the expression for x in equation 10,

equation 13 may be rewritten:

$$\alpha/P = A\, e^{-\frac{BV_i}{E/P}} \qquad \text{(Ref. 33:516)} \qquad (14)$$

where A and B are constants determined by the gas in the discharge and P is the gas pressure. In the present analysis, an analytic expression such as this, given by Lowke and Davies (Ref. 11:4994), was used to calculate the Townsend ionization coefficient in argon. However, for methane, Cookson's experimental values of the "net ionization coefficient," which included electron losses by attachment, were used (Ref. 14:18). From the appropriate Townsend ionization coefficient, the rate of such ionization, ν_i, i.e. the number density of electron-ion pairs produced in one second by a single electron, is obtained from the product of α and the average drift velocity of an electron betweem collisions, W_e:

$$\nu_i(1/\text{sec}) = \alpha(1/\text{cm}) \cdot W_e(\text{cm/sec}) \qquad (15)$$

Metastable Ionization.

Townsend's first ionization coefficient accounts for ionization from the ground state of an atom or molecule. Another means must be used to include the effect of ionization from metastable excited states of atoms or molecules. This metastable ionization is particularly important for rare gases, such as argon and krypton, and molecular gases, such as O_2 and N_2. To include this effect, the number density of metastable neutrals and the rate of ionization from these states had to be determined. The rate of ionization of metastables was approximated by assuming that the electrons had a Maxwellian energy distribution and that the magnitude of this cross-section was similar to that of the ground state ionization

cross-section, although this cross-section was shifted to much lower energies. The number density of neutral argon metastables was approximated by using a Boltzmann distribution, at the electron temperature, between the ground and metastable states. The effect of metastable ionization was included in the investigation of argon, but not in the investigation of methane.

Secondary Emission. One additional source of charged particles considered in this investigation was secondary electron emission from the cathode. (Although electrodes can also emit positive ions in certain circumstances, the rate of positive ion emission is usually very low and was therefore neglected in this analysis.) These electrons are produced by the bombardment of the cathode by positive ions. In a metallic electrode, which has "free" electrons, an electron is emitted if it is given enough energy by the incident ion to overcome the work function (potential barrier at the surface) of the material. This effect was also described by Townsend, who defined a secondary emission coefficient, γ, which is the cathode yield in electrons per incident ion. The value of γ is determined by the cathode material, the nature of the gas in the discharge, and the positive ion energy, which is a function of the electric field strength in the discharge. The values for γ given in the literature for positive argon ions in the ground and metastable states range from less than one percent to almost forty percent for various values of electric field strength and cathode material. Thus, a range of secondary emission coefficients, each constant with respect to field strength, was used in this analysis (Ref. 19:118).

Recombination. Recombination may occur when a positive ion collides with an electron or negative ion. The free electron or the extra electron

from the negative ion recombines with the positive ion, producing one or two neutral particles. The initial kinetic energy of the particles and the potential energy of ionization may be dissipated in one of three major ways (see Table I). The energy may be radiated away (radiative recombination); it may be transferred to a third particle (an electron or a heavy particle) as kinetic energy (three-body recombination); or it may be used to dissociate the neutral molecule formed from a molecular ion and an electron (dissociative recombination).

The probability of recombination decreases as the relative velocity of the oppositely-charged particles increases. Consequently, the probability of electron-ion recombination is usually much less than that of ion-ion recombination because electrons typically have much higher velocities than ions. However, in methane and argon, their very small attachment cross-sections result in correspondingly low number densities of negative ions and thus low rates of ion-ion recombination. Therefore, electron-ion recombination was considered to be the dominant recombination mechanism in both methane and argon.

By comparing typical rates for the various types of electron-ion recombination, it was found that dissociative recombination was the dominant recombination mode for the discharge conditions considered in both argon and methane. The radiative recombination rate for electrons and ions is estimated by von Engel to be of order 10^{-13} cm^3/sec (Ref. 17: 141). In contrast, because of the multiplicity of energy absorption possibilities in molecules, dissociative recombination coefficients are usually of order 10^{-7} cm^3/sec (Ref. 17:142-143). Also, at the intermediate gas pressures (240 and 760 Torr) and low electron number densities investigated, the rate of three-body recombination, with an

electron as the third body, is approximately 10^{-9} cm^3/sec. When the third body is a heavy particle, the rate is even lower, at 10^{-11} cm^3/sec (Ref. 18:36).

As noted previously, the electron-ion recombination rate is greater for lower relative velocities between electrons and ions. As a result, recombination is, in turn, greater at lower field strengths. In the investigation of argon, the results using various recombination coefficients were compared. Both the constant coefficient used by Lowke and Davies and a coefficient with a functional dependence on electron temperature, offered by them as an alternative, were used (Ref. 11:4994). In addition, a recombination coefficient with a field strength dependence, given by Kline, was used for comparison (Ref. 14:13). The investigation of methane made use of a recombination coefficient, also with a functional field dependence, which was calculated by Kline (Ref. 14:19) using measured recombination cross-sections. Detailed information on the values and analytic expressions used for these rates are provided in Appendix A.

Attachment. An electron which collides with a neutral particle may become "attached" to the neutral, forming a negative ion, in the process called attachment. In order for this process to occur, the neutral particle must have an electron affinity resulting from a nearly filled atomic electron shell or molecular orbital. Strong attachment rates are exhibited by only a few species of particles, including atomic and molecular oxygen and the halogen gases (e.g. fluorine and chlorine). Similar to recombination, the kinetic energy of the incident particles and the binding energy (affinity) of the resulting neutral particle must be dissipated in some way. Consequently, attachment may take one of three

forms: radiative attachment, dissociative attachment, or three-body attachment (see Table I) (Ref. 15:29). However, in this analysis, these forms of attachment were not distinguished from each other and attachment itself was only implicitly accounted for in methane. For methane calculations, an experimentally measured "net ionization coefficient" was used which considered attachment as a reduction in the Townsend ionization coefficient. For argon calculations, attachment effects were completely neglected because of argon's inert nature.

Diffusion. Charged particles are also lost through the process of diffusion. The rate of this loss is directly proportional to the diffusion coefficient

$$D = \frac{KT}{m\nu} \tag{16}$$

as shown previously in the discussion of charge carrier kinetics. In this expression, T is the temperature of the particle species, m is the particle mass, and ν is the average collision frequency of the particle. Thus, diffusion is greater for higher temperatures and smaller masses, and collision frequencies (and thus lower gas pressures). Because the mass of an ion is usually over 2000 times that of an electron, the diffusion of positive ions was neglected in this analysis. Values for the longitudinal diffusion coefficient of electrons, as a function of E/N, were obtained from calculations (for argon) and from experimental measurements (for methane). The sources for these values are listed in Appendix A.

Classification and Characterizatics of Gas Discharges

In a steady-state gas discharge, the voltage applied to the electrodes determines how the charged particle generation and loss processes interact in the production of a steady state distribution of charged

particles in the discharge. This distribution of charged particles then determines the magnitude of the discharge current. Discharges may be divided into two basic categories using the breakdown voltage, mentioned previously in the discussion of Townsend ionization, as the dividing point. At voltages below breakdown, a discharge is said to be non-self-sustained, while, above breakdown, the discharge is self-sustained. Non-self-sustained discharges require an external source of ionization to provide sufficient numbers of current-carrying charged particles. A self-sustained discharge generates enough current-carrying charged particles, from internal discharge processes such as Townsend ionization, secondary emission, or thermionic emission, to compensate for any loss processes in the discharge.

Non-Self-Sustained Discharge. If no ionization is produced by the discharge itself, and the only source of charged particles is natural radioactivity and cosmic rays, at very low applied voltages the discharge current is measured in random bursts. This intermittent current reaches a maximum when the applied voltage is increased to the point that the field thereby created sweeps all of the ions and electrons to the electrodes before they can recombine. (See Figure 1, which shows the variation of current with voltage (I-V characteristic) in a low pressure (~1 Torr) gas discharge. Thus, if the external ionization source produces electron-ion pairs at a rate S ($1/cm^3/sec$), between electrodes separated a distance d(cm), the saturation current density J_s (A/cm^2) is given by

$$J_s = edS \tag{17}$$

where e is the electronic charge in Coulombs (Ref. 15:48).

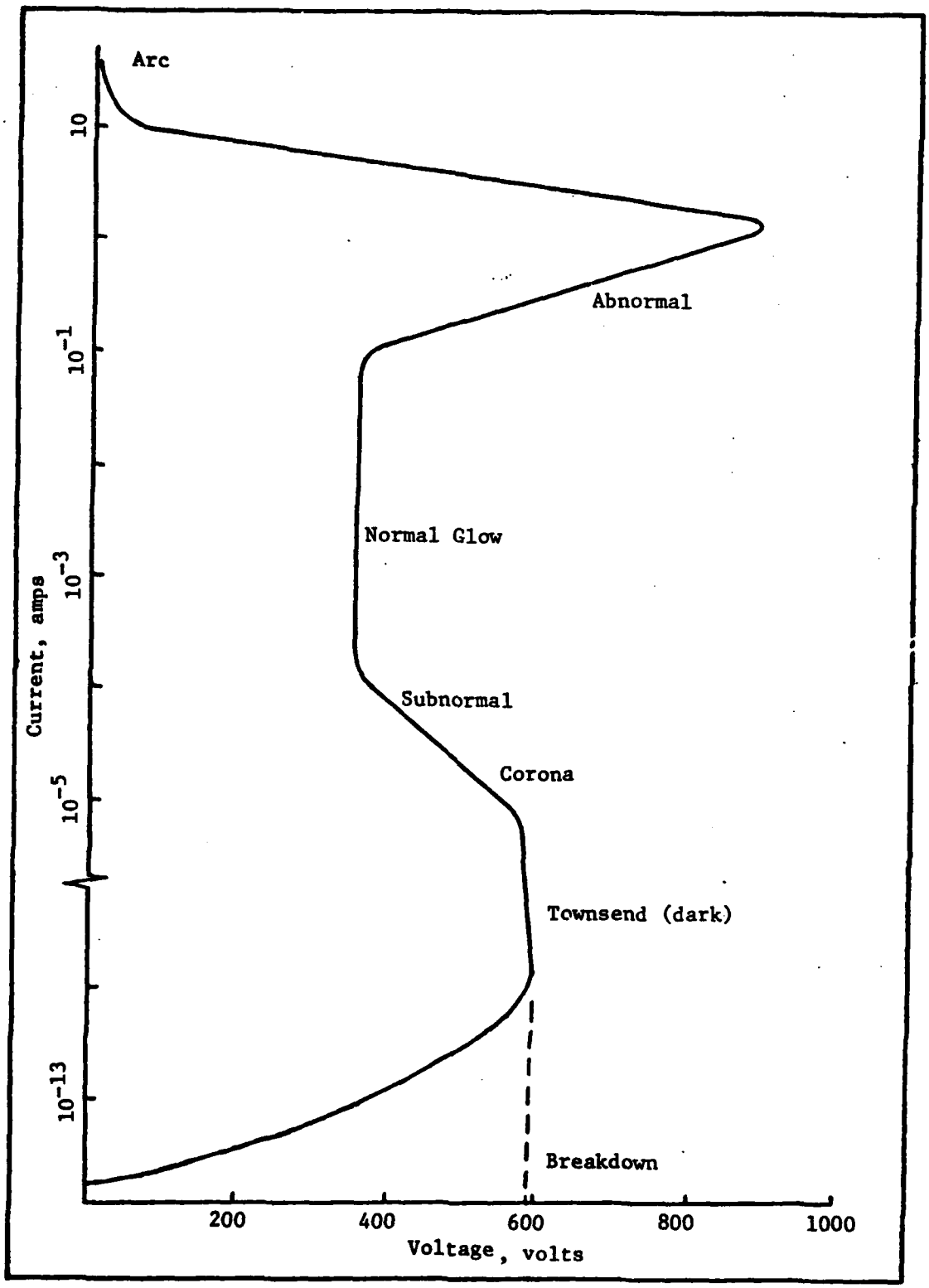

Figure 1. General Current-Voltage Characteristic (Ref. 49:211)

With a further increase in the applied voltage, Townsend ionization begins to occur, additional electrons and ions are produced, and the discharge current increases from its saturated value. At a certain voltage, the number of electrons and ions produced by Townsend ionization and secondary emission are sufficient to replenish the number lost by recombination, diffusion, attachment, and the external circuit current. At this voltage, the discharge is said to have "broken down," and is thus self-sustained.

Self-Sustained Discharge. Breakdown occurs at the beginning of what is known as the Townsend discharge region. This discharge is also known as a dark discharge since it emits very little visible radiation. The Townsend discharge and current saturation regions are indicated in Fig. 1.

As the discharge current increases, the voltage across the electrodes drops considerably as the discharge transitions to a more efficient operating regime. This region of the I-V characteristic, where the voltage falls as the current increases, is known as a subnormal or corona discharge. (See Fig. 1.) In this region, the effective electrical resistance of the discharge is negative (Ref. 15:82).

As the voltage drops, the discharge begins to glow. At a certain current, the discharge voltage stabilizes and remains relatively constant as the current is further increased. In this region of the I-V characteristic, known as a glow discharge, the luminous column covers only a portion of the cathode surface. As the current in the discharge is increased, this "cathode spot" increases in size, keeping the current density constant (Ref. 15:82). When the cathode spot covers the entire cathode surface, a further increase in current requires the voltage across the electrodes to increase rapidly to a maximum. This region of

the I-V characteristic is termed an abnormal glow discharge (Ref. 15: 82).

If the discharge is driven to higher currents, the discharge voltage drops by over an order of magnitude as a new mechanism of electron production becomes operative. At these higher currents, electrons are also produced by thermionic emission at the cathode. This type of gas discharge, which is known as an arc discharge, is much more luminous than a glow discharge. In addition, the current carried by an arc discharge is determined primarily by the external electric circuit of which the discharge is a part, while the current carried by a glow discharge is also very dependent upon the properties of the discharge itself (Ref. 15:88). This difference occurs because the physical processes responsible for producing a glow discharge are very sensitive to the discharge current and voltage, while the thermionic emission which allows an arc to form is very stable once it is initiated.

Externally-sustained Discharge. However, none of the previous discharge descriptions allow for strong external ionization sources. If such sources are considered, it is found that although a discharge may appear to resemble a glow discharge, it may not necessarily be self-sustained, as required by the previous description. In fact, the discharges produced under strong external ionization may not exactly resemble any of the various self-sustained discharges mentioned previously. However, since the currents carried by glow and arc discharges are similar to those desired for electron-beam-sustained switches, some of the features of these discharges will be presented. These characteristics will later be compared to those predicted by this investigation of externally-sustained gas discharges.

Low Pressure Glow Discharge. A low pressure glow discharge may be divided longitudinally into several distinct regions, as shown in Fig. 2. Not all of these regions produce visible radiation. Light is emitted only in those regions of the discharge in which excited ions or neutrals transition to lower energy levels or in which electrons and ions radiatively recombine. The major features in each of four longitudinal regions of a glow discharge are described in the following sections.

Cathode sheath. The electrons required to maintain the discharge are produced primarily by positive-ion bombardment of the cathode. These electrons are quickly accelerated by the strong negative electric field through the region known as Aston's dark space (see Fig. 2). Incoming positive ions colliding with the slowest of the exiting electrons emit light as they recombine in the region referred to as the cathode glow. These electrons may also produce excited atoms, which emit light of discrete frequencies as they return to their ground states. The remaining higher-energy electrons are quickly accelerated through the cathode dark space, leaving a net positive space charge in this region. (No light is emitted from this region because, as mentioned previously, the recombination coefficient is very small at high relative velocities. The net positive space charge produces a strong electric field in these three regions, which are collectively known as the cathode sheath (Ref. 16:83). Typically, most of the voltage drop across the discharge occurs in the cathode sheath (of thickness d_c) and is referred to as the cathode fall, V_c.

Negative Glow. The large negative electric field in the cathode sheath causes large numbers of electrons to be created through Townsend ionization. However, these electrons are rapidly accelerated out of the

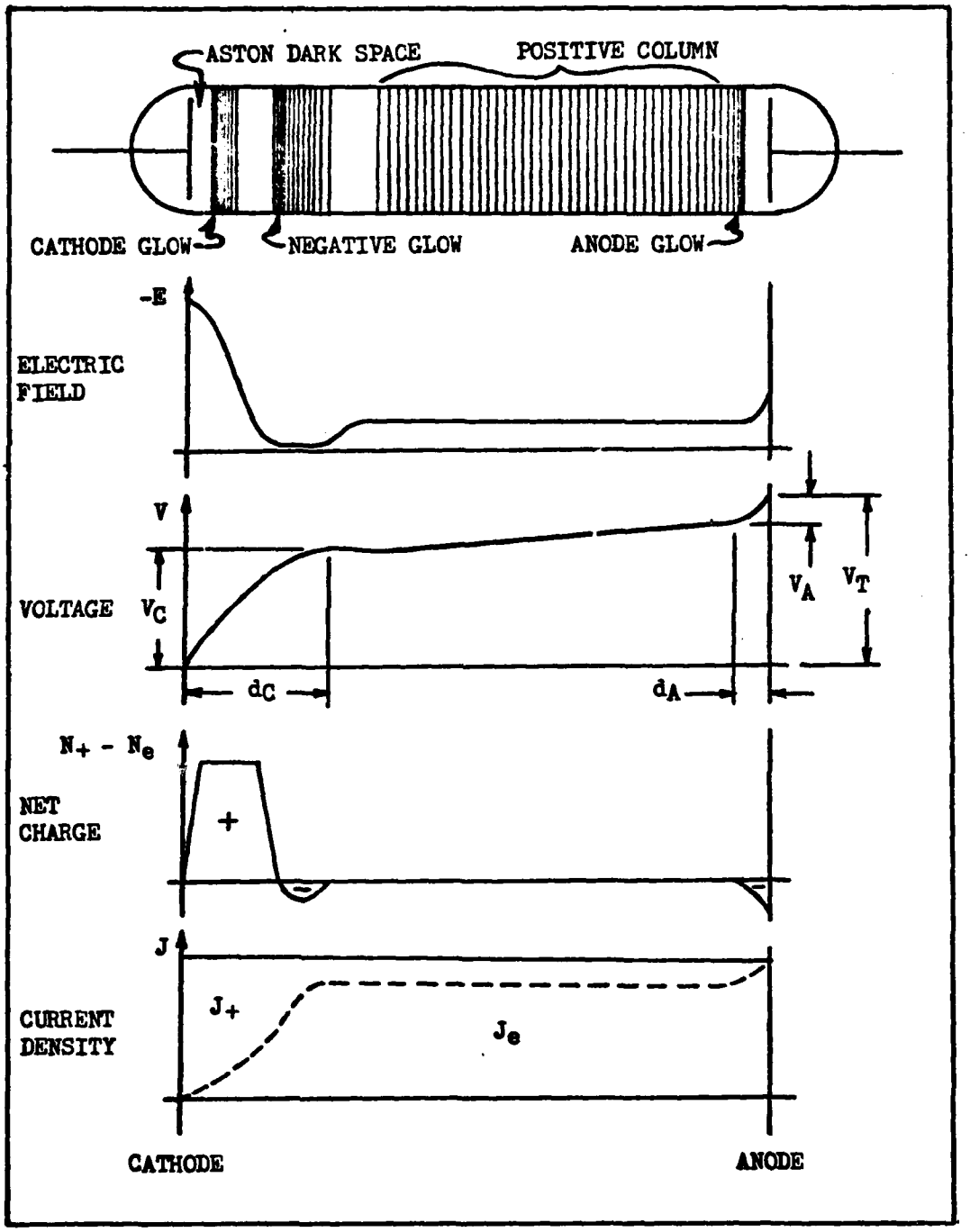

Figure 2. Glow Discharge Parameter Profile

sheath region and into the negative glow region, where they produce a slightly negative net space charge. With a much smaller field in this region, the electrons quickly lose their energy through ionization and recombination. The resulting recombination and de-excitation is responsible for producing the "negative" glow. As the swarm of electrons pass through this region, recombination gradually reduces the net space charge to zero as the electrons enter the next region, the positive column (Ref. 16:85).

Positive column. In spite of its name, the positive column has little or no net space charge. Although the region is neutral overall, the more rapid diffusion of electrons to the walls of the discharge tube causes a "column" of positive charge to develop along the axis of the tube. To maintain this overall neutrality, the small negative field within the positive column is of sufficient strength for Townsend ionization to balance electron loss by recombination and diffusion (Ref. 16:86). These electrons also cause electron impact excitation, so that de-excitation and recombination combine to produce a luminous positive column. However, this luminous region does not perform any essential function in the production of a glow discharge. It merely serves to connect the cathode and anode sheaths ends of the discharge. Thus, as the discharge parameters (gas pressure, tube length, etc.) are varied, the positive column adjusts its length to compensate for any required charges in the sheath thicknesses.

Anode sheath. A short distance from the anode, the positive column gives way to the anode sheath, which somewhat resembles a compressed cathode sheath. (The anode sheath thickness is often less than 1% of the cathode sheath thickness.) (Ref. 11:4999) Also, in the anode sheath,

the space charge produced is negative since electrons are attracted to this electrode. This negative space charge causes the negative electric field in the discharge to increase in magnitude in the sheath. Some electrons accelerated by this enhanced field gain enough energy to excite or ionize neutral gas particles. The resulting de-excitation and recombination produce another luminous region, known as the anode glow, some small distance from the anode surface (Ref. 16:87). The increase in magnitude of the anode field produces a voltage drop, V_A, across the anode sheath, of thickness d_A. Since the field is negative throughout a glow discharge, the voltage drops across the cathode and anode sheaths and the positive column are all positive. Thus, the total discharge voltage, V_T, is the sum of these voltage drops (See Fig. 2).

High Pressure Discharge. If the pressure is increased in a normal glow discharge (in the same external electrical circuit), the thickness (d_c) of the cathode sheath will decrease and the current density in the sheath will increase. In addition, the field in the positive column will be greater: the increase in recombination losses at higher pressures must be compensated for by an increase in electron impact ionization and thus an increase in the electric field. However, at higher pressures (atmospheric or greater), a normal glow discharge may not exist as a stable discharge (Ref. 16:88): the drop in voltage upon entering the normal glow region (see Fig. 1) may no longer exist. As a result, a dark discharge may transition directly to an arc discharge at high gas pressures.

Arc Discharge. Although an arc discharge may be divided into regions similar to those in a glow discharge, an arc discharge is able to carry a much higher current, at a lower voltage, than a glow discharge. (The

total voltage drop across an arc discharge is roughly an order of magnitude less than the drop across a glow discharge.) The higher current that an arc carries is also carried at a higher current density. This high current density causes the discharge to be intensely luminous, which prevents the observation of variations in the sheath regions. The sheath regions are compressed and the voltage drops across them are decreased. However, the electric field in what may still be called a positive column is greater than for a glow discharge.

Experimentally-measured I-V Characteristics. The longitudinal variation of the electric field, voltage, and number and current densities in a gas discharge can usually be obtained experimentally, although with some difficulty. However, it is usually the total behavior of a discharge which is of interest in practical applications. I-V characteristics of the variation of the discharge (circuit) current with total discharge voltage drop are experimentally obtained using a circuit as shown in Figure 3. The I-V characteristic is "traced out" by varying the supply voltage, V_o, for a particular resistor value, R. Thus, given V_o and R, and measuring the external circuit current, I, the discharge voltage, $V_T(I)$, is obtained. The relationship between these circuit parameters is represented by what is termed a "load line." Several load lines are superimposed on a general discharge characteristic in Fig. 3. As V_o is varied, the load line "scans" the characteristic. If the characteristic has a complicated behavior, some ambiguity may occur if the resistance in the external circuit is too small, as shown by load line 3 in Fig. 3. Thus, particularly large-valued resistors must be used to trace out reversals in I-V characteristics, as in the Townsend discharge region.

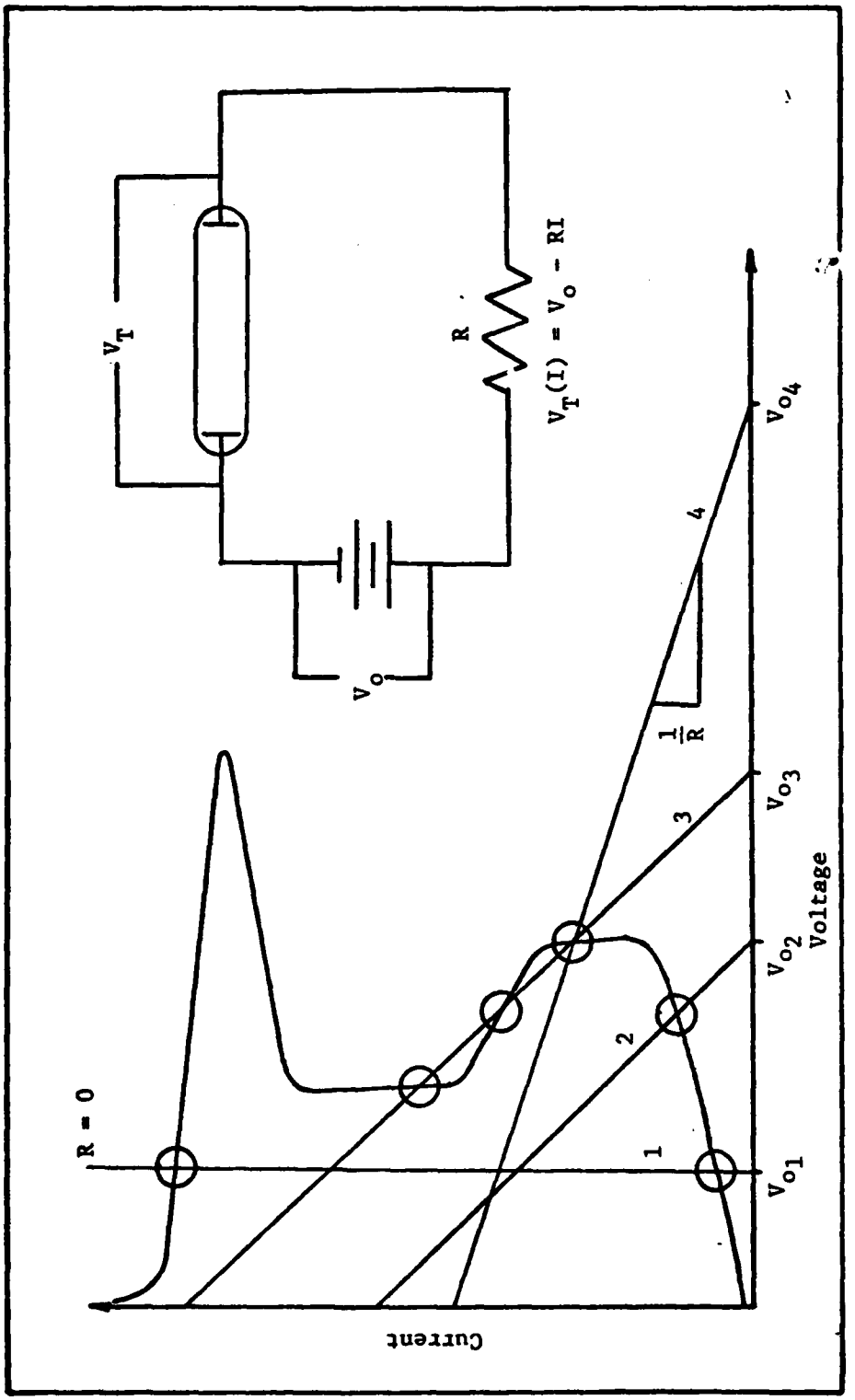

Figure 3. Experimental I-V Measurements in Gas Discharges

III. Numerical Method

Externally-sustained gas discharges may contain some features of each of the types of discharges just described. This chapter explains how an externally sustained gas discharge between parallel electrodes was modeled using the continuity equations for electrons and ions and Poisson's equation. With the boundary conditions imposed by the electrodes, this set of equations was solved numerically to obtain the steady-state spatial distributions of the electric field and electron and ion number densities and current densities. Three methods of solution, subsequently referred to as Cases I, II, and III, were used. These methods, each of which corresponds to a particular type of discharge, were used by Lowke and Davies in their analysis (Ref. 11:4999-5000). However, before these individual methods are described, the physical setup of the components of the discharge tube, the sign conventions used, the differential equations describing the discharge's behavior, and the boundary conditions at the electrodes are presented. Additional boundary conditions are discussed separately for each case.

Setup and Sign Conventions

The components of the model discharge tube are shown in Fig. 4. The problem was restricted to one dimension between plane, parallel electrodes placed a distance d apart: the cathode was at x = 0 and the anode was at x = d. It was also assumed that an external ionization source created electron-ion pairs uniformly throughout the electrode gap at a constant rate S($1/cm^3/sec$). (In some electron beam-sustained discharges, this source is produced by directing a high energy electron beam through a foil at the cathode end of the discharge tube. To allow

the electron beam to penetrate the entire interelectrode gap, the cathode is in the form of a conducting grid.)

The positive directions of the electric field, current densities, and spatial coordinates are defined to be from cathode to anode. Thus, when subjected to a negative electric field, an electron, with a negative charge, will have a positive drift velocity and move toward the anode. Conversely, a positive ion will have a negative drift velocity and move toward the cathode. Thus, when an electron-ion pair is created by Townsend ionization or an external ionization source, the charged particles migrate to opposite electrodes. Although the electron drifts much faster than the ion, and would thus seem to carry more current, it exists as a charge carrier for a time inversely proportional to its velocity. Thus, the total contributions to the current of the electron and ion are exactly the same. Consequently, the current carried by an electron-ion pair created in the center of the interelectrode gap is equivalent to that carried by an electron created at the cathode or a positive ion created at the anode (Ref. 17:154).

However, the current carried at a particular longitudinal point in the interelectrode gap may be shared unequally by electrons and ions if their number densities do not exactly compensate for differences in their drift velocities. At all longitudinal points, however, the total current density, which is the sum of the magnitudes of the electron and ion current densities, must be constant. Thus, in terms of particle fluxes, and recalling the sign convention adopted, the total particle flux at a point x is:

$$J/e = j_e(x) - j_+(x) \qquad (18)$$

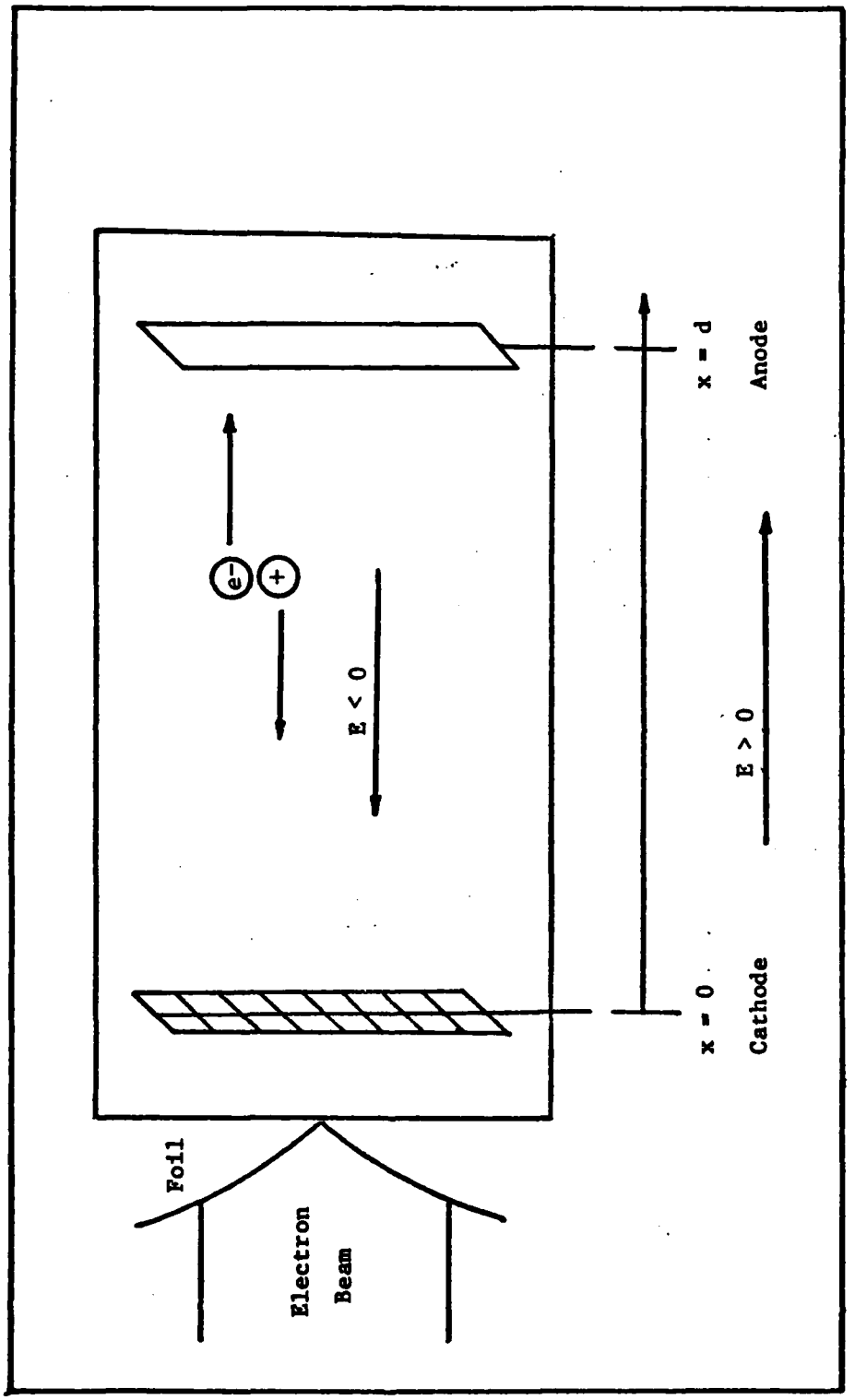

Figure 4. Setup and Sign Conventions

Equations

The continuity equations for electrons and positive ions and Poisson's equation were solved simultaneously to obtain the spatial variation, in the steady-state, of the electric field, the electron and positive ion number densities, and the electron and positive ion fluxes. Not all of the physical processes described in the previous chapter were included in every calculation. Initially, only those processes considered by Lowke and Davies (Ref. 11), namely electron ionization and recombination, were used. Both argon and methane discharges were modeled in this way. Subsequent calculations included the effect of metastable ionization in argon discharges and the effect of secondary emission in both argon and methane discharges. Including terms describing metastable ionization, the continuity equations for electrons and positive ions are (secondary emission affects the boundary conditions but not the form of the differential equations):

$$\frac{\partial n_e}{\partial t} = S + \alpha|W_e|n_e - R_r n_e n_+ + R_{im} n_e n_m - \frac{\partial j_e}{\partial x} \qquad (19)$$

$$\frac{\partial n_+}{\partial t} = S + \alpha|W_e|n_e - R_r n_e n_+ + R_{im} n_e n_m - \frac{\partial j_+}{\partial x} \qquad (20)$$

where n_e, n_+ = number density of electrons and positive ions ($1/cm^3$)

j_e, j_+ = flux of electrons and positive ions ($1/cm^3/sec$)

n_m = number density of metastable neutrals ($1/cm^3$)

x = distance from cathode (cm)

t = time (sec)

S = electron-ion pair production rate ($1/cm^3/sec$)

α = Townsend's first ionization coefficient (1/cm)

R_{im} = metastable ionization rate coefficient (cm^3/sec)

R_r = electron-ion recombination rate coefficient (cm^3/sec)

W_e = electron drift velocity (cm/sec)

Equation 19 states that the temporal rate of charge of the number density of electrons at a particular point in the discharge is equal to the rate at which electrons are produced by the source function, Townsend ionization, and metastable ionization, minus the rate at which electrons are lost by recombination and the gradient in electron flux. Similarly, equation 20 states that the temporal rate of charge of the number density of positive ions is equal to the rate at which positive ions are produced by the source function, Townsend ionization, and metastable ionization, minus the rate at which they are lost by recombination and the gradient in positive ion flux. Thus, the continuity equations for electrons and positive ions are identical. In the steady-state, the temporal derivatives vanish, and the result is:

$$\frac{\partial j_e}{\partial x} = \frac{\partial j_+}{\partial x} = S + \alpha|W_e|n_e - R_r n_e n_+ + R_{im} n_e n_m \qquad (21)$$

In equation 21, an expression for the flux of electrons at a particular point in the discharge, j_e, may be obtained from the fluid equation of motion (equation 1) for electrons. Assuming, as before, one dimension, steady-state, and negligible pressure gradients, and using the ideal gas law:

$$-en_eE = KT(dn_e/dx) + m_e n_e \nu W_e \qquad (22)$$

Dividing by $m_e\nu$:

$$\frac{-en_e}{m_e\nu} E = \left(\frac{KT}{m_e\nu}\right)\left(\frac{dn_e}{dx}\right) + n_e W_e \qquad (23)$$

Rewriting this equation in terms of the conductivity, σ,

$$\sigma = \frac{-ej_e}{E} = \frac{-e^2 n_e}{m_e \nu} \tag{24}$$

and the diffusion coefficient (equation 5),

$$-\frac{\sigma}{e}E = -D_e \frac{\partial n_e}{\partial x} + n_e W_e \tag{25}$$

$$+j_e = +n_e W_e - D_e \frac{\partial n_e}{\partial x} \qquad \text{(Ref. 11:4992)} \tag{26}$$

Equation 26 states that the flux of electrons at a particular longitudinal point is due to the electron drift velocity (which is positive for negative electric fields) and diffusion, which opposes the gradient in the electron number density. Because the mobility of ions is usually several orders of magnitude less than the mobility of electrons, and the diffusion coefficient is directly proportional to mobility, the diffusion of positive ions was neglected in this analysis (Ref. 16:34). Thus, the flux of positive ions was assumed to be given by

$$j_+ = n_+ W_+ = n_+ K_+ E \tag{27}$$

(The experimentally determined mobility, k_+, of Ar_2^+ ions was also used for the mobility of positive ions in methane, although their relative masses indicate that the mobility of positive methane ions should be approximately five times greater than that of argon ions.)

The potential, V, in the region between the electrodes is given by Poisson's equation:

$$\frac{\partial^2 V}{\partial x^2} = \frac{e}{\varepsilon_o}(n_+ - n_e) \tag{28}$$

where $e = 1.6 \times 10^{-19}$ Coulombs and $\varepsilon_o = 8.85 \times 10^{-14}$ Coulombs/Volt/cm. Poisson's equation may also be written in terms of the electric field, E, since:

$$E = -\frac{\partial V}{\partial x} \tag{29}$$

In summary, the steady-state behavior of an externally-sustained gas discharge may be described by a set of four coupled first-order differential equations with four independent variables:

$$\frac{\partial j_e}{\partial x} = S + \alpha |W_e| n_e - R_r n_e n_+ + R_{im} n_e n_m \tag{30}$$

$$\frac{\partial j_+}{\partial x} = S + \alpha |W_e| n_e - R_r n_e n_+ + R_{im} n_e n_m \tag{31}$$

$$\frac{\partial n_e}{\partial x} = \frac{n_e W_e - j_e}{D_e} \tag{32}$$

$$\frac{\partial E}{\partial x} = \frac{e}{\varepsilon_o} (n_+ - n_e) \tag{33}$$

where the independent variables are j_e, n_e, n_+, and E. The potential, V, is obtained directly from E by using equation 29. Also, j_+ is obtained directly from n_+ and E by using equation 27.

In using this set of equations, the value for the external ionization source strength had to be stipulated and the values for the reaction rates, ionization coefficients and the electron diffusion coefficient and drift velocity had to be known as functions of the electric field. The values used for some of these terms were obtained by experimental measurement of the quantities in a uniform field. The values used for other terms were obtained from solutions of the collisional Boltzmann

equation, in which electron velocity distributions for constant fields and electron number densities were used. The validity of using the values obtained by these methods was thoroughly discussed by Lowke and Davies in their report. They also emphasized that the alternative to this equilibrium approach, which would probably require a Monte Carlo technique, would be considerably more complex without significantly affecting the major features of the solutions obtained (Ref. 11:4993).

Methods of Solution

Three methods were used to solve the system of equations describing an externally-sustained discharge. These methods were used by Lowke and Davies in their investigation, which covered a very wide range of ionization source strengths. In the first two methods, which were applicable in low current and source strength situations, Lowke and Davies found that no plasma region was produced. However, a plasma region was produced at higher source strengths and currents, which required the third method of solution. Although all of Lowke and Davies' methods were successfully duplicated, the high currents and source strengths of interest in switching applications made their third method much more useful than the others in this investigation.

In all three methods, integrations were begun at a particular point (or points) in the discharge at which all of the independent variables were either known or iteratively assigned a value. The position of these starting points depended upon the case being considered: in Case I, the anode was the starting point; in Case II, the point at which the field vanished was the starting point; and in Case III, two starting points, at opposite ends of the positive column, were used. With these starting values, and with all of the transport coefficients and material

functions known as a function of the field, the integration procedure of C. W. Gear (Ref. 25) was used to obtain values for the independent variables at various points in the discharge. Gear's method was particularly useful because it automatically decreased the step size only in those regions for which the system of equations was stiff.

Boundary Conditions

For all three methods of solution, the boundary conditions at the electrodes were deduced from physical requirements on the ratio of electron to ion fluxes at the electrodes. The resulting boundary conditions are the same as those used by Lowke and Davies, but their rationale for them is based upon the electrodes' perfect absorptivity of electrons (Ref. 11:4993). The boundary conditions used in this analysis will first be described at the cathode. It will be seen that a similar development applies for positive electric fields at the anode, while some modification is required if the field is negative at the anode.

At the cathode, the applied voltage produces a negative field which drives positive ions into the electrode. As a consequence, electrons are liberated through the process of secondary emission. Assuming that there are no other sources of electron or ion currents, the secondary emission yield of the cathode determines the ratio of the electron and ion current densities at that point.

$$j_e = \gamma j_+ = \left(\frac{\gamma}{\gamma-1}\right) \frac{J}{e} \tag{34}$$

(The last equality is obtained from the requirement that the total current density be a constant: $J/e = j_e - j_+$.) This requirement may also be expressed in terms of the value of n_e at the cathode. Since $j_+ = n_+ K_+ E$, and using Piosson's equation (33) to rewrite n_+ in terms of

n_e and $\frac{\delta n_e}{\delta x}$, equation 34 becomes

$$n_e = \frac{D_e \frac{\delta n_e}{x} - \frac{\varepsilon_o \gamma K_+ E}{e} \frac{\delta E}{\delta x}}{W_e - \gamma W_+} \tag{35}$$

Then, in the case of no secondary emission, $\gamma = 0$, and the boundary conditions simplify to:

$$j_e = 0 \tag{36}$$

or

$$n_e = \frac{D_e}{W_e} \frac{\delta n_e}{\delta x} \tag{37}$$

and the entire current is carried by positive ions. In most of the discharge calculations, this value for n_e was over eight orders of magnitude less than the maximum value for n_e in the discharge, thus, this boundary condition was approximated as

$$n_e \approx 0 \tag{38}$$

which agrees with Lowke and Davies' development (Ref. 11:4999). This approximation resulted in exaggerated values for the cathode fall, V_c, although they were usually in error by less than one per cent.

At the anode, if the electric-field there is positive, positive ions are driven toward the electrode and it should behave as a cathode. Thus, the number density of electrons at the anode, for no secondary emission, is the same as at the cathode:

$$n_e = \frac{D_e}{W_e} \frac{\delta n_e}{\delta x} \approx 0 \tag{39}$$

Although it is also required that $j_e = 0$, this alternate boundary

condition could not be satisfied because of an error in the treatment of electron diffusion. This error occurs whenever there is appreciable electron diffusion into a retarding electric field. Although these electrons should lose energy, if the diffusion is into a region with a stronger electric field, the material functions used assign the electrons a larger diffusion coefficient. This problem is particularly evident in Case II discharges, in which diffusion has a significant effect (Ref. 11: 4998). Thus, as seen in Figure 7, the electron flux continues to increase in the anode "sheath" although the electron number density is decreasing and the retarding field is also increasing. A similar problem does not occur in the cathode region because the electric field there decreases with increasing x. The anode sheath in Case III discharges suffers from the same problem, although its overall effect is not as important because the anode sheath is usually much smaller than the cathode sheath in this case. Thus, if the anode electric field is positive, the most that can be required of the particle fluxes at the anode is

$$j_e - j_+ = J/e \tag{40}$$

If the anode electric field is negative, electrons are driven toward the cathode and the ratio of positive ion to electron fluxes is again a constant

$$j_+ = \eta j_e$$

In this case, however, η is always zero because the probability for an electron to induce the emission of a positive ion is vanishingly small. Thus, $j_+ = 0$, and the entire current is carried by electrons. In terms of number densities, then, the number density of positive ions at the anode is:

$$n_+ = 0 \tag{41}$$

while the number density of electrons is (using Poisson's equation):

$$n_e = \frac{-\varepsilon_o}{e} \frac{\delta E}{\delta x} \tag{42}$$

If $\delta E/\delta x$ at the anode is very small, as in a Case I discharge, this boundary condition becomes

$$n_e \approx 0 \tag{43}$$

These electrode boundary conditions are summarized in Table II. Additional boundary conditions at the ends of a Case III positive column and at the center of a Case II discharge are discussed as they are encountered in the following descriptions of the three methods of solution.

Case I. This method was used for low, saturated current densities and low ionization source strength discharges. In this situation, the sheath thickness is greater than the inter-electrode gap and there is no plasma region with $n_e \sim n_+$. In fact, n_e is generally much less than n_+ throughout the inter-electrode gap. An example of this situation is shown in Fig. 5, for conditions identical to those used by Lowke and Davies (Ref. 11:4995). At this low applied voltage, the field in the discharge is correspondingly small and Townsend ionization is minimal. Thus, the maximum current density that can be carried at these low voltages is just the saturation current density, $J_s = edS$ (Equation 17). However, the Case I method is only designed to handle discharges at the saturation current density. At voltages lower than that required to just sweep all electrons and ions to the electrodes before recombining, the Case II method should be used. This dividing point can also be

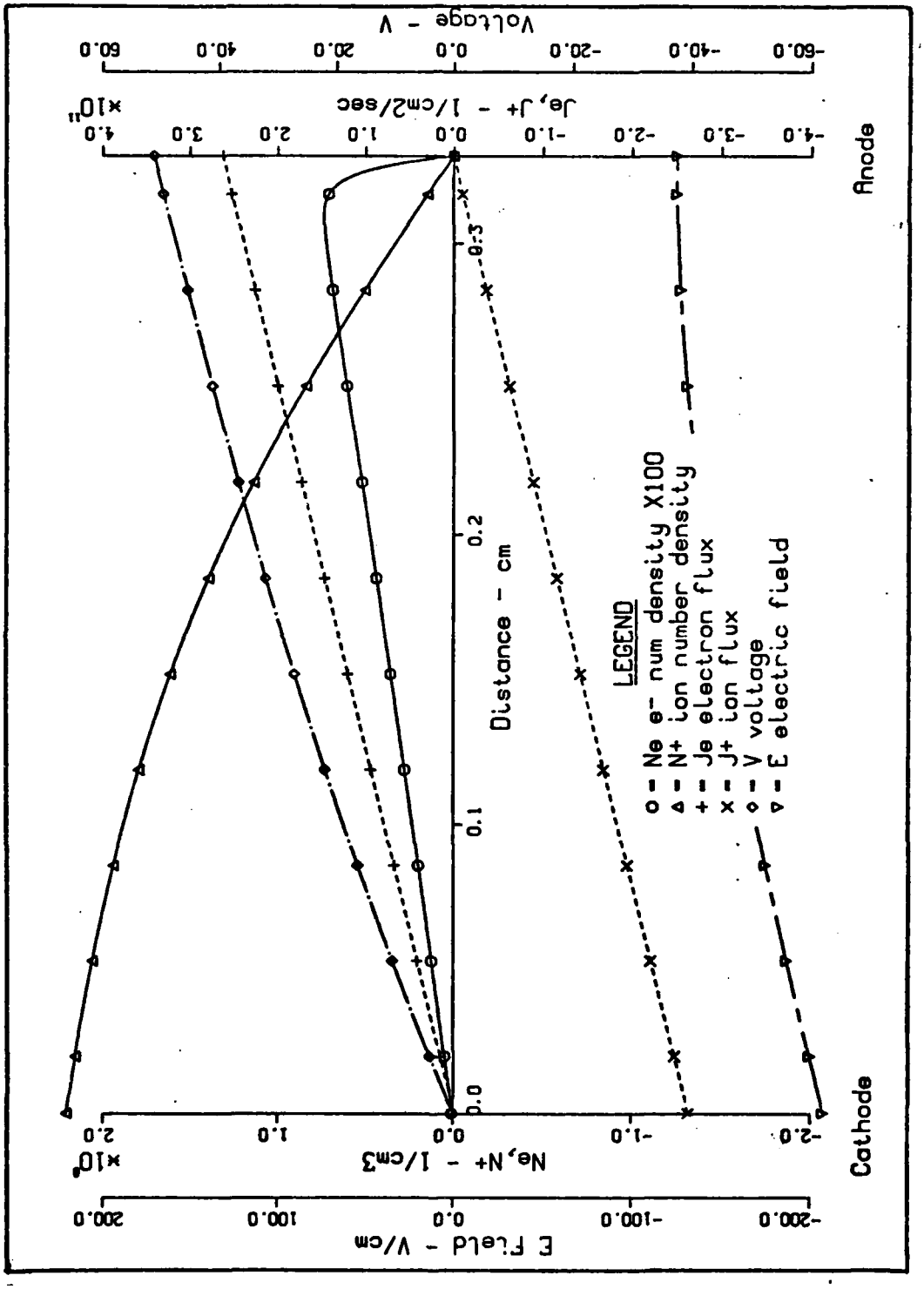

Figure 5. Case I Discharge (Argon, 240 Torr, S = 8 x 10^{11} 1/cm^3/sec, J = .042 μA/cm^2)

described as the discharge voltage for which the cathode sheath thickness, d_c, equals the electrode separation, d. Thus, at voltages for which Townsend ionization is negligible, Case I applies if $d_c \geq d$ and Case II applies if $d_c \leq d$. The regions of applicability of these methods are shown in Fig. 6, which is taken from Lowke and Davies' report.

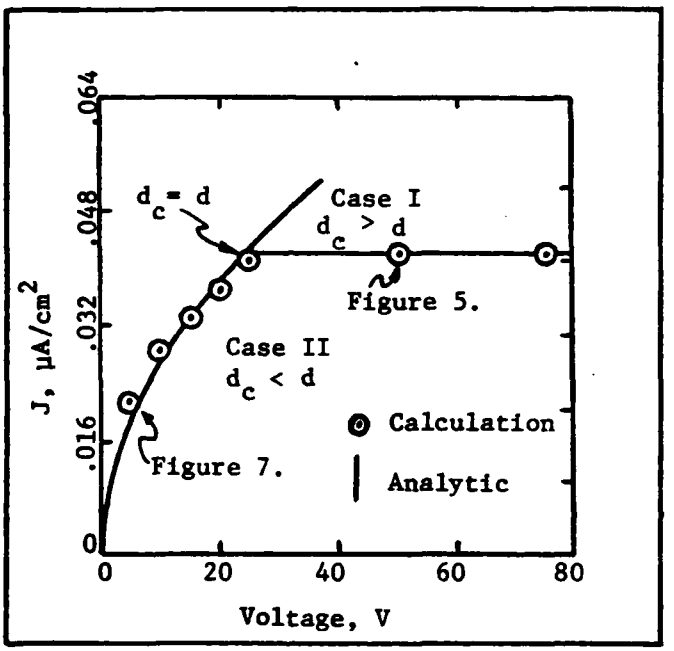

Fig. 6. I-V Characteristic for Case I and Case II ($S = 8 \times 10^{11}$) (Ref. 11:4995)

In order to solve the system of equations (30-33) using the Case I method, a "shooting" technique is used because three boundary conditions are known at the anode and one is known at the cathode. At the anode, as discussed previously, the improbability of positive ion emission requires $j_+ = 0$, which in turn requires that $n_+ = 0$ and $j_e = J/e$. Then, since $n_+ = 0$, Poisson's equation requires, at the anode, that (equation 42):

$$n_e = \frac{-\epsilon_o}{e} \frac{\delta E}{\delta x} \tag{44}$$

Table II

Boundary Conditions

	Cathode	Positive Column C Shth/Pos Col Interface	Positive Column Pos Col/A Shth Interface	Anode
Case I	(E < 0) $j_e = \gamma j_+$ or $n_e = \frac{D_e}{W_e} \cdot \frac{\partial n_e}{\partial x} \approx 0$	not exist		(E < 0) E = trial values V = 0 (arbitrary) $n_+ = 0$ $n_e = \frac{-\epsilon_o}{e}\frac{\partial E}{\partial x} \approx 0$ $j_+ = 0$ $j_e = J/e$
Case II	(E < 0) same as Case I	E = 0 V = 0 (arbitrary) $j_+ = 0$ $j_e = J/e$ n_e = trial values n_+ = function of n_e (equation 47)		(E > 0) $n_e = \frac{D_e}{W_e} \cdot \frac{\partial n_e}{\partial x} \approx 0$
Case III (Low current density)	(E < 0) same as Case I	V = 0 (arbitrary) V = equation 55 E = FLD (j_e/n_e) E = .10 $n_e = n_+ = (S/R_r)^{1/2}$ $j_+ = n_+ k_+ FLD(j_e/n_e)$ $j_e = J/e + j_+$		(E > 0) $n_e = \frac{D_e}{W_e} \cdot \frac{\partial n_e}{\partial x} \approx 0$
Case III (High current density)	(E < 0) same as Case I	V = 0 (arbitrary) V = equation 55 $n_e = n_+ = (S/R_r)^{1/2}$ E = FLD (j_e/n_e) $j_+ = n_+ k_+ E$ $j_e = J/e + j_+$		(E < 0) $n_+ = 0$ $n_e = \frac{-\epsilon_o}{e} \cdot \frac{\partial E}{\partial x} \approx 0$ $j_+ = 0$ $j_e = J/e$

In a Case I discharge, however, $\delta E/\delta x$ at the anode is essentially zero, so that another anode boundary condition is that $n_e = 0$. Also at the anode, the voltage is arbitrarily assigned a value of zero and the field is iteratively assigned values in order to satisfy the cathode boundary condition that $n_e = 0$, or $j_e = \gamma j_+$ if secondary emission is included. Thus, with the total discharge current density (J) the only input parameter, the spatial variation of n_e, n_+, j_e, j_+, E, and V is obtained, with the total voltage drop across the discharge, V_T, calculated by taking the difference between the anode and cathode voltages.

Case II. At voltages below the value for which $d_c = d$, the current in the discharge falls below the saturated value and the spatial variation of the independent variables takes on a form very different from that of a Case I discharge. (See Fig. 7, which duplicates Lowke and Davies' solution for a Case II discharge.) The existence of central maxima in n_e and n_+ is a result of space charge effects, which are much more important than in Case I: while the electric field in a Case I discharge is farily uniform, positive space charges at both the electrodes in a Case II discharge cause the field to be negative near the cathode and positive near the anode. This field reversal forces electrons to the center of the discharge and positive ions to the electrodes, creating maxima in n_e and n_+ at the point where E passes through zero. However, these maxima in the number densities are prevented from becoming a plasma, with $n_e \sim n_+$, because of the "influence of diffusion together with the boundary conditions that $n_e = 0$ at the electrodes (Ref. 11:4995). Because positive ion diffusion is neglected, the number density of positive ions may be expressed as

$$n_+ = \frac{j_+}{K_+ E} \tag{45}$$

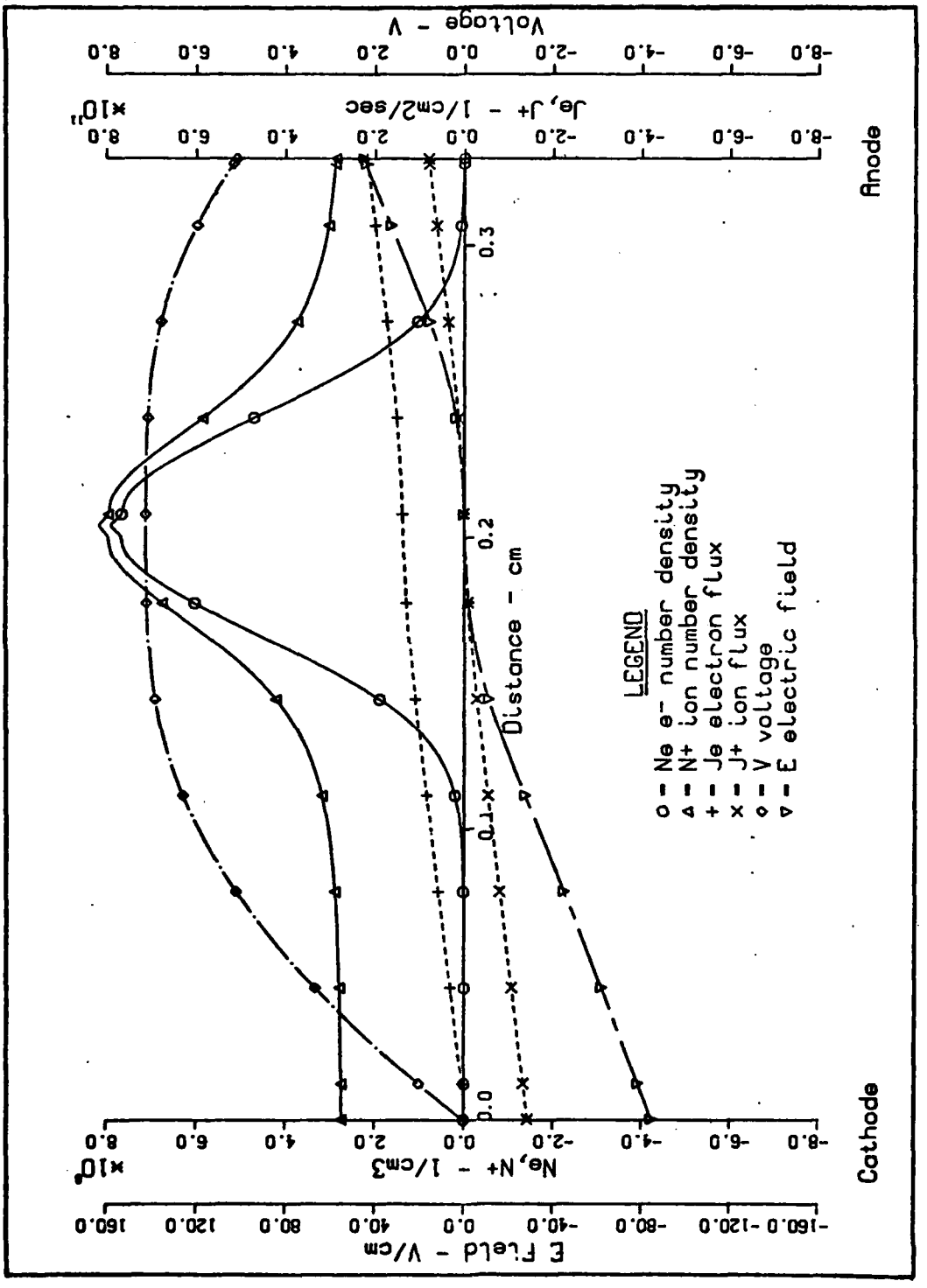

Figure 7. Case II Discharge (Argon, 240 Torr, S = 8 x 10^{11} 1/cm^3/sec, J = .022 μA/cm^2)

Thus, at the point where E = 0, j_+ must also be zero to avoid a singularity in n_+. The value for n_+ at this point is obtained by using L'Hospital's rule:

$$n_+ = \left(\frac{dj_+}{dx}\right) / \left(k_+ \frac{dE}{dx}\right) \tag{46}$$

Making use of the continuity equation for positive ions and Poisson's equation, the expression obtained for n_+ is:

$$n_+ = \frac{(k_+ e/\varepsilon - \gamma) n_e + [(\gamma - k_+ e/\varepsilon)^2 n_e^{\,2} + 4k_+ eS/\varepsilon]^{1/2}}{2k_+ e/\varepsilon} \tag{47}$$

Thus, with a trial value for n_e at this point, n_+ is also determined. In addition, with $j_+ = 0$, j_e must equal J/e. Integrating toward the cathode from this central point, the position of the cathode is defined to be at that point for which $n_e = 0$ or $j_e = \gamma j_+$, depending upon whether secondary emission is allowed or not. Integrating toward the anode, the anode's position is defined to be where $n_e = 0$. The value of n_e at the central point is iteratively varied so that the calculated distance between the anode and cathode is exactly the physical separation of the electrodes (Ref. 11:4999).

Case III. This method, which is applicable at higher current densities and much higher source strengths than the previous two methods, produces two types of solutions determined by the magnitude of the discharge current (see Figs. 8 and 9). In both types, a plasma region is created with $n_e \sim n_+$ and an electric field much less than that in the cathode sheath. At current densities below $1 mA/cm^2$ (for $S = 3.6_{16}$), a constant number density, positive-ion space charge is formed in both the cathode and anode sheaths as a result of the differing drift velocities

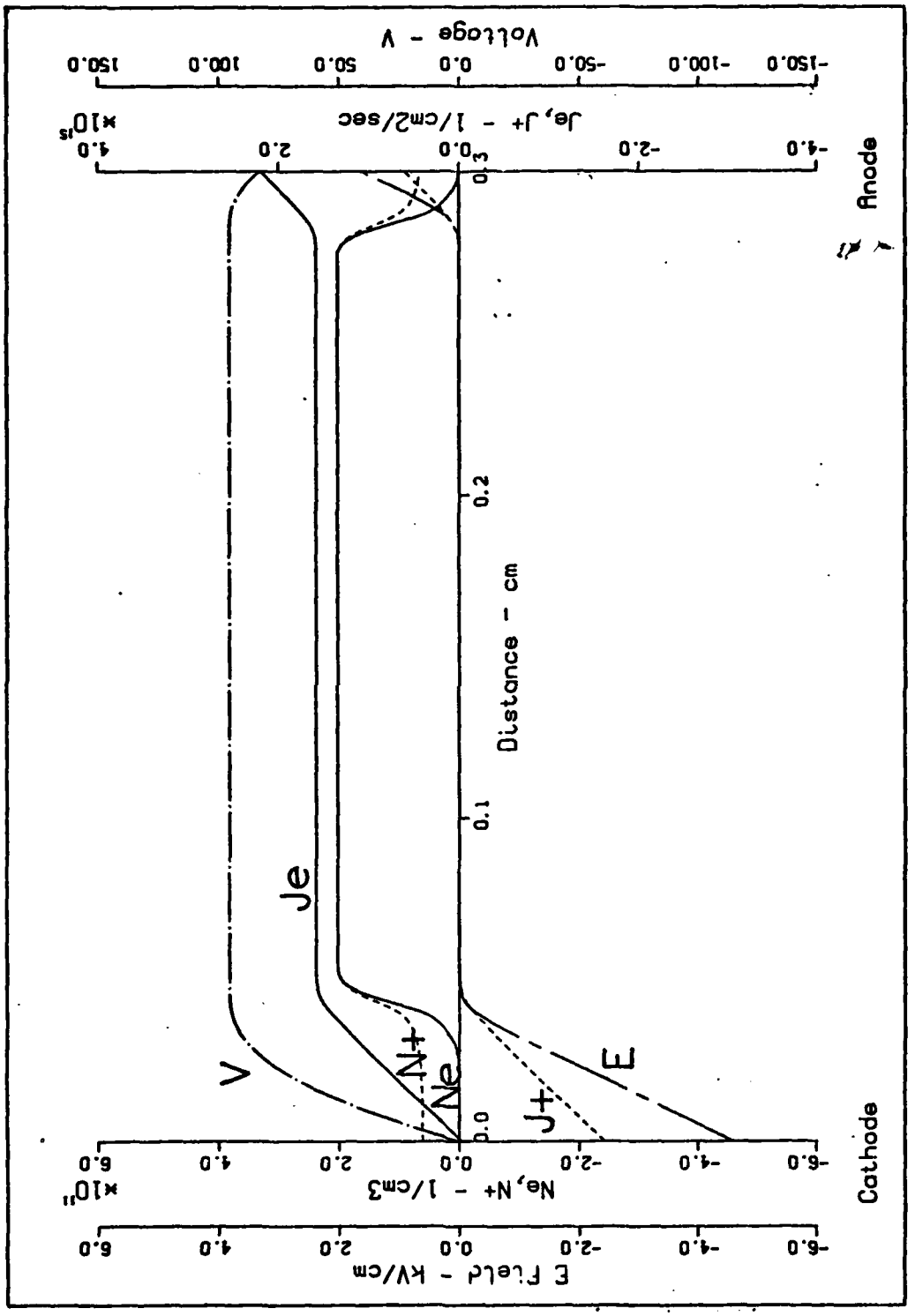

Figure 8. Case III Discharge (Argon, 240 Torr, S = 3.6×10^{16} $1/cm^3/sec$, J = .254 mA/cm^2)

of electrons and positive ions and the relatively weak electric field in the discharge (Ref. 11:4996). However, at current densities above ~25 mA/cm^2, the increased electric field in the cathode sheath causes significant Townsend ionization to occur, producing a positive-ion number density maximum which is greater than the number density in the plasma region. The maximum in n_+ exists because Townsend ionization, which is represented by the term $\alpha|W_e|n_e$, is small near the cathode, where $n_e = 0$, and also near the plasma region, where the electric field strength (and thus the electron drift velocity) is small (Ref. 11:4997). At these high current densities, the electric field is also much stronger in the positive column. This causes a larger portion of the total voltage drop across the discharge to occur in the positive column ($\delta V/\delta x = -E$). In addition, these high fields are able to draw positive ions away from the anode sheath, leaving an excess of electrons there. Thus, the anode sheath has a negative space charge, which drives the field further negative in the sheath and reinforces these tendencies.

For both the low and high current Case III solutions, integration is begun in the positive column, where the values of all of the independent variables can be determined. In the positive column, which is quasi-neutral, the number densities of electrons and ions are assumed to be equal. Also, at the relatively low electric fields in the plasma, Townsend ionization is minimal and the external source's production of electrons and positive ions is balanced solely by recombination losses. Thus, in the plasma:

$$n_e = n_+ = (S/R_r)^{1/2} \tag{48}$$

Also, because of their higher mobility, the electrons in the plasma are assumed to carry the total discharge current density, J,

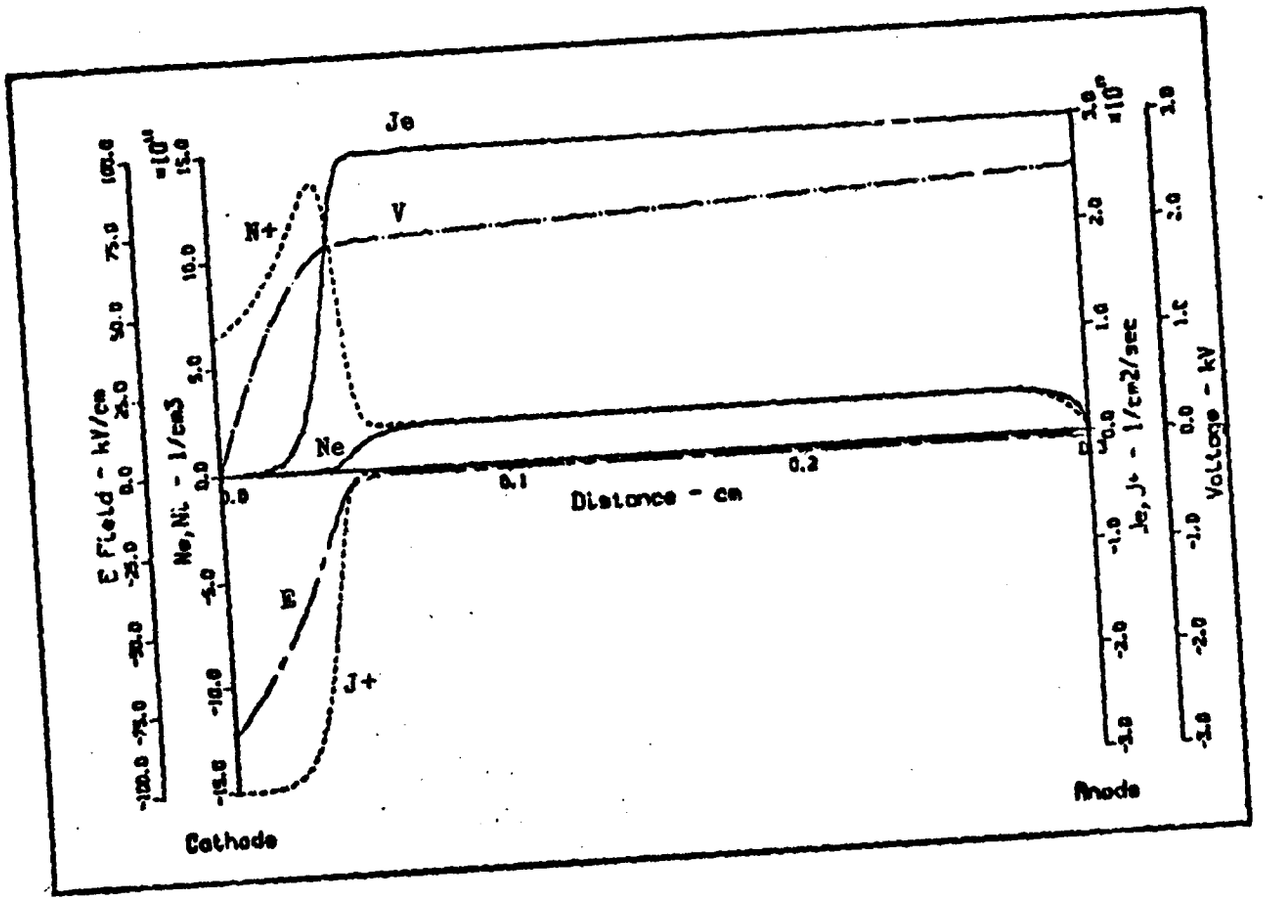

Figure 9. Case III Discharge (Argon, 240 Torr, S = 3.6 x 10^{16} $1/cm^3/sec$, J = 48. mA/cm^2)

$$j_e = J/e \tag{49}$$

at a constant velocity, W_e,

$$W_e = j_e/n_e \tag{50}$$

since the electron number density is uniform throughout the plasma region. Using tabulated values for the drift velocity versus E/N (see Appendix A), the positive column field is also determined. Then, since

$$j_+ = n_+ k_+ E \tag{51}$$

the positive ion current density can be obtained and the electron current density recalculated:

$$j_e = J/e + j_+ \tag{52}$$

Thus, using equations 50 and 51 in 52, an expression is obtained for j_e:

$$j_e = J/e + n_e k_+ FLD(j_e/n_e) \tag{53}$$

where FLD is a tabulated function which gives the electric field for a particular electron drift velocity. This expression is iteratively evaluated until the values converge. Thus, values for all of the independent variables (n_e, n_+, j_e, and E) are determined at the cathode end of the plasma region (see Table II). With these starting values, the cathode sheath region is integrated and the cathode is defined to be at that point where $n_e = 0$, or $j_e = \gamma j_+$, if secondary emission is considered.

The starting values used for the anode sheath integration are determined by the discharge current density. At low current densities ($J \leq 10$ mA/cm^2 for $S = 3.6 \times 10^{16}$), the field in the positive column is also low. Thus, the positive ions produced by the external source are

not removed from the anode sheath, and a positive space charge is formed. This positive space charge causes the electric field to become positive in the anode sheath. Thus, the anode acts as a cathode and the anode boundary conditions are similar to those at the cathode. To start this integration, the field is assigned a very small positive value of .1 V/cm. Then, with the positive column values for n_e and n_+, j_+ is calculated as described previously. Since the total current density is constant, j_e is also determined. With these starting values, the anode sheath is integrated and the anode is defined to be where $n_e = 0$, or $j_e = \gamma j_+$, if secondary emission at the anode is considered. (In this analysis, secondary emission at the anode was not considered, so the boundary condition used in this case was $n_e = 0$.)

In contrast, at high current densities ($J \geq 500$ mA/cm^2 for $S = 3.6 \times 10^{16}$), the anode sheath has a negative space charge and the electric field goes to larger negative values. In this case, the starting value for the electric field at the positive column/anode sheath boundary is just the field value in the positive column. Using the positive column values for n_e and n_+, j_+ and j_e are also calculated. With these starting values, the anode sheath is integrated and the anode is defined to be where $n_+ = 0$.

At intermediate currents, two anode sheath solutions are possible for each value of the discharge current. For one solution, corresponding to the low current density case, the generally negative electric field reverses and goes positive in the anode sheath; for the other solution, corresponding to the high current density case, the field goes further negative in the sheath. Using the low current density method, as the current density is increased, the value of the field at the anode

decreases. At high current densities, this method can no longer produce a solution. Using the high current density method, as the current density is decreased, a solution is obtained only if the starting value for the field is perturbed positively from the positive column value. When the required starting value approaches zero, the set of equations becomes unsolvable (See Figure 10).

To calculate the total voltage drop across a Case III discharge, these different methods of solution had to be considered. Using the high current method for high currents, the field is assumed to be constant throughout the positive column. Thus, since $\delta V/\delta x = -E$, the voltage drop across the positive column, V_p, is

$$V_p = -E_{CS} \cdot d_p \tag{54}$$

where d_p is the length of the positive column and E_{CS} is the value of the field at the cathode sheath/positive column interface. However, the fields at opposite ends of the positive column are different when using the low current method and for low currents when using the high current method. In these instances, it is assumed that the field varies linearly between these values. Thus, the voltage drop across the positive column is reduced, being given by

$$V_p = -E_{CS} \cdot d_p - (E_{as} - E_{CS}) \cdot d_p/2 \tag{55}$$

where E_{as} is the value of the field at the anode sheath/positive column interface and $E_{as} > E_{CS}$.

At intermediate currents, for which both the high and low current density methods produce a solution, the total voltage drop across the discharge can have two different values. As a result, there must be some

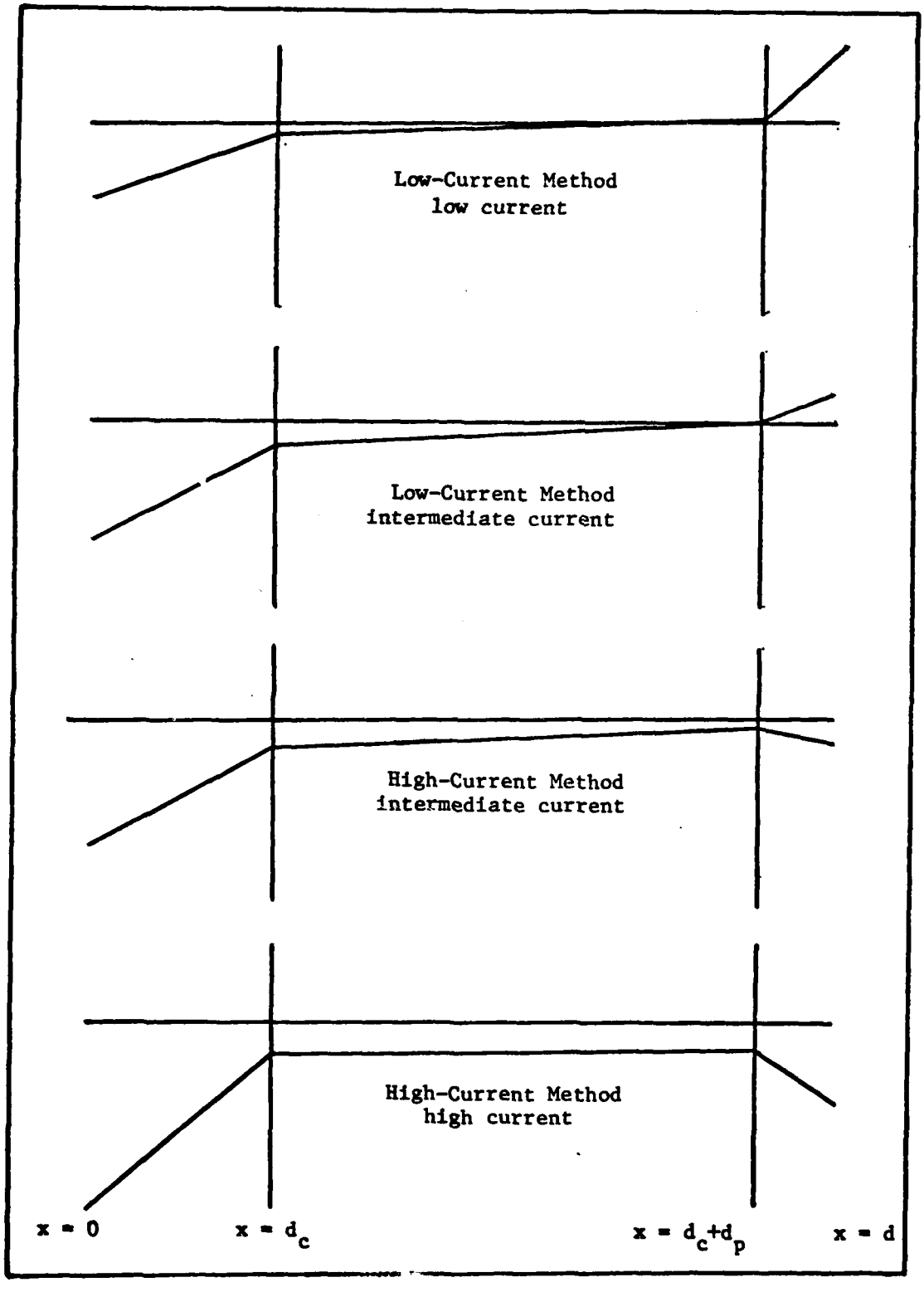

Figure 10. Discharge Electric Field for Variations of Case III Method

criteria to judge which is physically correct. In this investigation, the voltage drop given by the high current density method was used whenever both the high and low current density methods produced a solution. As a result, the voltages chosen were higher than their alternatives, although the difference was usually less than ten percent.

IV. Results

The validity of the computer codes written to model externally-ionized gas discharges was ascertained by comparing their results to the results of Lowke and Davies' calculations. For each of the codes, the spatial variation of the number and current densities, the electric field, and the voltage (the discharge's "profile") was calculated for the same parameters specified by Lowke and Davies. The profile calculated for a Case I discharge is shown in Fig. 5. Although the profile shown nearly duplicates the profile calculated by Lowke and Davies (Ref. 11:4995), there is one major discrepancy. In order to obtain this profile, Lowke and Davies' cathode boundary condition, $n_e = 0$, was relaxed and assumed to be satisfied if $n_e \leq 1 \times 10^4$. Without this modification, the total voltage drop across the discharge was about an order of magnitude too large. The proper boundary condition at the cathode was given previously in equation 37:

$$n_e = \frac{D_e}{W_e} \cdot \frac{\delta n_e}{\delta x} \tag{37}$$

Although this more exact cathode boundary condition was not incorporated in any of the computer codes written, the effect of its neglect was decreased in both Case II and Case III discharges. Their larger electron number densities and gradients allowed the approximate boundary condition of $n_e \approx 0$ to be quite adequate, especially for Case III discharges. However, this particular problem was completely avoided in most of the calculations because the secondary emission boundary condition ($j_e = \gamma j_+$) was usually used at the cathode.

The profile calculated for a Case II discharge also nearly duplicated Lowke and Davies' results (Ref. 11:4995) (See Fig. 7.) In

addition to the error in the cathode boundary condition, the peaks in n_e and n_+ also exhibited a small, sharp, non-physical peak centered on the starting point for the integration. Although this "cosmetic" defect could be overcome simply by taking a larger step at the start of each integration, this defect may be the result of starting conditions at the peak which are not completely consistent.

The validity of the Case III code was checked more thoroughly than the Case I and Case II codes. Both individual discharge profiles and I-V characteristics generated from a large number of profiles were checked against Lowke and Davies' calculated and theoretical results. The profiles obtained for current densities of .254 mA/cm^2 and 48. mA/cm^2, shown in Figs. 8 and 9, were nearly identical to Lowke and Davies' calculated profiles (Ref. 11:4996-4997). Although the cathode discrepancies seen in the Case I calculation were also present in these profiles, their effects were negligible in this case. A profile was also obtained in which electron diffusion was effectively neglected by setting its coefficient to one thousandth of the electron mobility (see Fig. 11). The calculated cathode sheath thickness in this case was 0.0441 cm, which compared very favorably with the thickness of 0.044 cm predicted by Lowke and Davies' theoretical development (Ref. 11:4996).

The effect of diffusion can be seen by comparing Figs. 8 and 11. Ions produced in the plasma region by the source function are lost to recombination. Since these ions never get to the electrodes, they cannot contribute to the total current in the discharge. Diffusion shortens the plasma region and reduces the number of charge carriers which must be produced by Townsend ionization in the sheath. Thus, when diffusion is significant, a smaller sheath field (and voltage drop) are sufficient to supply the charge carriers needed for a given current to flow.

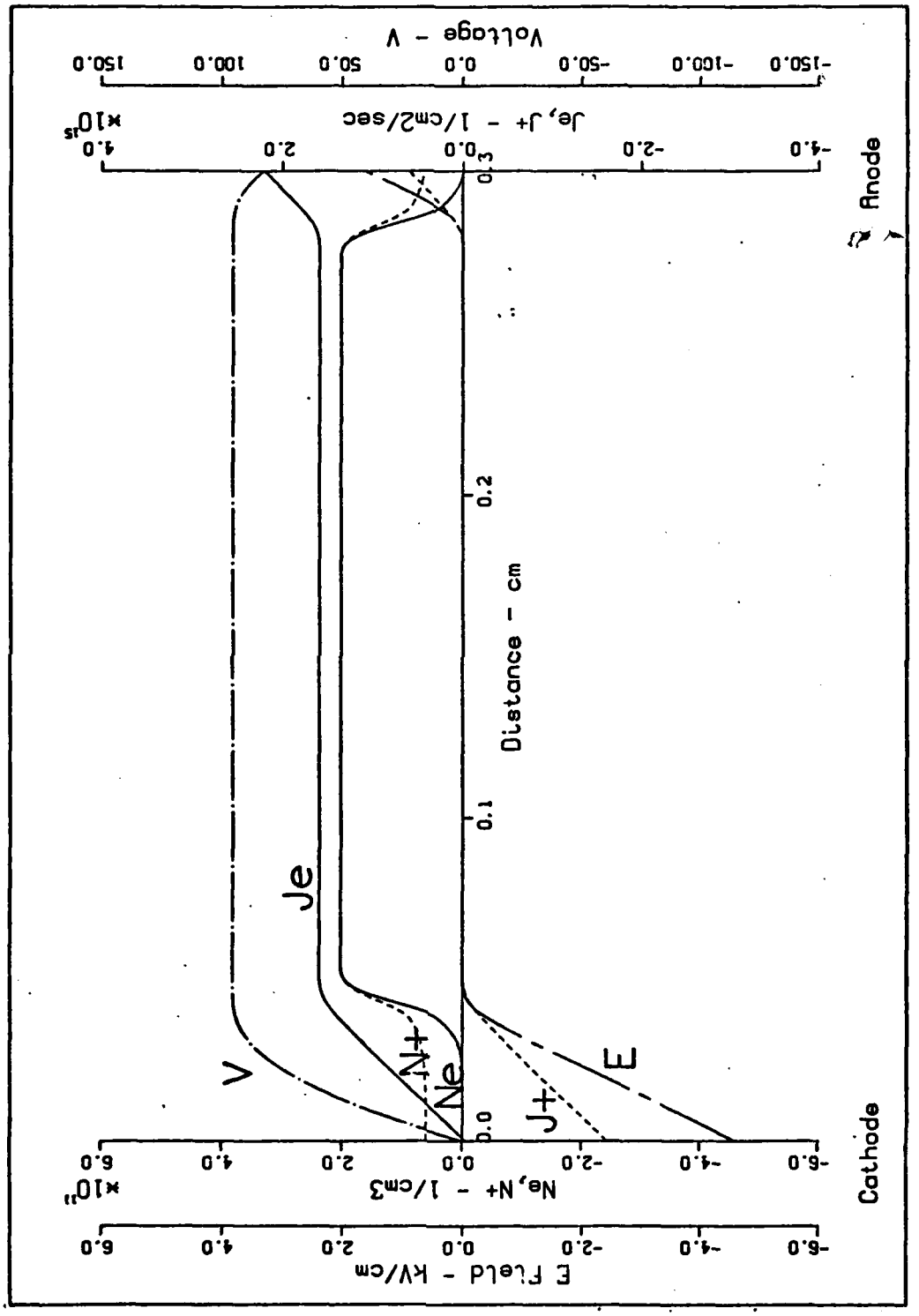

Figure 8. Case III Discharge (Argon, 240 Torr, S = 3.6×10^{16} $1/cm^3/sec$, J = .254 mA/cm^2)

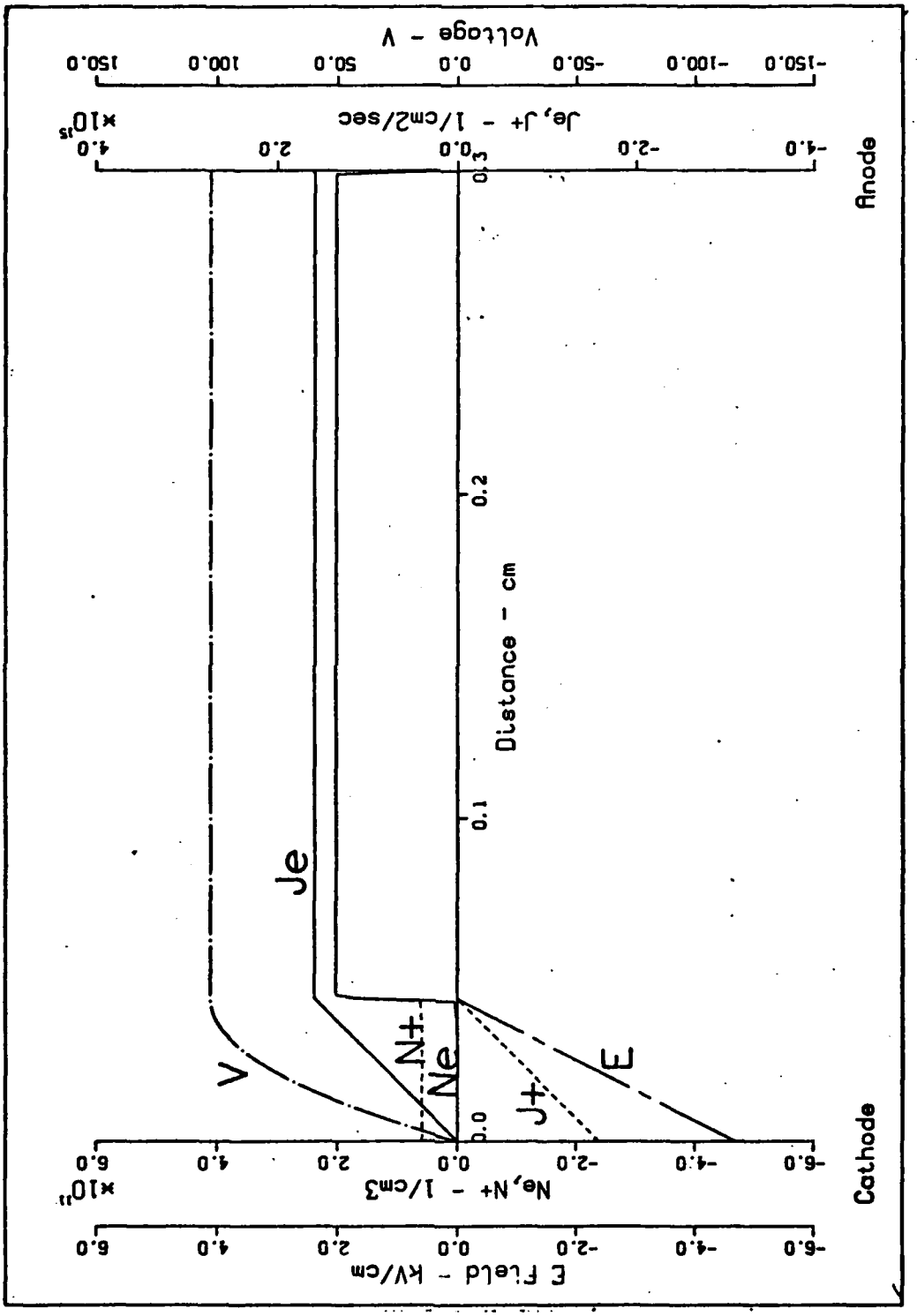

Figure 11. Case III Discharge (Argon, 240 Torr, S = 3.6×10^{16} $1/cm^3/sec$, J = .254 mA/cm^2, D_e = .001 x k_e)

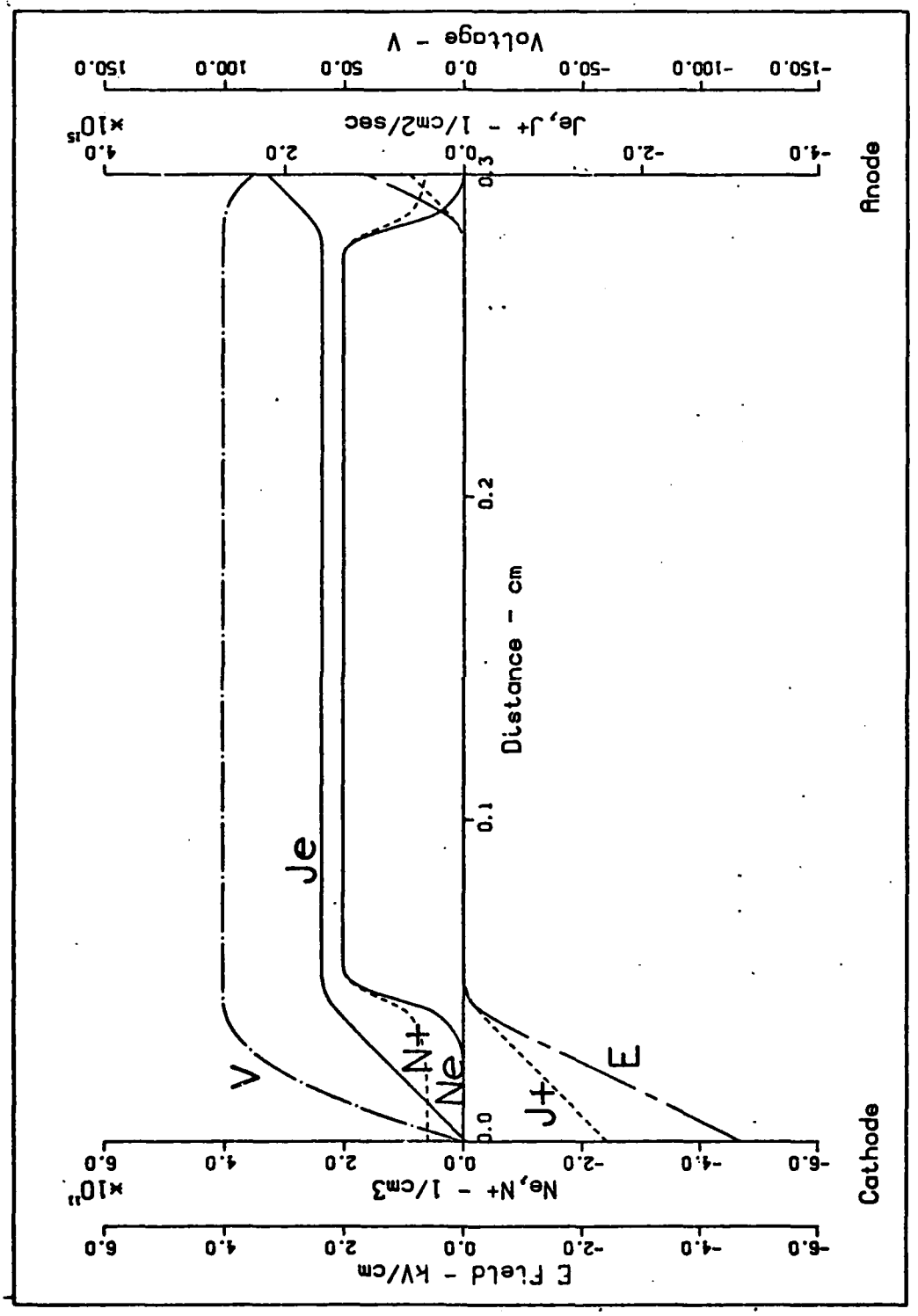

Figure 12. Case III Discharge (Argon, 240 Torr, S = 3.6×10^{16}, J = .254 mA/cm^2, α = 0)

Townsend ionization also decreases the total voltage, particularly at higher sheath field strengths (which occur for higher current densities). This effect can be seen by comparing Figs. 8 and 12. Figure 8 shows the discharge profile for a Case III discharge with both diffusion and Townsend ionization, while Figure 12 shows the profile obtained when Townsend ionization is neglected. The increase in the total voltage when Townsend ionization is neglected (Fig. 12) is most easily observed at the anode, where it is apparent that the cathode fall in this case is larger than in Fig. 8.

These results are summarized for a number of discharge currents in the I-V characteristics shown in Fig. 13. As shown there, with the addition of Townsend ionization, diffusion, or both, the total voltage drop is decreased at each current. Note that the decrease due to Townsend ionization is most pronounced at higher current densities, while the decrease due to diffusion is more pronounced at lower current densities (and therefore lower cathode fields). Although these results agree very closely with those of Lowke and Davies (Ref. 11:4996), both sets of calculations underestimate the voltage drop observed in Leffert's experiments (Ref. 13). Lowke and Davies offered two explanations for this discrepancy. First, the set of equations does not properly account for the diffusion of electrons into a retarding electric field, as in the cathode sheath. Although electrons should lose energy when moving contrary to such a field, the increase in the diffusion coefficient with E/N produces the opposite effect in electrons diffusing from the low field positive column through the high field cathode sheath. Thus, the calculated effect of diffusion is overestimated and the cathode fall is underestimated (Ref. 11:4998). Lowke and Davies also ventured a second

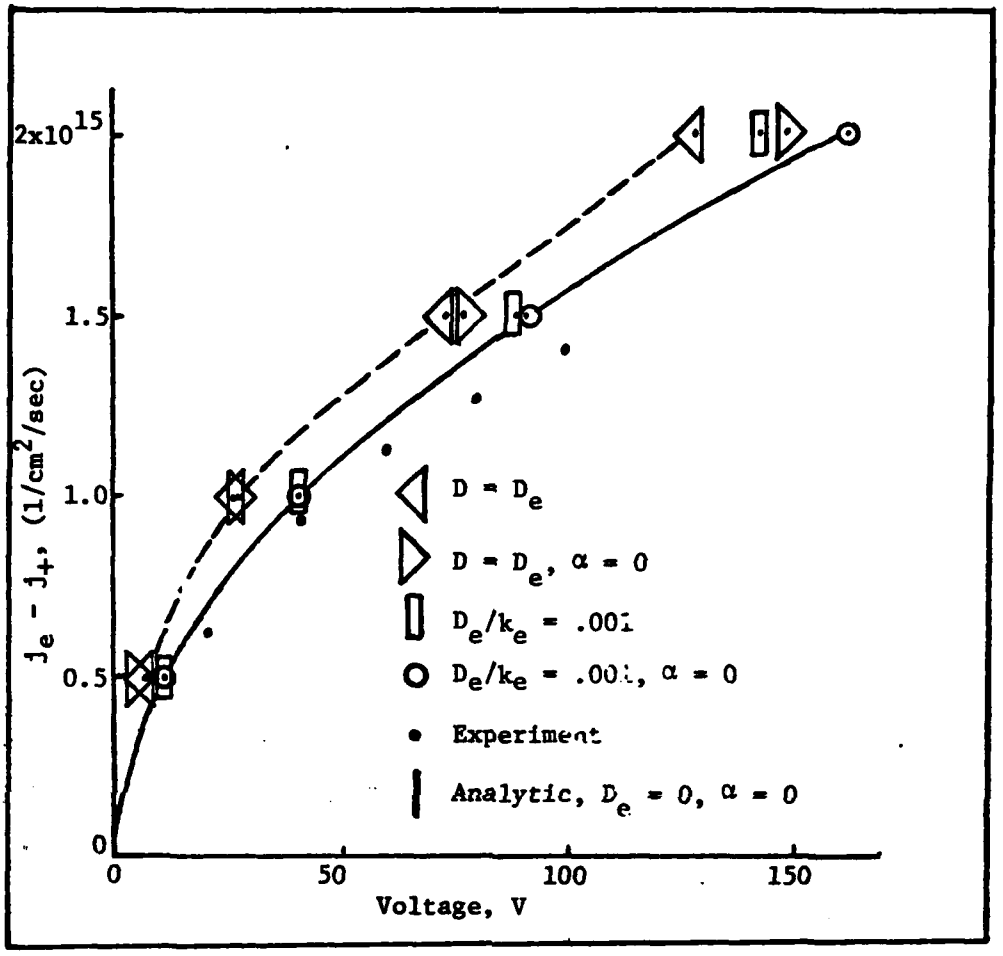

Fig. 13. Calculated and Analytic I-V Characteristics (Argon, 240 Torr, S = 3.6 x 10^{16} 1/cm^3/sec, with and without α and D_e)

explanation based upon nonuniformities in the external ionization in Leffert's gas discharge. (They noted that Leffert's source function at the electrodes was about half of its value at the center of the inter-electrode gap.) (Ref. 11:4996) To see if this second idea could be used to explain the discrepancy between the calculated and experimental I-V curves, the effect of varying the source function was investigated.

Discharge profiles were calculated for an argon discharge at 240 Torr and J = 15 mA/cm^2. Townsend ionization and electron diffusion were

included. The results obtained for three different source strengths are shown in Figs. 14, 15, and 16. At higher source strengths, the cathode sheath is compressed, the cathode fall (and total voltage drop) is decreased, and the electric field at the cathode is decreased. Since the number of electrons in the cathode sheath is larger at higher S, the cathode sheath field need not be as large for the discharge to carry the same current. With a decrease in the field, the voltage drop also decreases since $\frac{\partial V}{\partial x} = -E$. This effect is predicted by Lowke and Davies' analytic solution, although it did not include the effects of ionization or diffusion. The expression they obtained for the total current density in the discharge is

$$J = (4\varepsilon_o k_+ e^3 S^3)^{1/4} V_T^{1/2} \qquad (56)$$

Thus, the total current density is proportional to $S^{3/4}$ and $V_T^{1/2}$, and, at a given current, V_T is proportional to $S^{-3/2}$. However, the voltage drop predicted by this relationship is much larger than that calculated for a current density of 15 mA/cm^2. At this current, ionization in the cathode sheath is substantial, as shown by the peak in n_+. At lower currents, ionization is less important, and Lowke and Davies' relationship is more closely obeyed. I-V characteristics for three different source strengths are shown in Fig. 17. At a current density of .5 mA/cm^2, increasing S by a factor of four decreased V_T to about .13 times its former value, which is close to the value of .125 predicted by Lowke and Davies' relationship. At lower current densities, the decrease in V_T is not as large, so that the relationship between V_T and S is given approximately by $V_T \sim 1/S$. Using this new relationship, the discrepancy between Leffert's experiment and the present calculations can be partially explained. With a 50% decrease in S at the electrodes, or an average

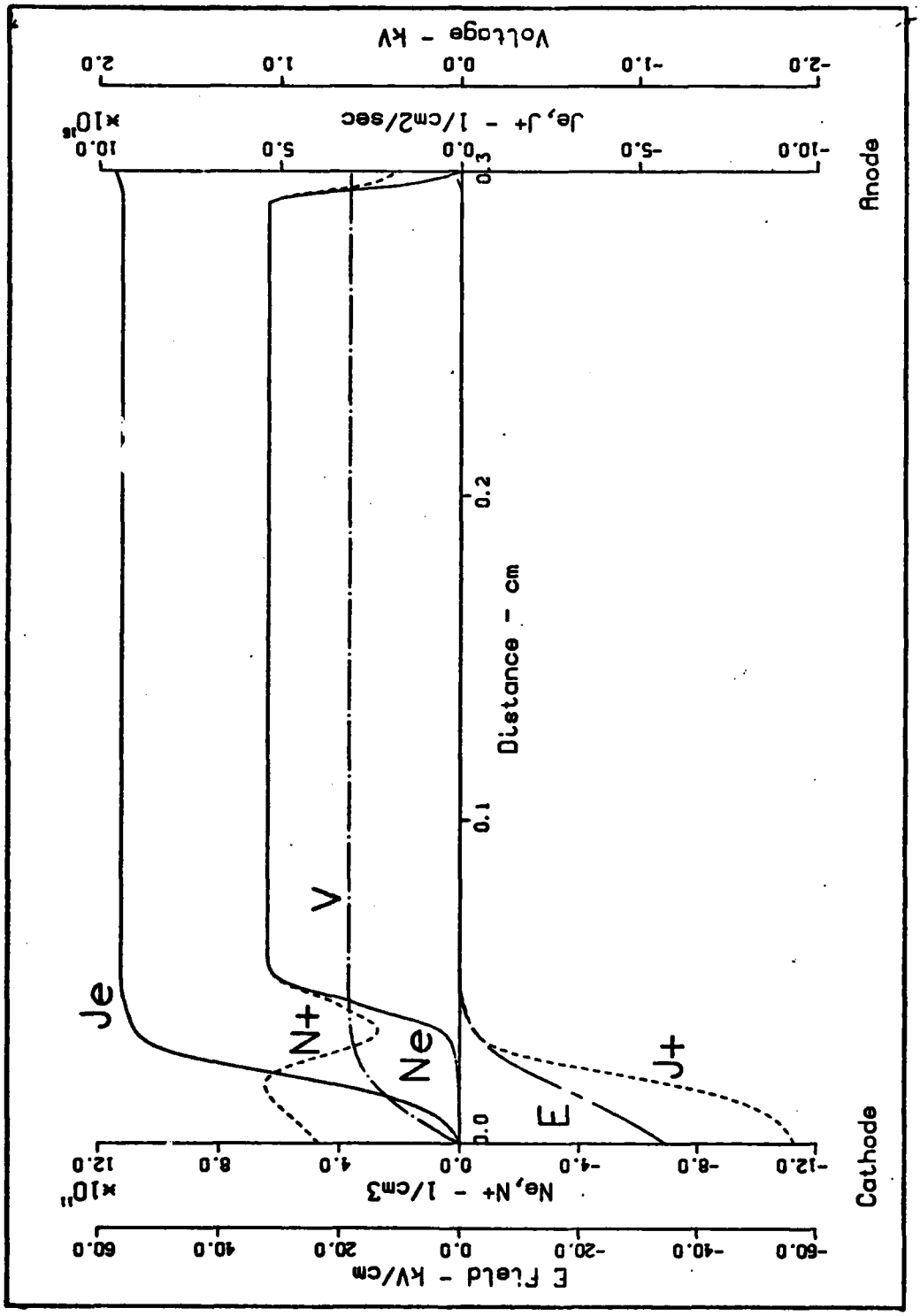

Figure 14. Case III Discharge (Argon, 240 Torr, S = 3.6×10^{17}, J = 15. mA/cm^2)

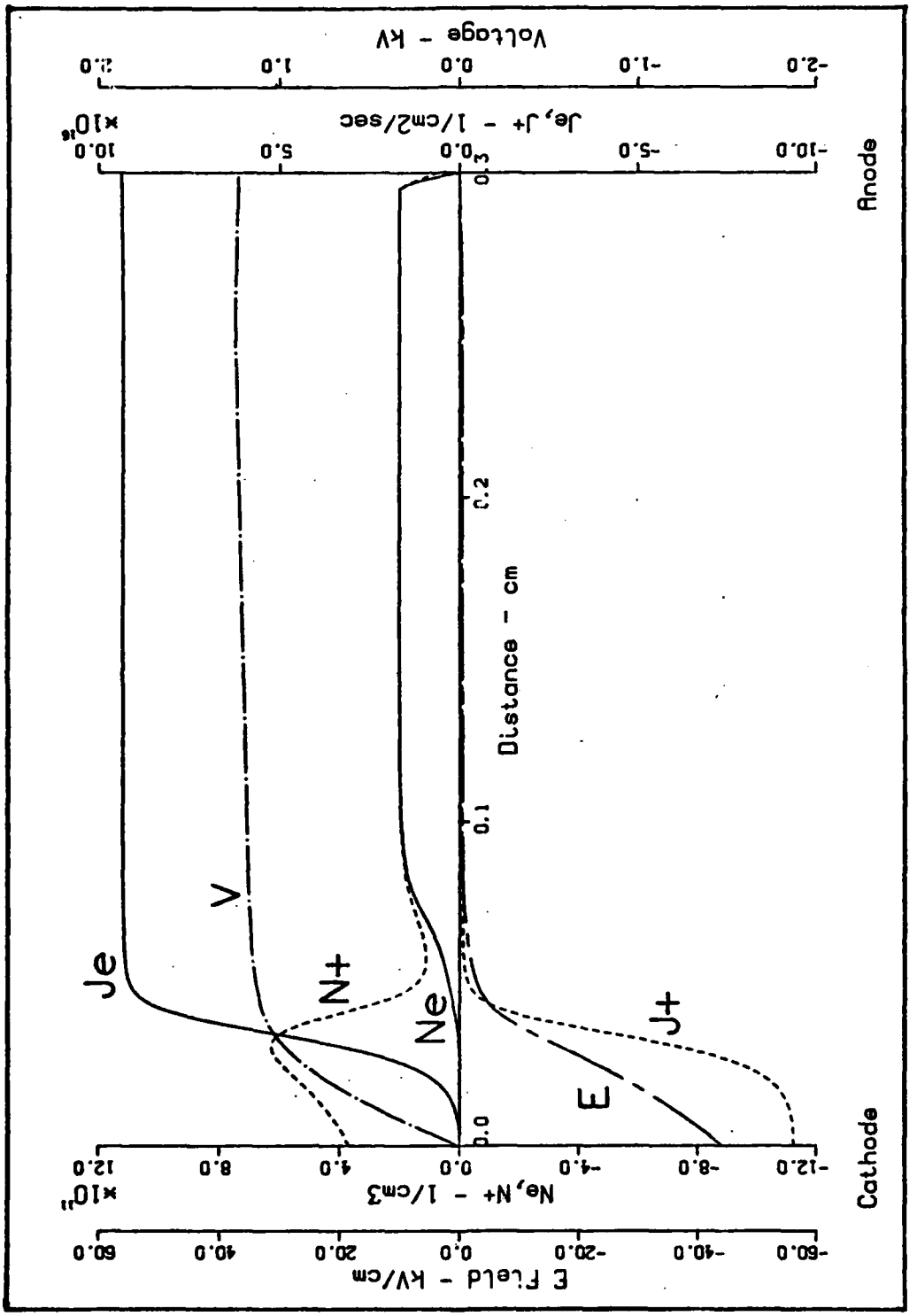

Figure 15. Case III Discharge (Argon, 240 Torr, S = 3.6×10^{16}, J = 15. mA/cm^2)

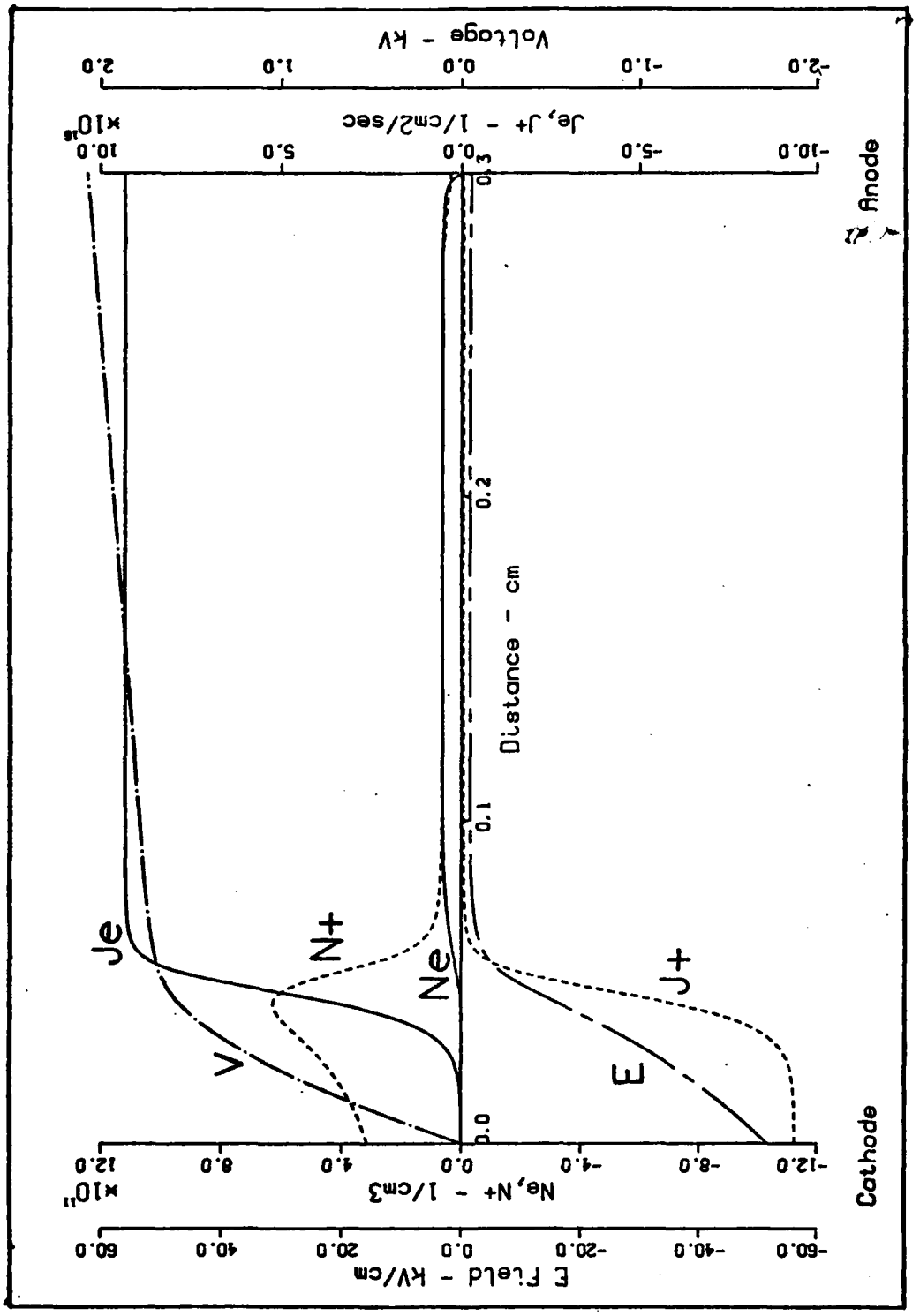

Figure 16. Case III Discharge (Argon, 240 Torr, S = 3.6 x 10^{15}, J = 15. mA/cm^2)

of about 58% within the cathode sheath (using a sheath thickness of .044 cm), and assuming $V_T \sim 1/S$, the predicted increase in voltage is approximately 1.72. Extrapolating the experimental I-V curve in Fig. 13 to 2×10^{15} $1/cm^2/sec$ (.32 mA/cm^2), the expected experimental voltage is approximately 1.67 times the calculated value, which agrees favorably with the predicted increase.

However, the reason for this departure from Lowke and Davies' theory is not completely understood. The source strength does affect the processes of ionization and diffusion. These processes could have opposite effects upon the voltage drop in the cathode sheath, and also, therefore, upon the total discharge voltage. At various current densities, one of these effects could be dominant, which could explain the departure from the relationship between V_T and S predicted by Lowke and Davies, who neglected these effects.

At increased source strengths, the effect of collisional ionization is decreased, as can be seen in Figs. 14, 15, and 16. The peak in the positive-ion number density, which is a direct result of ionization in the sheath, changes little in magnitude for different source strengths. As S is increased, greater numbers of electrons diffuse into the cathode sheath and more electron-ion pairs are produced in the sheath, so that ionization need not supply as many electrons and ions as before in order to carry the same current. Thus, the cathode field is reduced and the maximum in n_+ is reached nearer to the cathode. Adjacent to the positive column, in the region known as the negative glow in glow discharges, recombination occurs as the electrons lose energy. At higher source strengths, the cathode field is smaller and larger numbers of electrons are present in this region. Thus, recombination increases and the number

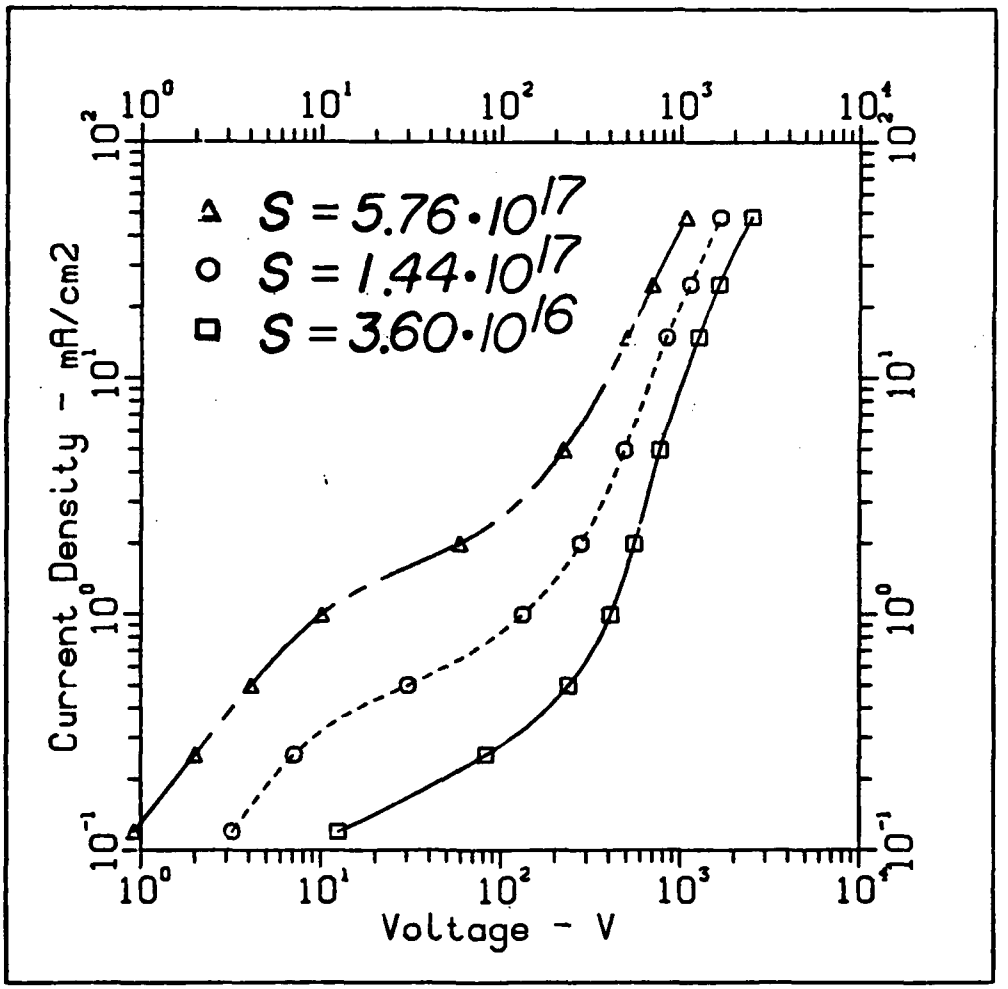

Figure 17. Calculated I-V Characteristics for Three Source Strengths (Argon, 240 Torr)

density of positive ions is reduced. This effect is more pronounced at higher source strengths, as can be seen by comparing the cathode sheath minima in the n_+ profiles in Figures 14, 15, and 16. At these higher source strengths, the cathode sheath field is reduced, Townsend ionization is thereby decreased, and a greater portion of the discharge current is due to the external source. Thus, the conductivity of the discharge is more completely controlled by the external source. However, the large energies invested in producing these high source strengths reduces the gain in switching applications. High-gain switching seeks to make use of the weakest source able to sustain a high-current discharge, forcing the cathode sheath to generate the necessary charge carriers.

One method of increasing the effectiveness of the cathode sheath in achieving this goal is by coating the cathode with a material which has a high secondary emission coefficient in the gas being used. With an increase in γ, the electron current density (and thus the electron number density) at the cathode is increased. The effect of these additional electrons is magnified by the cascade of ionization which each produces. Thus, the cathode field required to produce the additional required electrons and ions is reduced. Consequently, a given current can be carried at a much lower total discharge voltage. This effect can be seen by comparing Fig. 18, with no secondary emission, to Fig. 19, which includes a 2% secondary emission coefficient at the cathode. The peak in n_+, which is a result of Townsend ionization in the sheath, is shifted nearer the cathode as γ is increased. As a result, an increase in γ causes a decrease in the cathode fall voltage. (Note the shift in the voltage profile from Fig. 18 to Fig. 19.) For discharges in which electrons and ions are produced solely by Townsend ionization, von Engel predicts a

linear relationship between the cathode fall and the natural logarithm of γ (Ref. 10:1077). As shown in Fig. 20, this is nearly the case for low source strengths. However, at higher source strengths, the effect of Townsend ionization is decreased and small values of γ do not appreciably decrease the cathode fall. Thus, larger values of γ are required for ionization effects to come into play. At the source strengths required in electron-beam controlled switches, the cathode fall voltage is relatively insensitive to the secondary emission coefficient. However, some gas/electrode material combinations have unusually high secondary emission coefficients (e.g. for cesium electrodes in argon, γ = .4 electrons per incident metastable argon atom) (Ref. 17:84). In these instances, the decrease in cathode fall voltage could be considerable.

This decrease in voltage with increasing γ is shown by the I-V characteristics in Fig. 21. As predicted by Lowke and Davies, secondary emission of electrons from the cathode causes the I-V characteristic to rise more rapidly with an increased γ. However, at current densities below a certain value (.3 mA/cm^2 in Fig. 21), ionization is minimal and the cathode fall is nearly the same as with $\gamma = 0$.

All of the I-V curves in Fig. 21 were calculated using the constant recombination rate coefficient given by Lowke and Davies (Ref. 11:4994). Because this value significantly overestimates the magnitude of this coefficient in the cathode sheath, the influence of including the functional dependence of the recombination rate on E/N was investigated. Two functional forms were considered for argon, while only one function was used for methane. One of the argon recombination coefficients was for Ar^+ ions, while the other was for Ar_2^+ ions. The total discharge voltages obtained using these functions differ by less than one percent

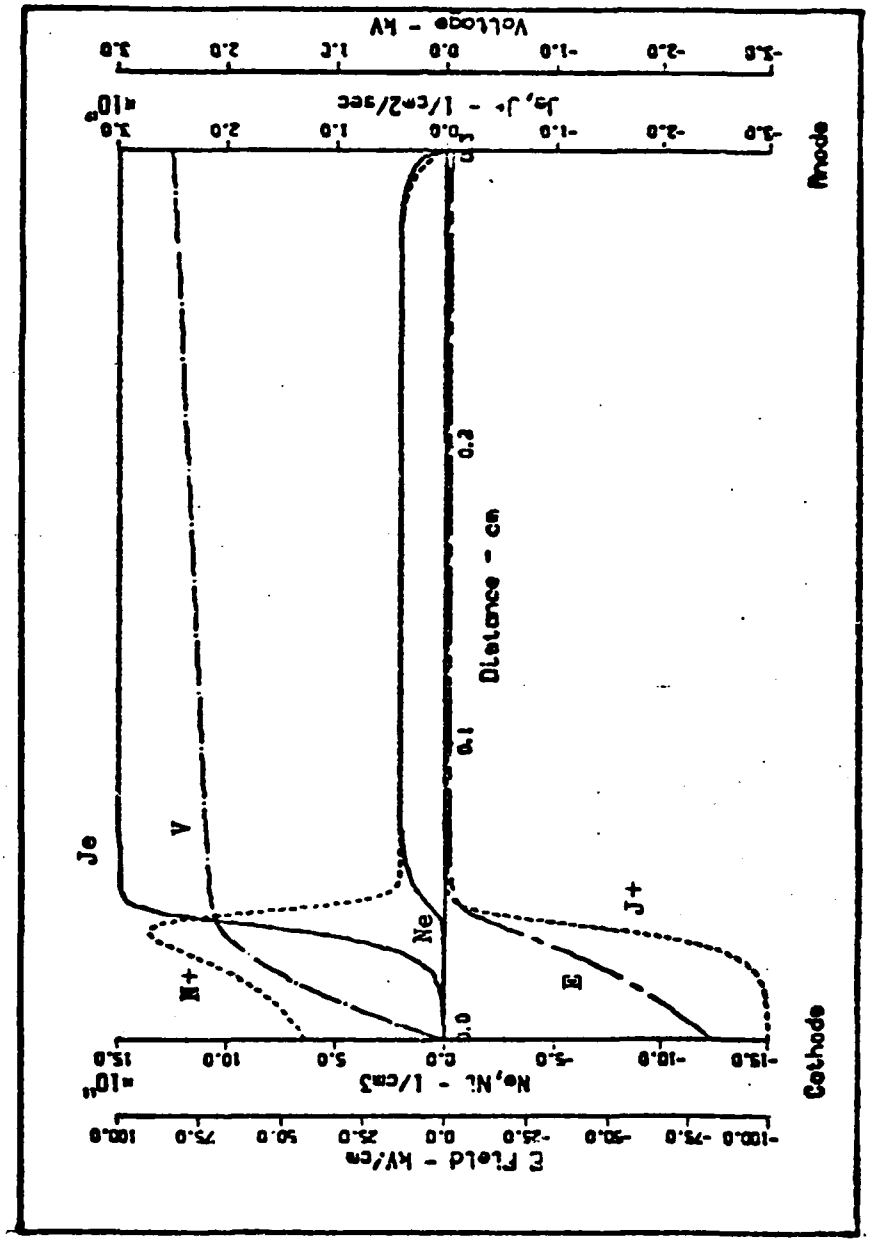

Figure 18. Case III Discharge (Argon, 240 Torr, S = 3.6×10^{16}, J = 48 mA/cm^2)

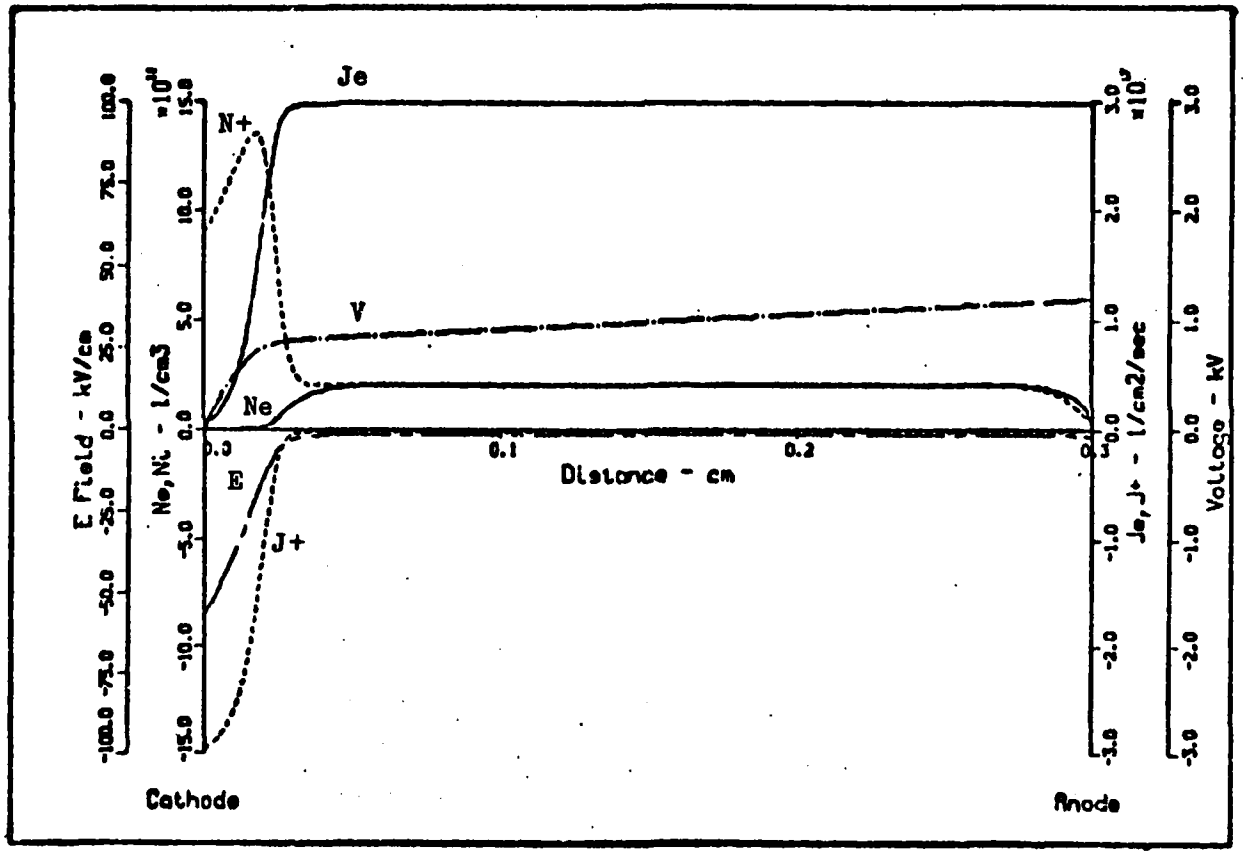

Figure 19. Case III Discharge (Argon, 240 Torr, S = 3.6 x 10^{16}, J = 48 mA/cm^2, γ = .02)

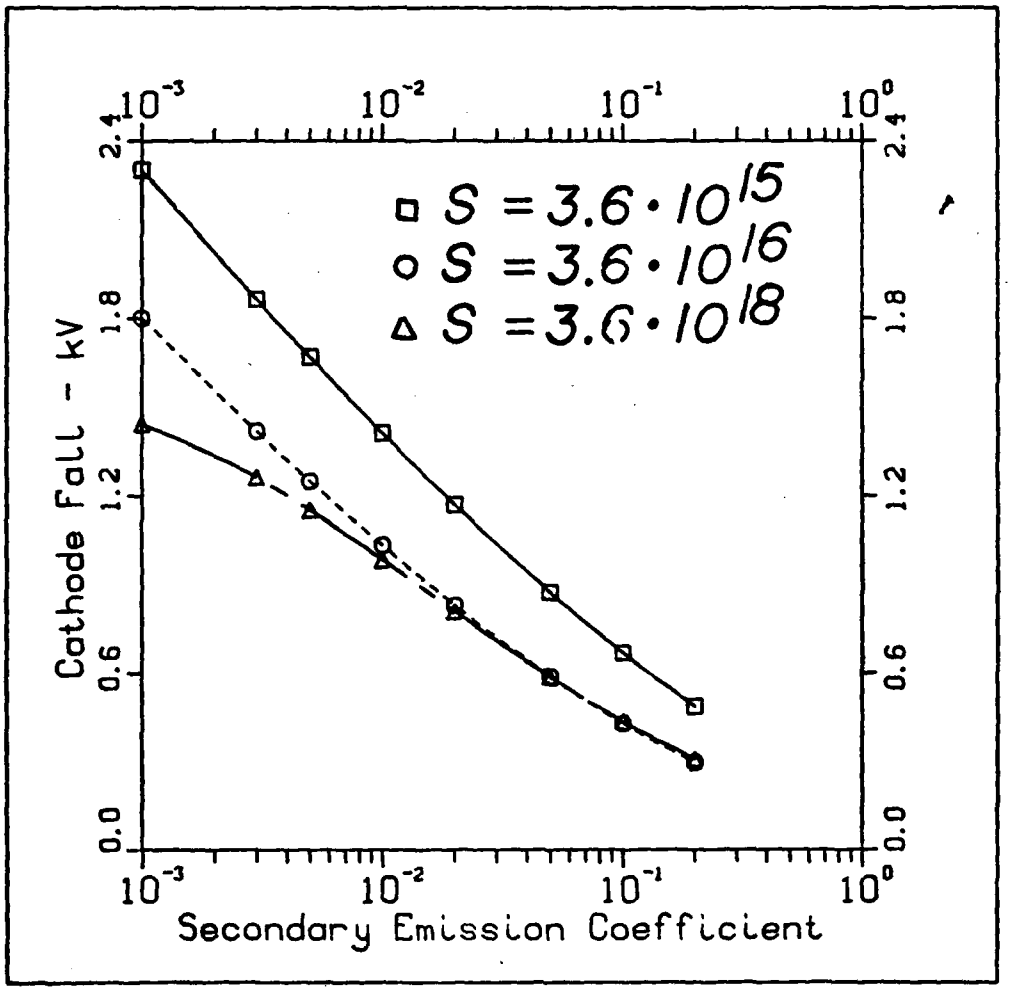

Figure 20. Cathode Fall Versus Secondary Emission Coefficient (Argon, 760 Torr, J = 500. mA/cm^2)

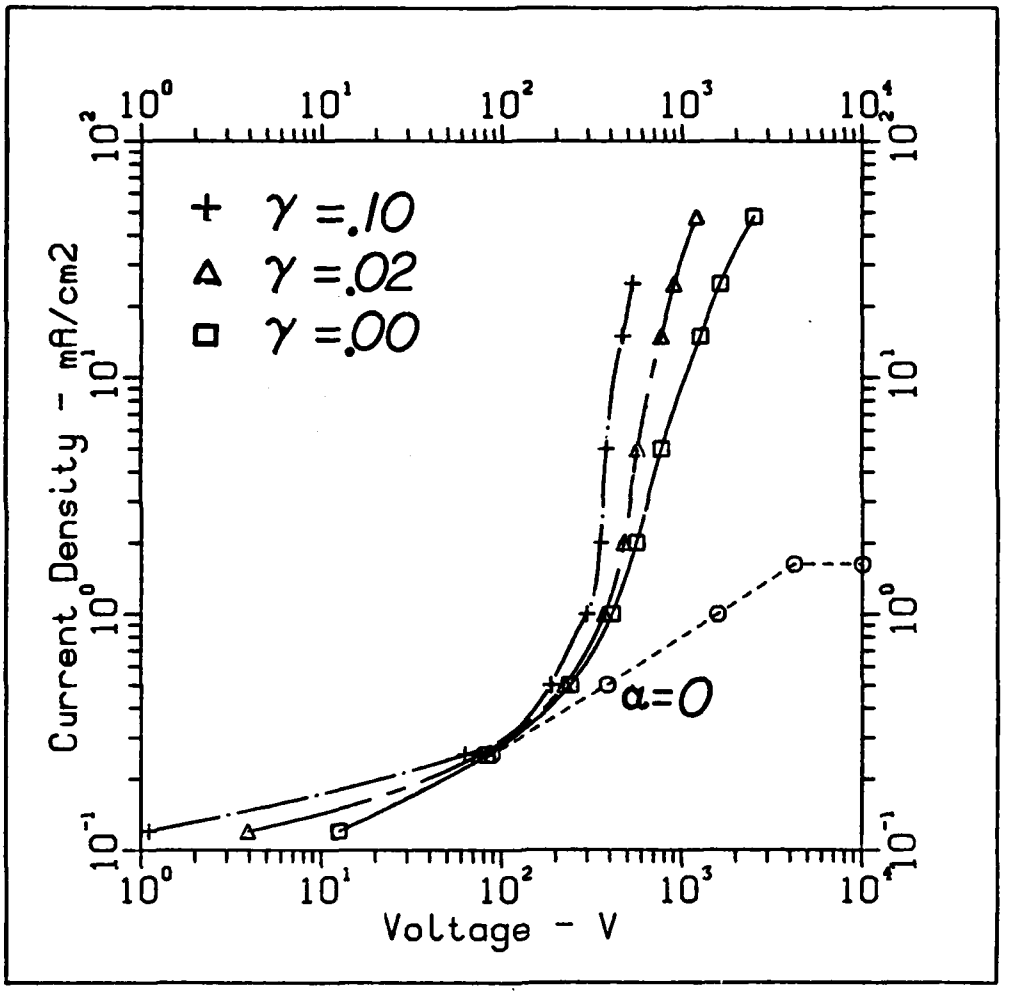

Figure 21. Calculated I-V Characteristics for Three Secondary Emission Coefficients (Argon, 240 Torr, S = 3.6×10^{16})

(only current densities below 48 mA/cm^2 were investigated), and both are less than five percent below the values obtained using a constant R_r characteristic of 300°K $A_{r_2}^+$ ions (See Appendix A). Although this result seemingly vindicates Lowke and Davies' assumption of a constant R_r, the functional form for A_r^+ ions was used for many of the calculations because it can be calculated more easily than the coefficient for $A_{r_2}^+$ ions. (See Appendix A.) However, the recombination coefficient's E/N dependence requires an iterative approach to obtain self-consistent starting conditions at the positive column interfaces with the sheaths. At high discharge current densities (field strengths), the rapid variation of the variables involved makes this calculation very unstable. In those instances in which a self-consistent set of parameters could not be found in this way, a large, constant R_r was used to start the integration, while subsequent calculations in the integration used the functional form of R_r.

Using this technique, or using a constant R_r, the argon I-V characteristics of Lowke and Davies were extended to higher current densities and expanded to include additional effects. These I-V characteristics were compared qualitatively to similar calculations by Zakharov, et.al. (Ref. 10:1077), and directly to experimental data by Bletzinger (Ref. 5:1-2). All of these calculations were done at 760 Torr with an electrode separation of .3 cm, no metastable ionization, and with $\gamma = .02$. The results obtained are shown in Figs. 22 and 23. At low current densities, almost the entire voltage drop in the discharge occurs in the cathode sheath and the discharge current density increases relatively slowly with increasing voltage (region AB in Figure 23). At a particular "ignition" voltage, however, there is a sharp increase in the

slope of the I-V curve. Beyond this ignition voltage the discharge current density increases rapidly (region CD in Figure 23) for small increases in the total discharge voltage. This sharp increase in the current density is due to the rapid increase of Townsend ionization in the cathode sheath at these currents and voltages. In this current density/voltage regime, the discharge current density is determined primarily by the mobility and density of electrons in the plasma region, and is approximately proportional to the total discharge voltage. As a result, the electric field in the positive column must increase to keep pace with the required increase in current density. (The number density of electrons, the primary current carriers in the positive column, is not allowed to increase since it is assumed that $n_e = (S/R_r)^{1/2}$.) With a larger electric field, the voltage drop across the positive column also increases, becoming comparable to the cathode fall voltage. At very high current densities, the cathode fall becomes negligible compared to the positive column voltage drop. The cathode fall may also be negligible at intermediate currents if the interelectrode gap is substantially increased.

The transition from the low to high conductivity regions occurs smoothly for large external ionization source strengths. However, at lower source strengths, regions of negative differential conductivity occur, as in curve BC in Figure 23. In this I-V regime, the effective resistance is negative as the discharge reconfigures itself into a more efficient operating mode. This behavior is similar to that of a subnormal discharge, as described previously, in the transition to a stable, glow discharge. Also, the subsequent rapid rise in current density is similar to that observed in normal glow discharges (See Fig. 1). These regions of negative differential conductivity at low

current densities and source strengths were also observed in similar calculations by Velikhov (Ref. 28:593) and Zakharov (Ref. 10:1077) for N_2 discharges. Although Zakharov maintained that this region was not physical and could not be measured experimentally, Averin et.al. reported such a measurement in 1980 (Ref. 7). Zakharov described this region of negative differential conductivity as an unstable "transition region between a low-current discharge (in which the charges are produced only by the external ionization source) and a discharge in which the cathode sheath which is formed is an electron emitter" (Ref. 10:1077). As mentioned previously, this negative-differential conductivity region vanishes at higher ionization source strengths. For large S, the effect of Townsend ionization at low current densities is reduced because, as seen in Figs. 14, 15, and 16, the cathode sheath field and the sheath thickness are also reduced. Thus, large source terms "smooth" the transition from external ionization to Townsend ionization.

The Case III method was used to obtain the argon I-V characteristics in Figures 22 and 23. The low current density variation of Case III was used for current densities up to 48 mA/cm^2, while the high current density variation was used at higher currents. Thus, the observed regions of negative differential conductivity are not simply a result of using different variations of the Case III method. Also, because only this method was used to obtain the I-V characteristics, the curve for S = 3.6×10^{14} in Figure 23 is incomplete. At this low source strength, the Case III method is not applicable at low current densities, as explained previously. Thus, this characteristic could be completed at low current densities by using the Case II method.

In order to experimentally observe this negative differential conductivity region, the external circuit load line must be shallow enough to avoid simultaneous operation at more than one point of the discharge's I-V characteristic (See Fig. 3). To accomplish this, a very large circuit resistance must be used, as was done by Averin et.al. (Ref. 7) for discharges in nitrogen.

Bletzinger (Ref. 5:2) was also able to observe this negative differential conductivity region for discharges in argon at 760 Torr. The I-V characteristics which he obtained at two different source strengths (produced by an external electron beam), are compared with the calculated characteristics in Fig. 23. Although Bletzinger's electrode separation was 2.2 cm, while the electrode separation in the calculational model was only .3 cm, it is still reasonable to compare these characteristics. In Bletzinger's experiment, the positive column field was measured to be less than .01 Townsend. As a result, the cathode fall constituted nearly the entire discharge voltage. In the computational model, with an electrode separation less than 15% of the experimental model, most of the discharge voltage drop will occur in the cathode sheath only if the current density is below 25 mA/cm^2. Thus, the inconsistency between calculation and experiment which is observed in the positive column (i.e. the calculated positive column field is much larger than the observed field) has a minimal effect when the comparison is restricted to low current densities and small electrode separations. As the current density is increased, the calculated positive column field must increase and the unphysical behavior of the model's positive column in accentuated.

Comparing the calculated characteristics (Fig. 23), at source strengths of $3.6 \cdot 10^{15}$ and $3.6 \cdot 10^{16}$, to Bletzinger's characteristics

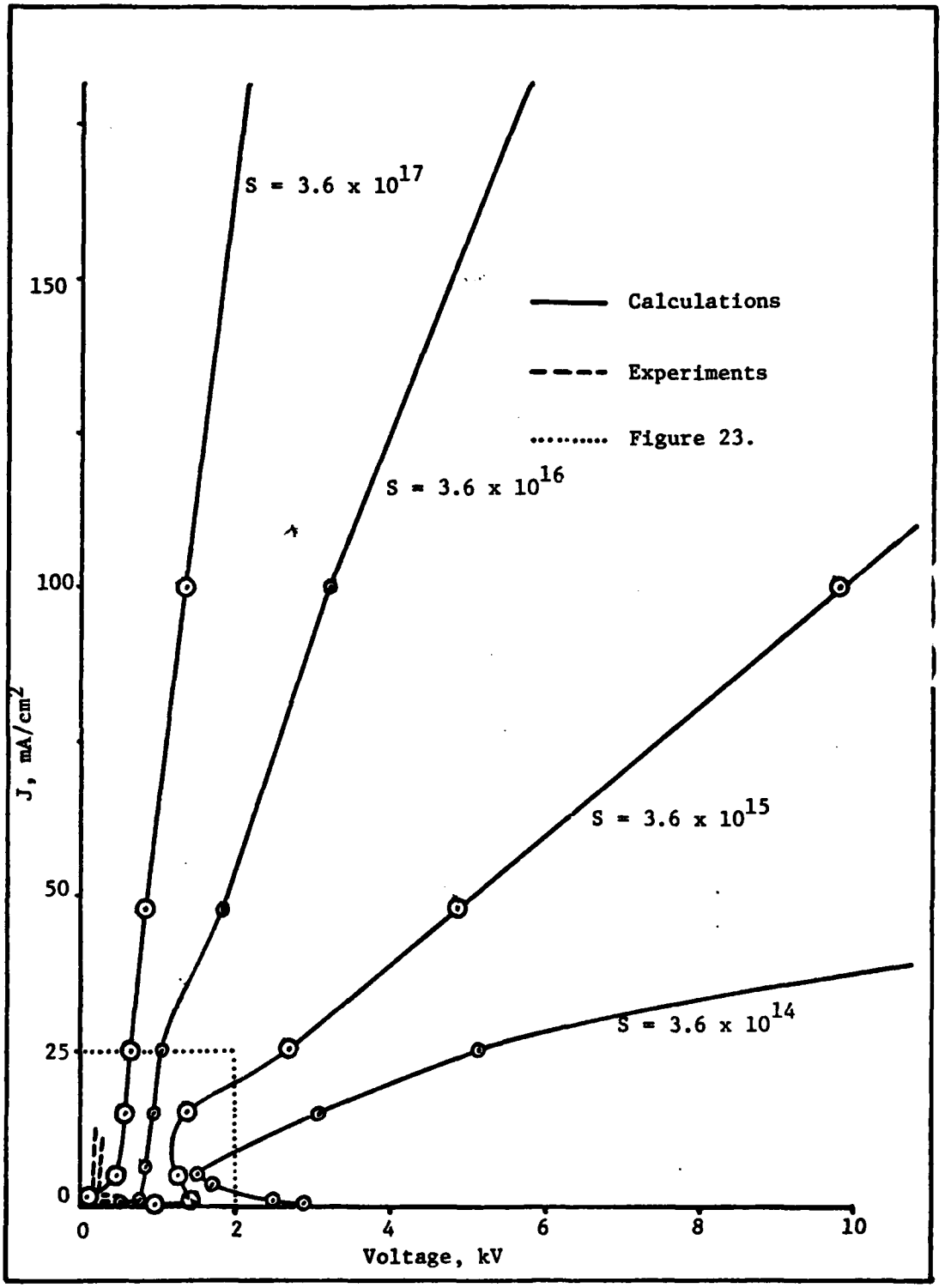

Figure 22. I-V Characteristics-Calculated for an Argon Discharge (760 Torr, γ = .02, d = .3 cm, no metastable ionization)

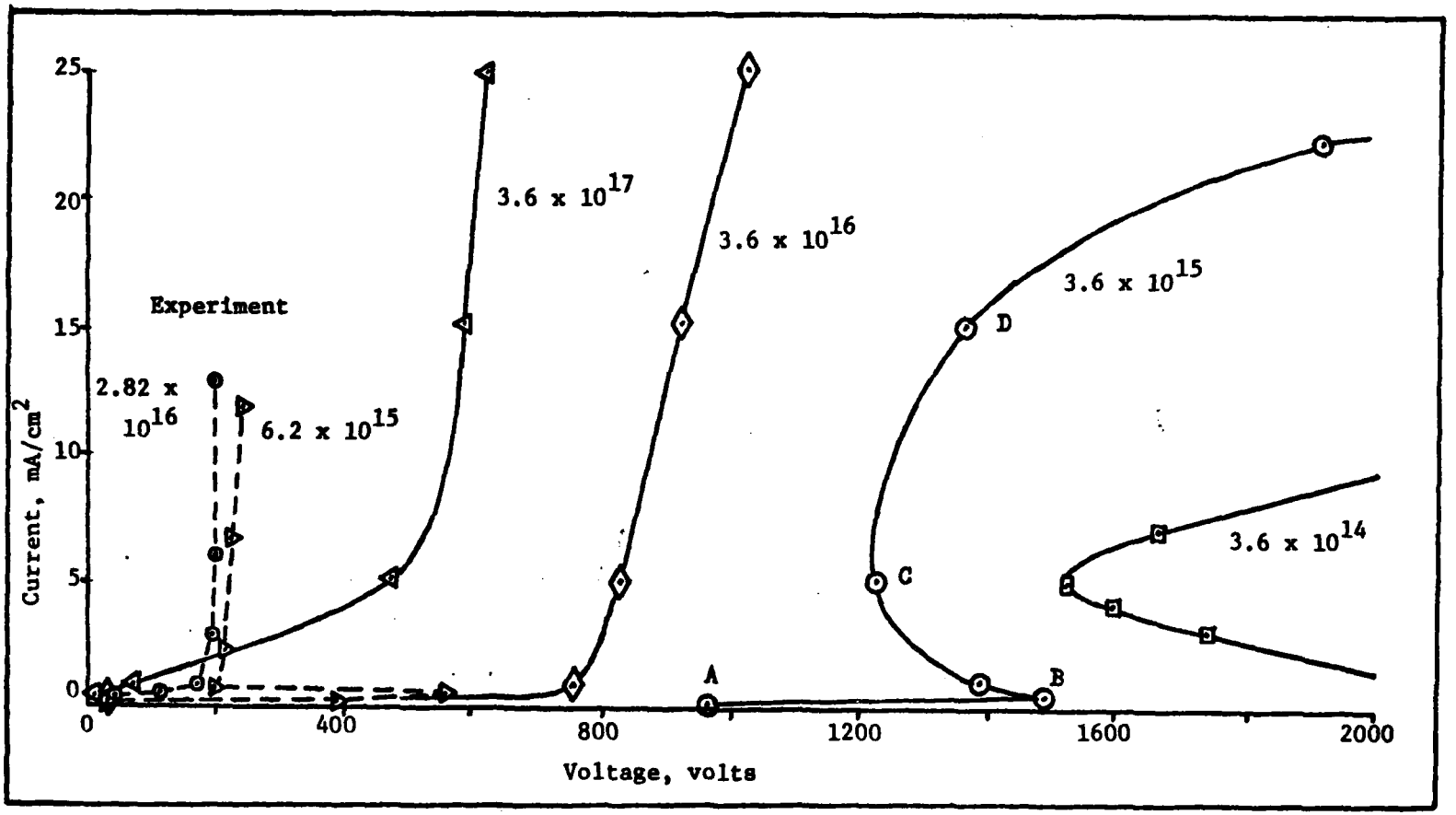

Figure 23. I-V Characteristics-Calculated for an Argon Discharge (expansion of low current and voltage region of Fig. 22.)

for source strengths of $6.2 \cdot 10^{15}$ and $2.82 \cdot 10^{16}$, it is seen that their general shapes are quite similar, especially at lower currents. As the current is increased, the calculated positive column field must increase more rapidly for lower source strengths. Thus, the calculated characteristic for $S = 3.6 \cdot 10^{15}$ rapidly diverges from the experimental curves. Comparing the more well-behaved calculated characteristic for $S = 3.6 \cdot 10^{16}$ to Bletzinger's $2.82 \cdot 10^{16}$ curve, it is seen that the slope of the calculated high conductivity region is not as great as that observed. This is partially due to the previously discussed problem in the positive column. However, it could also be the result of using too small a value for the secondary emission coefficient in the calculations. In the calculation done, the secondary emission coefficient was assumed to be 2%, but this may be considerably smaller than the actual value, since the secondary emission coefficient for metastable argon atoms (which may be present in large numbers) is 40%. With a larger secondary emission coefficient, the slope of the I-V characteristic is increased, as shown in Fig. 21. Thus, a secondary emission coefficient of two percent probably underestimates the magnitude of this effect in the discharges investigated experimentally. The slope of an I-V characteristic would probably also increase if the effect of secondary emission at the anode were considered. However, since such emission would only occur for low current densities (for which the anode sheath field is positive), the slope increase would probably be minimal.

It may also be observed in Fig. 23 that the voltage separation between the experimental characteristics is much less than the separation of the calculated characteristics. In the calculational model, an increase in S results in an increase in n_e in the positive column. For

a given current density, then, the electric field in the positive column must decrease. This results in a weaker electric field in the cathode sheath and thus the observed decrease in discharge voltage (See Fig. 17). If there were another process (in addition to the external ionization source) by which free electrons were generated in the positive column, and if the number of electrons produced by this process were proportional to the local field strength, the decrease in discharge voltage resulting from an increase in S would be less than when S is the only source of electrons in the positive column. The decrease in the field which would normally occur with an increase in S would also cause the other source of electrons to reduce its production, negating some portion of the increase in n_e due to S. Thus, the closer voltage spacing of the experimental characteristics seems to indicate that there is an additional source of electron-ion pairs in the positive column.

Since this process is probably operative in the cathode sheath as well, the electric field needed to support the required current density would be reduced. Thus, both the cathode fall and the total discharge voltage would be reduced, resulting in a shift of the entire characteristic to lower voltages, as demonstrated by the experimental characteristics in Figure 23.

A very likely candidate for this additional process is metastable ionization. Because argon has a very high energy metastable state, even the weak electric fields in the positive column may produce significant ionization from these excited states. With the addition of the effect of metastable ionization, an I-V characteristic was calculated for a source strength of $3.6 \cdot 10^{16}$ in a 760 Torr argon discharge. This characteristic and one of Bletzinger's experimental curves (for a similar

source strength and electrode gap) are shown in Figure 24. (The basic I-V characteristic in Figure 24 differs slightly from that in Figs. 22 and 23 because a constant value of R_r was used for the calculations represented in Figure 24, while an R_r with a functional E/N dependence was used for the calculations in Figures 22 and 23.) Although the metastable calculation was not carried to current densities below 7 mA/cm^2, the experimental and calculated curves are in reasonable agreement where they overlap. Thus, the addition of metastable ionization shifts the I-V characteristic to lower discharge voltages, while leaving the slope of the high-conductivity portion of the characteristic relatively unchanged. Consequently, to reproduce the very rapid current rise which is observed experimentally, the secondary emission coefficient must also be increased.

Metastable ionization may also be used to correct the inflated value for the electric field in the positive column. Assuming that the rate of ionization of metastables is of the same magnitude as the rate of recombination and the rate of external ionization, the number density of electrons in the positive column is obtained using the electron continuity equation (3). In the positive column, $\partial j_e/\partial x = 0$, and the weak electric field allows the neglect of Townsend ionization. Thus, a quadratic equation in n_e is obtained:

$$0 = S - \gamma n_e^2 + R_{im} n_e n_m$$

with solution

$$n_e = \frac{R_{im} n_m + \sqrt{(R_{im} n_m)^2 + 4S\gamma}}{2\gamma} \qquad (57)$$

(57)

(A negative value for the square root would not be physical.) When

AD-A115 513 AIR FORCE INST OF TECH WRIGHT-PATTERSON AFB OH SCHOO--ETC F/G 20/9
CATHODE SHEATH EFFECTS IN EXTERNALLY-IONIZED GAS DISCHARGES.(U)
DEC 81 M R HALLADA
UNCLASSIFIED AFIT/GEP/PH/81D-4 NL

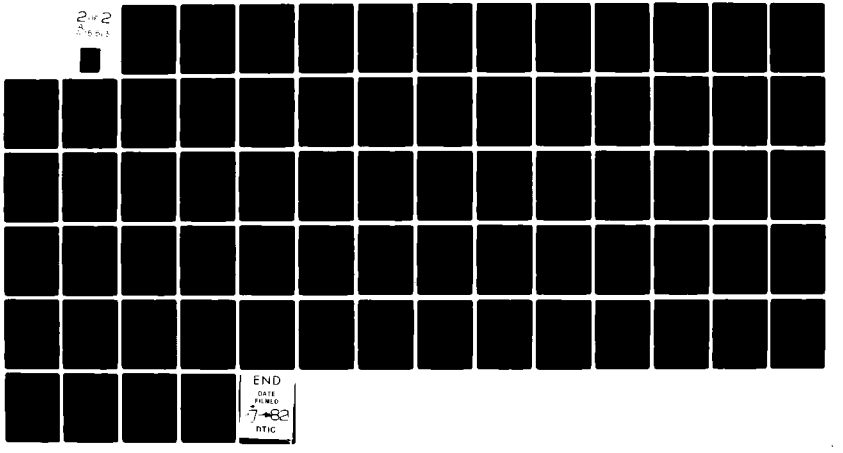

END
DATE FILMED
7-82
DTIC

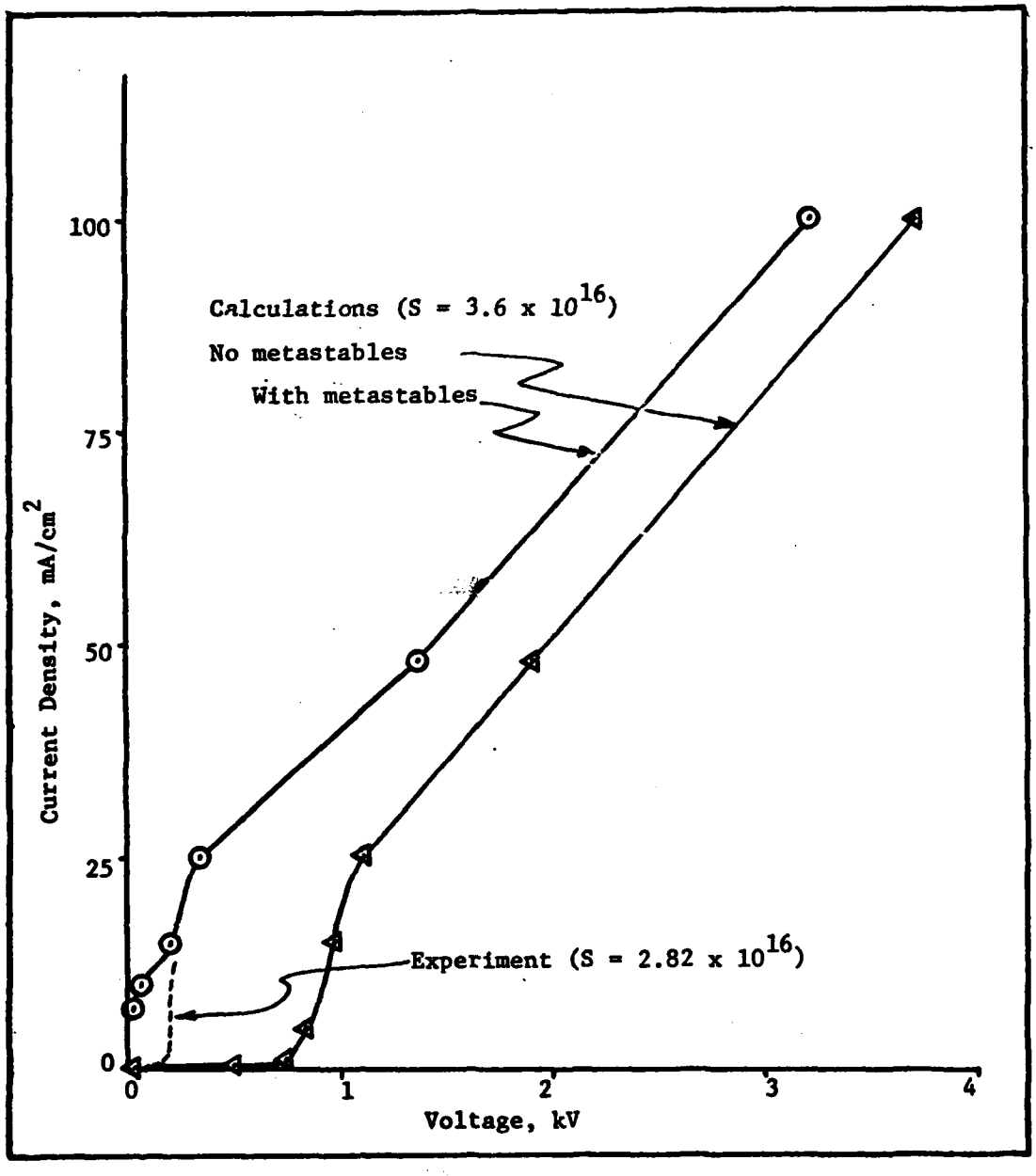

Figure 24. I-V Characteristics-Experimental and Calculated for an Argon Discharge (same parameters as Fig. 22, but with metastable ionization)

metastable ionization is significant, this equation will yield an increased n_e. For a given current, then, the electric field is reduced. For a metastable ionization rate of $R_{im} = 1 \cdot 10^{-6}\exp(-4.15/T_e)$, a metastable number density of $n_m = 2.5 \cdot 10^{19} \cdot \exp(-11.65/T_e)$ (See Appendix A), a source strength of $S = 3.6 \cdot 10^{16}$, a recombination coefficient of $R_r = 8.81 \cdot 10^{-7}$, and at an electron temperature of 1 eV, the number density of electrons in the positive column is:

$$n_e \approx 4 \cdot 10^{12}$$

Then, for a current density of 25 mA/cm^2, slightly above Bletzinger's largest current density, E/N in the positive column is about .004 Townsend. Therefore, although the rates and number densities used are quite crude, and the decrease in T_e with decreasing E/N was not accounted for, it is apparent from this analysis that the minute positive column fields observed experimentally in argon discharges could possibly be accounted for by considering metastable ionization occurring in the positive column.

Although argon is not very attractive for switching applications because of its low dielectric strength, the effects observed for secondary emission and metastable ionization may be applied to the modeling of other, more useful gases (Ref. 5:2).

One such gas which is currently being investigated is methane. Because of its very high drift velocity and high dielectric strength, it seems to be well suited for switching applications. I-V characteristics were calculated for methane discharges at 760 Torr. In Figure 25, these calculated characteristics are compared against experimental measurements made by Bletzinger (Ref. 11:2). Although the calculated curves are shifted to higher discharge voltages, the spacing between different

source strength curves in nearly the same for both pair of experimental and theoretical curves. In addition, both sets of curves exhibit transition regions of negative differential conductivity, although these regions are accentuated both in voltage and current density for the calculated curves. However, it should be noted that these discrepancies are relatively minor, considering the inaccuracies inherent in the experimental measurements. For example, the values assigned to the experimental source strengths are only approximate. These values were assigned based on average stopping powers, while a more exact calculation requires a statistical approach, using Monte Carlo techniques. Thus, the values for the experimental source strengths may be in error by up to an order of magnitude. Thus, if the actual experimental source strengths are a factor of ten larger than those listed in Fig. 25, the calculated and experimental curves for $S \sim 1 \times 10^{18}$ would nearly coincide. This explanation would also reconcile the discrepancy in the voltage spans of the negative differential conductivity regions. As seen previously for argon discharges (Fig. 22), with an increase in S, the voltage span of this region decreases and eventually disappears. Thus, if the experimental source strengths are in error as indicated, the voltage spans of the negative conductivity regions would be comparable for the experimental and calculated characteristics. The exaggerated extent in current density of the calculated negative conductivity regions could possibly be the result of an inflated secondary emission coefficient. The value of two percent, which was used in these calculations, may be much too large. As shown in Figure 21, a decrease in γ decreases the slope of the high current density region of an I-V characteristic. Such a decrease in γ could cause a calculated I-V curve to return more quickly to a positive slope

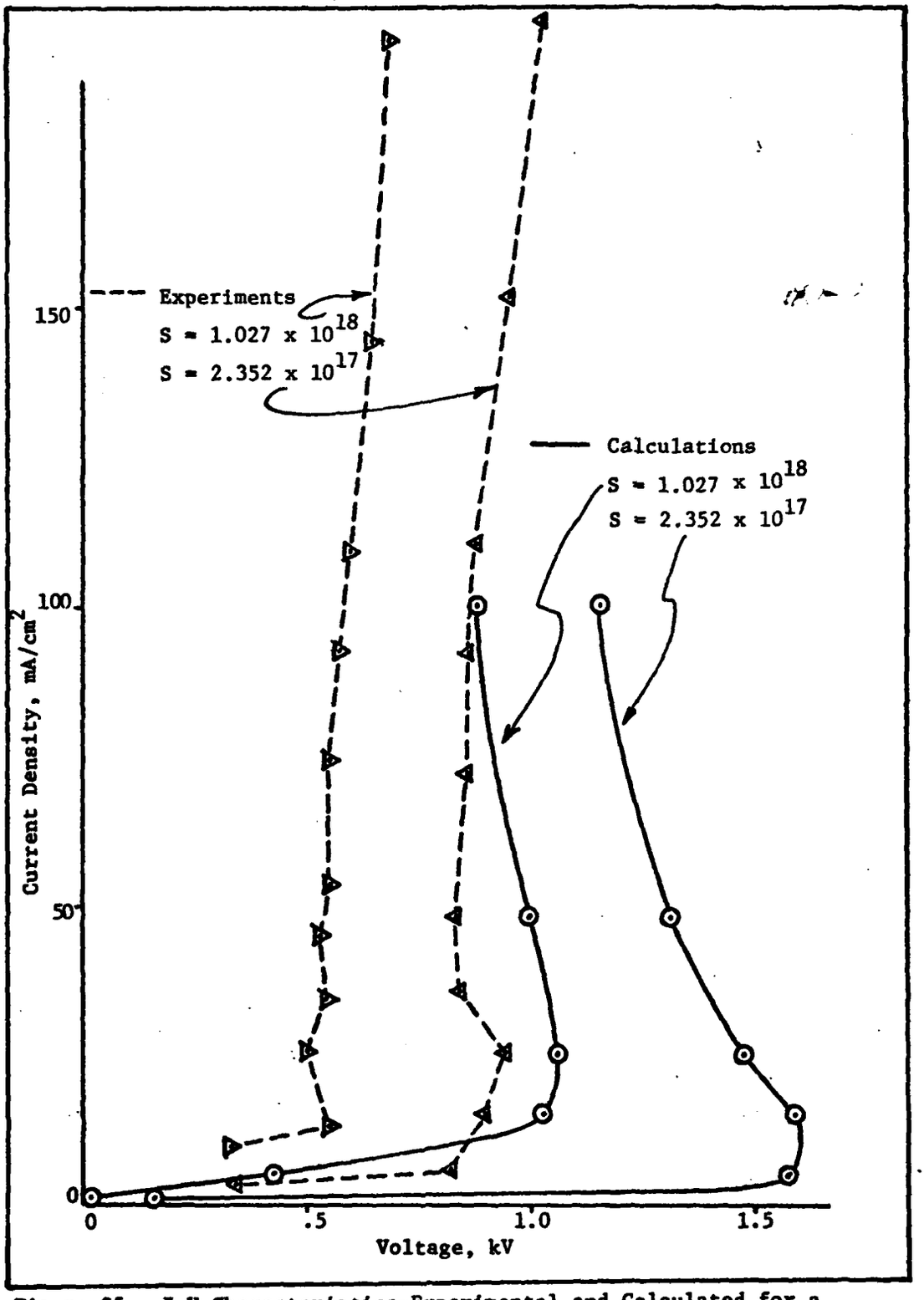

Figure 25. I-V Characteristics-Experimental and Calculated for a Methane Discharge (760 Torr, γ = .02, d = 2.2 cm)

as the current density is increased. Thus, it may be that the actual value for the secondary emission coefficient in a methane discharge is much less than the two percent figure used in the calculations. It should be noted that these discrepancies between calculation and experiment cannot be explained by the addition of metastable ionization, as was done for argon. For one thing, only the rare gases and some molecular gases have such high energy metastable states. In addition, metastable ionization would also cause the experimental characteristics to be more closely spaced than the calculated characteristics, but this is not observed to occur.

IV. Conclusions and Recommendations

The behavior of argon and methane gas discharges was investigated. Particular attention was paid to processes occurring in the cathode sheath. It was found that these sheaths became strong electron producers at voltages above an "ignition" voltage characteristic of the discharge gas and the external circuit parameters. This strong electron production results in very high discharge conductivities. The I-V characteristics calculated for argon agree qualitatively with those observed experimentally, particularly if the comparison is restricted to the cathode sheath region. In order to decrease the large calculated positive column fields to experimentally-observed levels, it is hypothesized that metastable ionization makes a significant contribution to the ionization in the positive column. Metastable ionization also shifts the calculated I-V characteristics to lower voltages, which are observed experimentally. The experimental curves also have a larger slope in the high conductivity region of the characteristics. This larger slope can be obtained in the calculations by the inclusion of secondary emission at the cathode. Metastable ionization does not seem to play a role in methane discharges. The calculated I-V characteristics obtained for this gas agree very well with those measured experimentally. The shift in the calculated characteristics to somewhat higher voltages may be due to an underestimation of the external ionization source strength produced in the comparison experiments.

These observed effects in argon and methane discharges may be applied to the design of more efficient high-energy switches. Some of the desirable features of such a switches include: high conductivity when "on," very low conductivity when "off," high gain (ratio of energy switched to switching energy, i.e. the energy expended by a sustaining electron beam), and rapid

switching. To achieve high conductivity, gases with high drift velocities should be used. However, a gas with a lower drift velocity can also produce a highly conductive discharge if high γ coatings are used on the cathode. These coatings would also allow the use of lower external ionization source strengths to achieve the same high conductivity. (At lower S, the I-V characteristic above the ignition voltage has a shallower slope than that at higher S. This larger slope, i.e. conductivity, can also be achieved by increasing γ for lower source strengths.) Thus, the switch's gain would be increased without affecting the conductivity. In order to decrease the time required for a discharge to turn "off," additional loss processes, such as attachment, could be produced by the addition of small quantities of attaching gases. These materials would quickly eliminate any free electrons in the discharge once the external ionization source is turned off. To decrease the time required for a discharge to turn on, external excitation could be used to quickly populate metastable states of a discharge gas. This would cause the discharge to immediately transition to an I-V characteristic at much higher currents. (The amount of this shift is determined by the external circuit because the operating points of a discharge are at the intersections of the circuit's bad load and the I-V characteristic(s) of the discharge.

Although this investigation answered some questions about electron beam sustained gas discharges, it also suggested a number of questions and proposals for further investigation.

1) I-V characteristics for a 760 Torr argon discharge should be recalculated in an attempt to reduce the discrepancies between the calculated and the experimental characteristics. These calculations should include: metastable ionization, in both the cathode sheath and the

positive column; more accurate values for the rate of this ionization and for the number density of metastables; more accurate values for the secondary emission coefficient (taking into account the large coefficients associated with metastables); and source strengths which are the same as those used by Bletzinger (Ref. 5).

2) Experimental investigations of argon discharges should be extended to lower source strengths to determine if the I-V characteristics obtained in the first proposal are physically realistic. In particular, the region of negative differential conductivity should be explored.

3) The I-V characteristics calculated for methane should be extended to higher current densities and a wider range of source strengths. For these calculations, a more accurate value for the actual secondary emission coefficient should be obtained. Also, the validity of the method for determining the source strength produced by an external electron beam should be investigated.

4) High γ cathode coatings, which could reduce the source strength required to access the rapid current rise portion of discharge I-V characteristics, should be experimentally explored. These coatings would increase the gain of an externally-sustained gas discharge switch.

5) I-V characteristics should be calculated for a range of gas pressures. The effects produced may be a function of the discharge current density. There may be an optimal operating pressure for a given gas discharge switch.

6) The diffusion coefficient of electrons used in the computer calculations should be modified to correct for the inflated value of this coefficient when electrons diffuse into a retarding electric field.

7) Because of the importance of rapid "off" switching, the effect

of small quantities of attaching gases in externally-sustained discharges should be determined by calculating the I-V characteristics of these mixtures. Initially, a mixture of argon and oxygen should be investigated because Bletzinger (Ref. 5) has already measured I-V characteristics for such a discharge.

Bibliography

1. Hunter, R. O. "Electron-Beam Controlled Switching," Proceedings 1st IEEE International Pulsed Power Conference, IC8:1-5, Lubbock, TX (1976).

2. Daugherty, J. D., E. R. Pugh, and D. H. Douglas-Hamilton. Bulletin of the American Physical Society, 16:399 (1972).

3. Fenstermacher, C. A., M. J. Nutter, J. P. Rink, and K. Boyer. Bulletin of the American Physical Society, 16:42 (1972).

4. Leland, W. T. "Relation of Electric Discharge Parameters to Short-Pulse CO_2 Laser Efficiency," Sov. J. of Quant. Electronics, 6 (4): 466-470 (April 1976).

5. Bletzinger, P. "Electron Beam Switching Experiments in the High Current Gair Regime," 3rd International Pulsed Power Conference, Albuquerque, New Mexico, paper 5.4, (May 1981).

6. Koval'chuk, B. M., Yu. D. Korolev, V. V. Kremner, and G. A. Mesyats. "The Injection Thyraton-a Completely Controlled Ion Device," Soviet Radio Eng. and Electron Physics, 21:1513 (1976).

7. Averin, A. P., Ye. P. Glotov, et al. "Negative Differential Conductivity of Electron-Ionization Discharge in Nitrogen," Pis'ma V. Zhurnal Teknicheskoy Fiziki, 6 (7):405-408 (12 April 1980).

8. Wardlaw, A. B. Jr. and I. M. Cohen. "Continuum Analysis of the Photoionization Chamber in the Transition from Low to High Rates of Ionization," Physics of Fluids, 16 (5):637-650 (1973).

9. Ward, A. L. "Effect of Space Charge in Cold-Cathode Gas Discharges," Physical Review, 112 (6):1852-1857 (1958).

10. Zakharov, V. V. et al. "Gaseous Discharge in Nitrogen with Steady-State External Ionization," Sov. Phys. Tech. Phys., 21:1074 (Sep 76).

11. Lowke, J. J., and D. K. Davies. "Properties of Electric Discharges Sustained by a Uniform Source of Ionization," J. Appl. Physics, 48 (12):4991-5000.

12. Aleksandrov, V. V., V. N. Koterov, and A. M. Soroka. "Asymptotic Analysis of the Structure of a Semi-self-maintained Volume Gas Discharge," U.S.S.R. Computational Mathematics and Mathematical Physics, 18 (5):138-153, (May 1978).

13. Leffert, C. B., D. B. Rees, and F. E. Jamerson. Journal of Applied Physics, 37:133, (1966).

14. Dzimianski, J. W. and L. R. Kline. "High Voltage Switch Using Externally Ionized Plasmas," AFWAL-TR-80-2041, (April 80).

15. Howatson, A. M. An Introduction to Gas Discharges. Oxford, England: The Whitefriars Press Ltd, 1965.

16. Sharp, T. E. and J. T. Dowell. "Isotope Effects in Dissociative Attachment of Electrons in Methane," Journal of Chemical Physics, 46 (4):1530-1531, (February 1967).

17. von Engel, A. Ionized Gases. Oxford, England: Clarendon Press, 1955.

18. Mitchner, M. and C. H. Kruger, Jr. Partically Ionized Gases. New York: John Wiley and Sons, 1973.

19. Brown, S. C. Introduction to Electrical Discharges in Gases. New York: John Wiley and Sons, 1966.

20. Brown, S. C. Basic Data of Plasma Physics. Cambridge, Massachusetts: Technology Press of M.I.T., 1959.

21. Lowke, J. J. and J. H. Parker, Jr. "Theory of Electron Diffusion Parallel to Electric Fields. II. Application to Real Gases," Physical Review, 181 (1), (May 1969).

22. C. W. Duncan and I. C. Walker. Journal of Chemical Spectroscopy, Faraday Transactions II, 68:1514 (1972).

23. Cochran, L. W. and D. W. Forester. Physical Review, 126:1785, (1962).

24. Lakshminarasimha, C. S. and J. Lucas. J. Phys. D, 10:313, (1977).

25. Hindmarsh, A. C. "Gear: Ordinary Differential Equation System Solver," Lawrence Livermore Laboratory, UCID-30001 Rev. 3, (December 1974).

26. Pollock, W. J. Transactions of the Faraday Society, 64:2919, (1968).

27. Evdokimov, O. B., V. V. Kremnev, G. A. Mesyats, and V. B. Ponomarev. "Field Distribution in a Gas Discharge Excited by Fast Electrons," Sov. Phys. Tech. Phys., 18 (11):1478-1481, (May 1974).

28. Velikhov, E. P., V. D. Pis'mennyi, and A. D. Rakhimov. "The Non-Self-Sustaining Gas Discharge for Exciting Continuous-Wave Gas Lases," Sov. Phys. Usp., 20 (7):586-602, (July 1977).

29. Ward, A. L. "Calculations of Cathode-Fall Characteristics," Journal of Applied Physics, 33 (9):2789-2794, (September 1962).

30. Barnaov, V. Yu., et al. "Theoretical and Experimental Investigation of Pulsed Discharges in Gases," Soviet Journal of Quantum Electronics, 9 (12):1509-1515, (December 1979).

31. Long, W. H. Jr. "Plamsa Sheath Processes," Air Force Aero Propulsion Laboratory, AFAPL-TR-79-2038, (April 1979).

32. Specht, L. T., S. A. Lawton, and T. A. DeTemple. "Electron Ionization and Excitation Coefficients for Argon, Krypton, and Xenon in the Low E/N Region," Journal of Applied Physics, 51 (1):166-170, (January 1980).

33. Francis, Gordon. "The Glow Discharge Low Pressure," Encyclopedia of Physics, Gas Discharges II, Volume XXII. Berlin: Springer-Verlag, 1956.

34. Zeldovich, Ya. B., and Yu. P. Raizer. Physics of Shock Waves and High-Temperature Hydrodynamic Phenomena. Vol. I. New York: Academic Press, 1966.

35. Kruithof, A. A. and F. M. Penning. Physica (Utrecht), 3:515, (1936).

36. Duke. G. Private Correspondence Between the Author and G. Duke, Dayton, Ohio: Wright-Patterson AFB, 1981.

Appendix A

Transport Coefficients and Material Functions

Townsend Ionization Coefficient (α)

Argon: $\alpha = N \cdot 2.9 \cdot 10^{-17} \exp(-1.48 \cdot 10^{-15} \cdot N/E)(cm^2)$ This expression for α, which was obtained from experimental measurements (Ref. 35:515), was used by Lowke and Davies (Ref. 11:4994). This expression was used for Case II and Case III. However, recent experimental data indicates that this expression should be modified at low E/N (Ref. 32:167). This modified expression, as used in Case I, is:

$$\alpha = N \quad 1.76275 \cdot 10^{-17} \exp(-1.45027 \cdot 10^{-15} \cdot N/E)$$

Methane: Tabulated experimental values of Cookson et.al. were used for the net ionization coefficient, $(\alpha - A)$, which implicitly accounted for attachment occurring in methane (Ref. 14:18). Values for $(\alpha - A)$ at $E/N < 72Td$ (1 Townsend = 1 Td = $1 \cdot 10^{-17}$ Volt-cm^2) were obtained by logarithmic extrapolation.

Recombination Rate Coefficient (R_r)

Argon: $R_r = 7.6 \cdot 10^{-8} \cdot \bar{\varepsilon}^{-.67}$ (cm^3/sec) This expression for the recombination rate of Ar_2^+ ions, given by Lowke and Davies, was determined experimentally. It requires a knowledge of the average electron energy $\bar{\varepsilon}$ (in eV) as a function of E/N. This function was used only for comparison with another function (Ref. 11:4994).

$R_r = 8.81 \cdot 10^{-7}$ (cm^3/sec) This constant value, which was used by Lowke and Davies, was obtained from the expression above for an average electron energy of .026 eV. This greatly exaggerated the recombination rate at higher electron energies, and thus higher fields, i.e.

in the cathode sheath. However, since this rate is multiplied by n_e, which decreases rapidly away from the plasma region, Lowke and Davies maintain that it is not too inaccurate (Ref. 11:4994). This value was used in the present analysis for code verification and for I-V comparisons at different source strengths and with the addition of secondary emission.

$R_r = 7.5 \cdot 10^{-8} \cdot (E/N)^{-.23}$ (cm^3/sec) This analytic expression for the recombination rate of Ar^+ ions, given by Dzimianski and Kline, was used for most of the argon calculations (Ref. 14:13). The value for E/N in this expression must be given in Townsends. Although the region of validity of this function is from .1 to 10 Td, cathode sheath fields in this investigation sometimes reached 100 Td. Although Lowke and Davies maintain that the use of the Ar_2^+ R_r is more appropriate, the total discharge voltage obtained using Lowke and Davies' analytic R_r was less than 5% different from the voltage obtained using Dzimianski and Kline's R_r.

Methane: $R_r = 2.4 \cdot 10^{-7} \cdot (E/N)^{-.34}$ (cm^3/sec) This expression for the recombination rate in methane was obtained from Dzimianski and Kline. The value for E/N must be given in Townsends. This function, which was only valid from .2 to 10 Td, exaggerated R_r at the low fields in the positive column, although it probably did not appreciably affect the calculations in the cathode sheath, as indicated in the preceeding discussion. This insensitivity seemed to vindicate Lowke and Davies' assumption of a constant R_r (Ref. 11:4994).

Drift Velocity of Electrons (W_e)

Argon: Tabulated values for W_e (as a function of E/N), calculated by Engelhardt and Phelps (Ref. 31:A377), were used in Lowke and Davies' study (Ref. 11:4995) and in the present analysis.

Methane: Tabulated values for W_e (as a function of E/N) were obtained from calculations and experiments by a number of individuals (Refs. 22; 23; 24). The values used in this analysis were compiled and presented by Dzimianski and Kline (Ref. 14:17). Values at low E/N were obtained by logarithmic extrapolation.

Longitudinal Diffusion Coefficient of Electrons (D_e)

Argon: Tabulated values for D_e/k_e (volts) were obtained from the calculations of Lowke and Parker (Ref. 21:307). Values at higher field strengths were obtained from Lowke and Davies' extension (Ref. 11:4995) of the previous calculations. In order to determine D_e, values for the mobility, k_e, were obtained from the similarly tabulated values of W_e versus E/N.

Methane: Tabulated values for D_e/k_e (volts) were obtained from the calculations of several authors (Refs. 23; 24; 26). Values at low E/N were obtained by logarithmic extrapolation of the values compiled by Dzimianski and Kline (Ref. 14:17). In order to determine D_e, values for k_e were obtained from the similarly tabulated values of W_e versus E/N for methane.

Metastable Ionization Rate (R_{im})

Argon: $R_{im} = 5 \cdot 10^{-8} \cdot Te^{1/2} \cdot \exp(-4.15/Te)$ This rate was obtained by shifting the cross-section for ground state ionization by lower electron energies. Thus, for argon, with an ionization energy of 15.8 eV and a metastable energy of 11.65 eV, the metastable ionization energy is 4.15 eV. Thus, the rate of metastable ionization is:

$$R_{im} = W_e \sigma e^{-4.15/Te}$$

Assuming a Maxwellian electron velocity distribution and a cross-section linear in Te (Ref. 34)

$$R_{im} \simeq (6.7 \cdot 10^{7} \cdot Te^{1/2}) \cdot (2 \cdot 10^{-17} \cdot Te) \cdot (2 + \frac{4.15}{Te}) e^{-4.15/Te}$$

$$R_{im} \simeq 5 \cdot 10^{-8} \cdot Te^{1/2} \cdot e^{-4.15/Te}$$

(Te is the electron energy in eV.)

However, this rate is very conservative. Using the metastable ionization cross-section calculated by Duke ($\sigma \simeq 1 \cdot 10^{-15} cm^{2}$), the rate obtained is about 20 times that shown above (Ref. 36). This higher rate was used in the estimation of the contribution of metastable ionization in the positive column.

Metastable Number Density (n_m)

Argon: $n_m = (N_o - n_+) \cdot \exp(-11.65/Te)$ The number density of metastable argon atoms was approximately by using a Boltzmann distribution of energy level population for a total number density of $(N_o - n_+)$ unionized argon atoms. (The metastable excitation energy for argon is 11.65 eV and Te is the electron energy, also in eV.)

Electron Temperature (T_e)

Argon and Argon/Oxygen: The average electron temperature was determined as a function of E/N for pure argon. These values were obtained from Boltzmann calculations done with experimentally determined cross-sections (Ref. 36).

Appendix B

Computer Codes

```
      PROGRAM CASEI(INPUT,OUTPUT,TAPE3 = OUTPUT,TAPE99)
      DIMENSION YO(5),WI(20),D_MU(20),XI(20),T(150),JE(150),NE(150),
     C          JP(150),E(150),V(150),VI(150)
      COMMON/CONST/S,NO,EPSI,A_PHA,GAMMA,ECHG,MU,MUE,K,EFLD,DE_T,D
      COMMON/GEAR9/MUSED,NOUSE),NSTEP,NFE,NJE
      COMMON/PLT/T,JE,NE,NI,JP,E,V,VMIN,M
      EXTERNAL DIFFUN,PEDERV,M
      REAL ME,NO,NP,MU,MJE,MG,NEKI,JE,JP,NE,NI
C
C     DISSPLA PLOT OPTION (1-YES   0-NO)
      DPLT = 1.0
C
C                        SET CONSTANTS FOR GEAR PROGRAM
C     NUMBER OF DIFF EQNS IN SYSTEM
      N = 5
C     LOCAL ERROR TOLERANCE PARAMETER
      EPS = .0001
C     STEP SIZE IN GEAR
      HO = .0000033
C     GEAR METHOD
      MF = 12
C                        SET PHYSICAL CONSTANTS FOR PROBLEM
C
C     ELECTRONIC CHARGE (COULOMB)
      ECHG = 1.6E-19
C     PERMITIVITY OF GAS (COULOMB/VOLT/CM)
      EPSI = 8.85E-14
C     ELECTRON MASS
      ME = .911E-27
C     BOLTZMANN CONSTANT
      BK = 1.38E-16
C     TRIAL ANODE E FIELD (V/CM)
      EFLD = -125.
      C = 4.2E-8
C
C     L COUNTS THE NUMBER OF TRIAL ANODE E FIELDS USED
      L = 0
C
C     K USED TO NEGATE DIFF EQNS IN DIFFUN AND PEDERV
      K = 1
C
C     SGN USED LATER IN SELECTION OF ANODE E FIELD TO PRODUCE NE EQ ZE
C     AT CATHODE
      SGN = 1.0
C
C
C                        SET PARAMETERS FOR DISCHARGE
   30 CONTINUE
C     INDEX FOR FIRST CALL TO GEAR
      INDEX = 1
C     DISTANCE BETWEEN ELECTRODES (CM)
      D = .33
C     DISTANCE STEP SIZE
      DELT = .01*D
C     POINT AT WHICH INITIAL CONDITIONS GIVEN
      TO = 0.0
C     FIRST OUTPUT POINT DESIRED
```

```
      TOUT = .01*D
C     ELECTRON CURRENT DENSITY AT ANODE (1/CM2/SEC)
      YO(1) = C/ECHG
C     ELECTRON NUMBER DENSITY AT ANODE (1/CM2/SEC)
      YO(2) = 0.0
C     ION CURRENT DENSITY AT ANODE (1/CM2/SEC)
      YO(3) = 0.0
C     ELECTRIC FIELD AT ANODE  (V/CM)
      YO(4) = EFLD
C     POTENTIAL AT ANODE ARBITRARILY SET TO ZERO
      YO(5) = 0.0
C     GAS PRESSURE (DYNE/CM2)
      PRES = 240.*(1.01325E6/760.)
C     GAS TEMPERATURE (K)
      TG = 273.
C     ELECTRON TEMPERATURE (K)
      TE = 11605.
C     NUMBER DENSITY OF GAS
      NO = PRES/BK/TG
C     IONIZATION SOURCE STRENGTH (ION PAIRS/CM3/SEC)
      S = 8.0E11
C     POSITIVE ION MOBILITY (CM2/SEC/V)
      MU = 4.9E19/NO
C     RECOMBINATION COEFFICIENT
      GAMMA = 8.81E-7
C     CALCULATE ION NUMBER DENSITY AT ANODE
      NP = YO(3)/MU/YO(4)
C     CALCULATE CURRENT DENSITY (AMPS/CM2)
      C = ABS(YO(1)- YO(3))*ECHG
      WRITE (3,1000)
      WRITE (3,1001)
      WRITE (3,1002) TO,YO(1),YO(3),C,YO(2),NP,YO(4),YO(5)
C
C     M COUNTS THE NUMBER OF INTGRATION PTS BETWEEN ANODE AND CATHODE
      M = 1
C     LOAD BOUNDARY CONDITIONS INTO PRINT ARRAYS
      T(M) = D - TO
      JE(M) = YO(1)
      NE(M) = YO(2)
      NI(M) = NP
      JP(M) = YO(3)
      E(M) = YO(4)
      V(M) = YO(5)
C
C     SET INITIAL COMPARISON VALUE FOR VOLTAGE
      VMIN = 1000.
C
C     BEGIN LOOP TO SOLVE SYSTEM OF EQNS AT SEVERAL POINTS BETWEEN
C     ANODE AND CATHODE
   40 CONTINUE
      M = M + 1
C
      CALL DRIVE (N,TO,HO,YO,TOUT,EPS,MF,INDEX)
      C = ABS(YO(1) - YO(3))*ECHG
      NP = ABS(YO(3)/MU/YO(4))
      DRIFT = W(YO(4)/NO)
      MUE = DRIFT/YO(4)
```

```
      DIFF = DL(YO(4)/NO)
      DMU = DIFF/MUE
      WRITE(3,1008) M,ALPHA,MUE,DRIFT,DIFF,DMU,GAMMA
 1008 FORMAT (12X,I3,9X,7(1PE9.1,6X))
C
C     FILL ARRAYS WITH OUTPUT (AND WRITE OVER THEM UNTIL FIND THE VALU
C     FOR THE ANODE E FIELD WHICH PRODUCES NE .EQ. ZERO AT THE CATHODE
C
      T(M) = D - TOUT
      JE(M) = YO(1)
      NE(M) = YO(2)
      NI(M) = NP
      JP(M) = YO(3)
      E(M)  = YO(4)
      V(M)  = YO(5)
C     OVERALL POTENTIAL MINIMUM WILL BE SUBTRACTED FROM POTENTIAL AT
C     EACH POINT TO MAKE POTENTIAL AT CATHODE ZERO
      VMIN = AMIN1(YO(5),VMIN)
      WRITE(3,1002) TOUT,YO(1),YO(3),C,YO(2),NP,YO(4),YO(5),NOUSED
C     NORMAL CONTINUATION OF INTEGRATION WITH INDEX .EQ. ZERO
      IF (INDEX.EQ.0) GO TO 100
C     ELSE, ERROR TERMINATION AND EXIT
      WRITE (3,1003) INDEX
      GO TO 200
C     LOOP BACK TO LINE 40 UNLESS HAVE REACHED CATHODE
C     DECREASE STEP SIZE AS GET NEAR CATHODE
  100 IF (ABS(DELT).LT.ABS(5.E-4*D)) GO TO 120
      IF ((D-TOUT).LT.(2.*DELT)) DELT = DELT/2.
      IF((D-TOUT).LT.(DELT)) DELT = DELT/10.
      TOUT = TOUT + DELT
      GO TO 40
  120 WRITE (3,1004) NSTEP,NFE,NJE
C
C     DO DISSPLA PLOTS OF FIRST AND EVERY TENTH ITERATION
      IF((DPLT.EQ.1.).AND.((L.EQ.0).OR.(MOD(L,10).EQ.0))) CALL PLOT(L)
C
C
C     NOW, CHECK RESULTS OF CALCULATION TO SEE IF NE AT THE CATHODE IS
C     ZERO - IF NOT, MODIFY E FIELD AT ANODE AND REPEAT ENTIRE
C     INTEGRATION BY LOOPING BACK TO LINE 30
C
      L = L + 1
      IF (L.EQ.1) GO TO 130
      IF((NEK1*YO(2).LT.0.0).OR.(NEGFLG.EQ.1)) GO TO 140
C
C     BEGINNING AT AN E FIELD VALUE WHICH ASSURES THAT NE AT THE CATHO
C     WILL BE POSITIVE, THE E FIELD IS INCREMENTED (NEGATIVELY) UNTIL
C     GOES NEGATIVE - THE E FIELD IS THEN INCREMENTED POSITIVELY USING
C     THE SGN VARIABLE - EACH SUCCEEDING INCREMENT IS HALVED AND IS MA
C     POSITIVE OR NEGATIVE BASED UPON WHETHER NE CHANGES SIGN OR NOT -
C     WHEN THIS INCREMENT BECOMES LESS THAN ONE PERCENT OF THE E FIELD
C     VALUE, THE OPTIMIZATION LOOP IS EXITED TO LINE 300
C
  130 NEK1 = YO(2)
      EFLD1 = EFLD
      IF (ABS(YO(2)).LE.1.E4) GO TO 500
      EFLD = EFLD - 10.
```

```
      DELE = EFLD - EFLD1
      GO TO 30
  140 DELE = ABS(DELE/2.)
      NEGFLG = 1
      IF (NE*1*Y0(2).LT.0.0) SGN = -SGN
      NEK1 = Y0(2)
      EFLD1 = EFLD
      EFLD = EFLD - DELE*SGN
      IF (ABS(Y0(2)).LE.1.E4) GO TO 500
      IF (ABS(DELE).LT.ABS(.01*EFLD)) GO TO 300
      GO TO 30
  200 WRITE (3,1004) NSTEP,NFE,NJE
      GO TO 500
  300 CONTINUE
  350 CONTINUE
  500 CONTINUE
 1000 FORMAT(1H1,3X"DISTANCE"10X"JE"13X"J+"7X"CURRENT DENSITY"5X,
     C"NE"13X"N+"11X"E FIELD"8X"VOLTAGE"4X"ORDER")
 1001 FORMAT(6X"CM"10X"1/CM2/SEC"6X"1/CM2/SEC"6X"AMPS/CM2"8X,
     C"1/CM3"10X"1/CM3"8X"VOLTS/CM"9X"VOLTS"///)
 1002 FORMAT(8(1PE12.4,3X),I4)
 1003 FORMAT(//26H ERROR RETURN WITH INDEX =,I3//)
 1004 FORMAT(//21H PROBLEM COMPLETED IN,I5,6H STEPS/
     C         21X,I5,14H F EVALUATIONS/
     C         21X,I5,14H J EVALUATIONS///)
      CALL EXIT
      END
```

```
      SUBROUTINE DIFFUN(N,T,Y,YDOT)
      COMMON/CONST/S,NO,EPSI,ALPHA,GAMMA,ECHG,MU,MUE,K,EFLD,DELT,D
      DIMENSION Y(N),YDOT(N)
      EXTERNAL W,DL
      REAL MU,NO
      IF (1.48E-15*NO/ABS(Y(4)).GT.300.) GO TO 10
      ALPHA = NO*1.76275E-17*EXP(-1.45027E-15*NO/ABS(Y(4)))
      GO TO 20
   10 ALPHA = 0.0
   20 CONTINUE
C
C     SIGN CONVENTION IS THAT THE DRIFT VELOCITY, W, IS POSITIVE
C     WHEN THE ELECTRIC FIELD,E, IS NEGATIVE
      SGN = -1.0
      IF (Y(4).LT.0.0) SGN = 1.0
C
C     INITIAL VALUES FOR DIFFERENTIAL EQUATIONS AT ANODE (ROUNDOFF
C     ERRORS WOULD PREVENT YDOT(1) AND YDOT(3) FROM BEING EXACTLY S)
      IF (T.EQ.0.0) GO TO 50
      GO TO 100
   50 YDOT(1) = S
      YDOT(2) = -Y(1)/DL(Y(4)/NO)
      YDOT(3) = S
      YDOT(4) = 0.0
      YDOT(5) = -EFLD
```

```
      GO TO 200
  100 CONTINUE
      YDOT(1) = S*Y(2)*ALPHA*ABS(W(Y(4)/NO))-GAMMA*Y(2)*Y(3)/Y(4)/MU
      YDOT(2) = (Y(2)*W(Y(4)/NO)/SGN - Y(1))/DL(Y(4)/NO)
      YDOT(3) = YDOT(1)
      YDOT(4) = (ECHG/EPSI)*(Y(3)/Y(4)/MU - Y(2))
      YDOT(5) = -Y(4)
C     DIFF EQNS ARE NEGATED TO ALLOW FOR INTEGRATION FROM
C     SHEATH BACK TO CATHODE
  200 CONTINUE
      YDOT(1) = YDOT(1)*(-1)**(
      YDOT(2) = YDOT(2)*(-1)**(
      YDOT(3) = YDOT(3)*(-1)**(
      YDOT(4) = YDOT(4)*(-1)**(
      YDOT(5) = YDOT(5)*(-1)**(
      RETURN
      END
```

```
      FUNCTION W(XIN)
C     THIS FUNCTION CALCULATES ELECTRON DRIFT VELOCITY (CM/SEC) FOR
C     PARTICULAR VALUES OF E/N  (GRID VALUES FOR DRIFT VELOCITY ARE
C     FROM ENGELHART AND PHELPS)
      DIMENSION WI(33),XI(33)
      COMMON/CONST/ S,NO,EPSI,ALPHA,GAMMA,ECHG,MU,MUE,K
      REAL NO,MU,MUE
C     DATA FROM ENGELHARDT AND PHELPS,PHYS REV,(133),JAN 64,PA377
      DATA WI/3169.2,4894.3,7657.9,13002.,22293.,30209.,53691.,53691.,
     C72756.,90267.,104566.,113097.,118391.,133171.,148334.,173524.,
     C195821.,222439.,250207.,291743.,343518.,390211.,450547.,544565.,
     C693072.,1029840.,1350700.,1731450.,2323430.,3037390.,3970640.,
     C5614230.,6524840./
      DATA XI/5.3765E-21,9.1264E-21,1.409E-20,2.1543E-20,3.0262E-20,
     C3.3814E-20,4.2638E-20,4.2638E-20,4.8117E-20,6.0674E-20,8.4372E-2
     C1.2126E-19,1.7595E-19,2.5122E-19,4.3053E-19,8.6616E-19,1.4605E-1
     C2.4791E-18,4.4056E-18,8.2471E-18,1.6482E-17,2.9868E-17,4.8428E-17
     C6.1674E-17,7.7518E-17,1.139E-16,1.5592E-16,2.0249E-16,2.8907E-16,
     C3.9555E-16,5.5182E-16,8.4372E-16,9.9357E-16/
      XIN = ABS(XIN)
      CALL INTRP(XI,WI,33,2,XIN,YOUT)
      W = YOUT
      RETURN
      END
```

```
      FUNCTION DL(XIN)
C     THIS FUNCTION CALCULATES THE LONGITUDINAL DIFFUSION COEFFICIENT
C     FOR PARTICULAR VALUES OF E/N  (GRID VALUES FOR DLMU ARE
C     FROM LOWKE AND PARKER)
      DIMENSION DLMU(38),XI(38)
      COMMON/CONST/S,NO,EPSI,ALPHA,GAMMA,ECHG,MU,MUE,K,EFLD
      REAL NO,MU,MUE
      EXTERNAL R,INTRP
C     DATA FROM LOWKE AND PARKER,PHYS REV,181,P 307 AND LOWKE AND DAVIS
C     ,J APPL PHYS,48(12),DEC 77, P4995
      DATA DLMU/.0069242,.0069242,.007865,.008751,.015234,.03107,
     C.061224,.12401,.207139,.246053,.19269,.111456,.08289,.080085,
     C.084912,.111456,.171403,.257249,.36183,.48485,.571389,.647463,
     C.725177,.867117,.901086,
     C1.20595,1.58018,1.95908,2.31774,2.75962,3.1288,3.4653,3.5777,
     C3.6314,3.7016?,3.93726,4.24172,4.0186/
      DATA XI/3.26437E-21,6.04227E-21,1.11096E-20,1.42495E-20,
     C1.87932E-20,2.20343E-20,2.53922E-20,2.91608E-20,3.24638E-20,
     C3.71535E-20,4.46272E-20,5.90609E-20,7.84332E-20,9.58738E-20,
     C1.61065E-19,3.20627E-19,3.5055E-19,2.19432E-18,4.11908E-18,
     C7.91954E-18,1.02353E-17,1.5021E-17,1.65348E-17,2.2636E-17,
     C2.93833E-17,
     C3.2961E-17,3.8566E-17,4.2521E-17,4.6979E-17,5.4853E-17,6.5418E-17,
     C8.8044E-17,1.1529E-16,4.0926E-16,6.0214E-16,9.5433E-16,1.5816E-15,
     C2.8471E-15/
      XIN = ABS(XIN)
      CALL INTRP(XI,DLMU,38,2,XIN,YOUT)
C     DL IS DL/MUE TIMES MUE
      DL = ABS(YOUT*R(XIN)/(XIN*NO))
      RETURN
      END
```

```
      SUBROUTINE PEDERV(N,T,Y,PD,NDD)
      DIMENSION PD(NDD,NDD),Y(N)
      EXTERNAL DL,W
      COMMON/CONST/S,NO,EPSI,ALPHA,GAMMA,ECHG,MU,MUE,K,EFLD
      REAL MU,NO,MUE
C
C     SIGN CONVENTION IS THAT THE DRIFT VELOCITY, W, IS POSITIVE
C     WHEN THE ELECTRIC FIELD,E, IS NEGATIVE
      SGN = -1.0
      IF (Y(4).LT.0.0) SGN = 1.0
      MUE = W(Y(4)/NO)/Y(4)
      ALPHA = NO*1.76275E-17*EXP(-1.45027E-15*NO/ABS(Y(4)))
      GAMMA = 8.81E-7
      PD(1,1) = 0.
      PD(1,2) = ALPHA*ABS(W(Y(4)/NO)) - GAMMA*Y(3)/Y(4)/MU
      PD(1,3) = -GAMMA*Y(2)/Y(4)/MU
      PD(1,4) = GAMMA*Y(2)*Y(3)/MU/Y(4)**2 + Y(2)*ALPHA*MUE
      PD(1,5) = 0.0
      PD(2,1) = -1./DL(Y(4)/NO)
      PD(2,2) = SGN*W(Y(4)/NO)/DL(Y(4)/NO)
      PD(2,3) = 0.0
      PD(2,4) = Y(2)*MUE/DL(Y(4)/NO)
      PD(2,5) = 0.0
      PD(3,1) = 0.0
      PD(3,2) = ALPHA*ABS(W(Y(4)/NO)) - GAMMA*Y(3)/Y(4)/MU
      PD(3,3) = - GAMMA*Y(2)/Y(4)/MU
      PD(3,4) = GAMMA*Y(2)*Y(3)/MU/Y(4)**2 + Y(2)*ALPHA*MUE
      PD(3,5) = 0.0
      PD(4,1) = 0.0
      PD(4,2) = -ECHG/EPSI
      PD(4,3) = ECHG/EPSI/Y(4)/MU
      PD(4,4) = PD(4,2)*Y(3)/MU/Y(4)**2
      PD(4,5) = 0.0
      PD(5,1) = 0.0
      PD(5,2) = 0.0
      PD(5,3) = 0.0
      PD(5,4) = -1.
      PD(5,5) = 0.0
C     PARTIAL DERIVATIVES ARE NEGATED TO ALLOW FOR INTEGRATION
C     FROM SHEATH BOUNDARY BACK TO CATHODE
      PD(1,2) = PD(1,2)*(-1)**K
      PD(1,3) = PD(1,3)*(-1)**K
      PD(1,4) = PD(1,4)*(-1)**K
      PD(2,1) = PD(2,1)*(-1)**K
      PD(2,2) = PD(2,2)*(-1)**K
      PD(3,2) = PD(3,2)*(-1)**K
      PD(3,3) = PD(3,3)*(-1)**K
      PD(3,4) = PD(3,4)*(-1)**K
      PD(4,2) = PD(4,2)*(-1)**K
      PD(4,3) = PD(4,3)*(-1)**K
      PD(4,4) = PD(4,4)*(-1)**K
      PD(5,4) = PD(5,4)*(-1)**K
      RETURN
      END
```

```
C     SUBROUTINE INTRP
C
C     PURPOSE
C       INTERPOLATE BETWEEN DATA POINTS TO EVALUATE A FUNCTION
C
C     DESCRIPTION OF PARAMETERS
C       X           ARRAY OF DATA POINTS FOR INDEPENDENT VARIABLE
C       Y           ARRAY OF DATA POINTS FOR DEPENDENT VARIABLE
C       NPTS        NUMBER OF PAIRS OF DATA POINTS
C       NTERMS      NUMBER OF TERMS IN FITTING POLYNOMIAL
C       XIN         INPUT VALUE OF X
C       YOUT        INTERPOLATED VALUE OF Y
C
      SUBROUTINE INTRP(X,Y,NPTS,NTERMS,XIN,YOUT)
      DOUBLE PRECISION DELTAX,DELTA,A,PROD,SUM
      DIMENSION X(1),Y(1)
      DIMENSION DELTA(10),A(10)
C
C       SEARCH FOR APPROPRIATE VALUE OF X(1)
C
   11 DO 19 I = 1,NPTS
      IF (XIN - X(I)) 13, 17, 19
   13 I1 = I - NTERMS/2
      IF (I1) 15,15,21
   15 I1 = 1
      GO TO 21
   17 YOUT = Y(I)
   18 GO TO 61
   19 CONTINUE
      I1 = NPTS - NTERMS + 1
   21 I2 = I1 + NTERMS - 1
      IF (NPTS - I2) 23,31,31
   23 I2 = NPTS
      I1 = I2 - NTERMS + 1
   25 IF (I1) 26,26,31
   26 I1 = 1
   27 NTERMS = I2 - I1 + 1
C
C       EVALUATE DEVIATIONS DELTA
C
   31 DENOM = X(I1+1) - X(I1)
      DELTAX = (XIN - X(I1))/DENOM
      DO 35 I = 1,NTERMS
      IX = I1 + I - 1
   35 DELTA(I) = (X(IX) - X(I1)) / DENOM
C
C       ACCUMULATE COEFFICIENTS A
C
   40 A(1) = Y(I1)
   41 DO 50 K=2, NTERMS
      PROD = 1.
      SUM = 0.
      IMAX = K - 1
      IXMAX = I1 + IMAX
      DO 49 I = 1, IMAX
      J = K - I
      PROD = PROD*(DELTA(K) - DELTA(J))
```

```
   49 SUM = SUM - A(J)/PROD
   50 A(K) = SUM + Y(IXMAX)/PROD
C
C        ACCUMULATE SUM OF EXPANSION
C
   51 SUM = A(1)
      DO 57 J = 2, NTERMS
      PROD = 1.
      IMAX = J - 1
      DO 56 I = 1, IMAX
   56 PROD = PROD*(DELTAX - DE_TA(I))
   57 SUM = SUM + A(J)*PROD
   60 YOUT = SUM
   61 RETURN
      END
```

```
C     SUBROUTINE TRIMAT
C
C
      SUBROUTINE TRIMAT(A,N,NO,PW,SAVE1)
      RETURN
      END
```

```
C     SUBROUTINE PED
C
C
      SUBROUTINE PED(N,T,Y,PW,NO,CON,IER)
      RETURN
      END
```

```
      SUBROUTINE PLOT(L)
      DIMENSION T(150),JE(150),NE(150),NI(150),JP(150),E(150),V(150),
     CPT(150),PJE(150),PNE(150),PJP(150),PE(150),PNI(150),PV(150),
     CIPAK(150),X(2),Z(2)
      COMMON/PLT/T,JE,NE,NI,JP,E,V,VMIN,M
      REAL JE,JP,NE,NI
      CALL COMPRS
      CALL BGNPL(L)
      CALL BASALF(6HL/CSTD)
      CALL MIXALF(8HSTANDARD)
      CALL TITLE(" $",-100,
     C"(D)ISTANCE - CM$",100,"(N)E,(N)+ - 1/CM3$",100,8.0,6.0)
      CALL CROSS
      CALL GRAF(0.0,.1,.33,-2.E8,1.E8,2.E8)
      Z(1) = Z(2) = 0.0
      X(1) = .30
      X(2) = .33
      CALL CURVE (X,Z,2,0)
      CALL MESSAG("(C)ATHODE$",100,-.5,-.5)
      CALL MESSAG("(A)NODE$",100,7.7,-.5)
      CALL BLNKL(2.4,5.65,0.05,1.40)
C     FILL IPAK ARRAY WITH LEGEND INFORMATION
      IDUMMY = LINEST(IPAK,150,80)
      CALL LINES("(N)E E- NUM DENSITY (X)100$",IPAK,1)
      CALL LINES("(N)+ ION NUMBER DENSITY$",IPAK,2)
      CALL LINES("(J)E ELECTRON FLUX$",IPAK,3)
      CALL LINES("(J)+ ION FLUX$",IPAK,4)
      CALL LINES ("(V) VOLTAGE$",IPAK,5)
      CALL LINES ("(E) ELECTRIC FIELD$",IPAK,6)
C
C     REVERSE ANODE AND CATHODE, CHANGE ZERO IN POTENTIAL FROM THE
C     ANODE TO THE CATHODE, AND MAGNIFY NE BY 100
      DO 350 MM = 1,M
      MMM = M+ 1 - MM
      PT(MM) = T(MMM)
      PJE(MM) = JE(MMM)
      PNE(MM) = NE(MMM)*100.
      PJP(MM) = JP(MMM)
      PE(MM) = E(MMM)
      PV(MM) = V(MMM) - VMIN
      PNI(MM) = NI(MMM)
  350 CONTINUE
C     DO NOT PRINT ERRORS IN PLOT VALUES (OUT OF RANGE) FOR
C     PLOTS OTHER THAN THE FIRST
      IF (L.GT.0) CALL NOCHEK
      CALL SPLINE
      CALL CURVE(PT,PNE,M,10)
      CALL CURVE(PT,PNI,M,10)
      CALL YGRAXS(-4.0E11,1.E11,+4.0E11,6.0,"(J)E,(J)+ - 1/CM2/SEC$",
     C-100,8.0,0.0)
      CALL DASH
      CALL SPLINE
      CALL CURVE(PT,PJE,M,10)
      CALL CURVE(PT,PJP,M,10)
      CALL YGRAXS(-60.0,20.,60.0,6.0,"(V)OLTAGE - (V)$",-100,8.7,0.0)
      CALL CHNDOT
      CALL SPLINE
```

```
      CALL CURVE(PT,PV,M,10)
      CALL YGRAXS(-200.,100.,200.,5.,"(E) (F)IELD - (V)/CMS",100,-.7,0.
      CALL CHNDSH
      CALL SPLINE
      CALL CURVE(PT,PE,M,10)
      CALL RESET("3LNK1")
      CALL LEGEND(IPAK,6,2.5,0.20)
      CALL ENDPL(L)
      CALL DONEPL
      RETURN
      END
```

```
      PROGRAM CASEIII(INPUT,OUTPUT,TAPE3 = OUTPUT)
      DIMENSION YO(5),T(200),JE(200),NE(200),NI(200),JP(200),
     CE(200),V(200)
      COMMON/CONST/S,NO,EPSI,ALPHA,GAMMA,ECHG,MU,MUE,K,EFLD,NP
      COMMON/PLT/T,JE,NE,NI,JP,E,V,VMIN,DKSHTH,DASHTH,MA,MAS,O
      COMMON/GEAR9/ HUSED,NQUSED,NSTEP,NFE,NJE
      EXTERNAL DIFFUN,PEDERV,W,FLD
      REAL ME,NO,NP,MU,MJE,MG,JE,NE,NI,JP,MUCHEP,MGAM
C
C     DISSPLA PLOT OPTION (1-YES  0-NO)
      DPLT = 1.0
C     SET COUNTER FOR NUMBER OF LOOPS BACK TO 20
      L = 0
      YO(2) = SQRT(8.0E11/8.81E-7)*.85
      STEPNE = YO(2)*.01
   20 CONTINUE
C
C
C                SET CONSTANTS FOR GEAR PROGRAM
C
C     NUMBER OF DIFF EQUNS IN SYSTEM
      N = 5
C     LOCAL ERROR TOLERANCE PARAMETER
      EPS = .001
C     STEP SIZE IN GEAR
      HO = .00001
C     GEAR METHOD
      MF = 22
C
C
C                SET PHYSICAL CONSTANTS FOR PROBLEM
C
C     ELECTRONIC CHARGE (COULOMB)
      ECHG = 1.6E-19
C     PERMITIVITY OF GAS (COULOMB/VOLT/CM)
      EPSI = 8.85E-14
C     ELECTRON MASS
      ME = .911E-27
C     BOLTZMANN CONSTANT
      BK = 1.38E-16
C
C
C                SET PARAMETERS FOR DISCHARGE
C
C     DISTANCE BETWEEN ELECTRODES (CM)
      D = .33
      TO = 0.0
C     INDEX FOR FIRST CALL TO GEAR
      INDEX = 1
C     GAS PRESSURE (DYNE/CM2)
      PRES = 240.*(1.013E6/760.)
C     GAS TEMPERATURE (K)
      TG = 293.
C     ELECTRON TEMPERATURE (K)
      TE = 11605.
C     NUMBER DENSITY OF GAS
      NO = PRES/BK/TG
```

```
C       MOLECULAR WEIGHT OF GAS (GM)
        MG = 40.*1.67E-27
C       POSITIVE ION MOBILITY (CM2/SEC/V)
        MU = 4.9E19/NO
C       RECOMBINATION COEFFICIENT (CM3/SEC)
        GAMMA = 8.81E-7
C       IONIZATION SOURCE (ION PAIRS/CM3/SEC)
        S = 8.E11
C       NET CURRENT IN DISCHARGE (AMPS/CM2/SEC)
        C = .022E-6
        CC = C
C       ELECTRON NUMBER DENSITY AT START (1/CM3)
        MUCHEP = MU*ECHG/EPSI
        MGAM = MUCHEP-GAMMA
C       INITIAL DISTANCE STEP SIZE
        TSTEP = .01*D
        NP =(MGAM*YO(2)+((MGAM*YO(2))**2+4.*MUCHEP*S)**.5)/(2.*MUCHEP)
        WRITE (3,1002) YO(2),MUCHEP,MGAM,NP
C       ION CURRENT DENSITY AT START (1/CM2/SEC)
        EFLD = YO(4) = -1.E-6
        YO(3) = 0.0
        YO(1) = C/ECHG
C       POTENTIAL (VOLTS) AT START SET ARBITRARILY TO ZERO
        YO(5) = 0.0
C       FIRST OUTPUT POINT DESIRED
        TOUT = TO + 5.E-4
        WRITE (3,1000)
        WRITE (3,1001)
        WRITE (3,1009)
 1009 FORMAT (13X"M"12X"ALPHA"11X"NUE"13X"W"14X"DL"10X"DL/NUE"/)
        WRITE (3,1005)
        WRITE (3,1002) TO,YO(1),YO(3),C,YO(2),NP,YO(4),YO(5)
C       STORE PARAMETER VALUES AT BOUNDARY
  355 YO10 = YO(1)
        YO20 = YO(2)
        YO30 = YO(3)
        YO40 = YO(4)
        YO50 = YO(5)
        YO60 = NP
C       M IS THE NUMBER OF THE INTEGRATION POINT
        M = 0
C       SET INITIAL VALUES OF NE AND J+
        YO3 = +1.0
        YO2 = +1.0
C       SET COMPARISON VALUE FOR VOLTAGE
        VMIN = 1000.
C
        K = 1
   30 CONTINUE
C
C       SGN USED LATER TO FIND POSITION AT WHICH NE GOES TO ZERO
        SGN = 1.0
C
 1000 FORMAT(1H1,3X"DISTANCE"10X"JE"13X"J+"7X"CURRENT DENSITY"6X,
     C"NE"13X"N+"11X"E FIELD"8X"VOLTAGE"4X"ORDER")
 1001 FORMAT(6X"CM"10X"1/CM2/SEC"6X"1/CM2/SEC"6X"AMPS/CM2"9X,
     C"1/CM3"10X"1/CM3"8X"VOLTS/CM"9X"VOLTS"///)
```

```
      NI(M) = NP
      JP(M) = YO(3)
      E(M) = YO(4)
      V(M) = YO(5)
      VMIN = AMIN1(VMIN,V(M))
      IF (YO(2).LT.0.0) GO TO 390
      IF (TSTEP.LT.1.E-6*D) GO TO 390
      IF ((2.*YO(2)-YO2).LT.0.0) TSTEP = TSTEP/10.
      YO1 = YO(1)
      YO2 = YO(2)
      YO3 = YO(3)
      YO4 = YO(4)
      YO5 = YO(5)
      TOUT = TOUT + TSTEP
      GO TO 40
  390 CONTINUE
      MA = M
      DASHTH = TOUT
      GO TO 500
  400 CONTINUE
      DKSHTH = TOUT
C     MK IS THE INDEX NUMBER OF THE CATHODE
      MK = M
      WRITE (3,1006)
 1006 FORMAT (1X"CATHODE")
      K = 4
C     RECALL PARAMETERS AT PLASMA/SHEATH BOUNDARY
      YO(2) = Y020
      YO(3) = -Y030
      YO(4) = -EFLD
      YO(5) = Y050
      NP = Y060
      C = CC
      YO(1) = YO(3) + C/ECHG
      HO = .00001
      EPS = .001
      TSTEP = .01*D
      TO = 0.0
C     FIRST OUTPUT POINT DESIRED
      TOUT = TO + 5.E-4
      INDEX = 1
      WRITE (3,1000)
      WRITE (3,1001)
      WRITE (3,1009)
      WRITE (3,1011)
      WRITE (3,1002) TO,YO(1),YO(3),C,YO(2),NP,YO(4),YO(5)
      GO TO 30
 1012 FORMAT (1X,7(1PE15.7))
 1011 FORMAT (1X"ANODE SHEATH BOUNDARY")
  500 WRITE (3,1007)
 1007 FORMAT (1X"ANODE")
      DD = DASHTH + DKSHTH
      WRITE (3,1002) D,DASHTH,DKSHTH,DD
      L = L + 1
      IF (L.EQ.1) GO TO 600
      IF (L.GT.10) GO TO 300
      IF ((DELD*(DD-D).LT.0.0).OR.(NEGFLG.EQ.1)) GO TO 700
```

```
 1005 FORMAT (1X"CATHODE SHEATH BOUNDARY")
C
   40 CONTINUE
C
C                  BEGIN LOOP TO SOLVE DE SYSTEM AT VARIOUS POINTS
C                  BETWEEN ANODE AND CATHODE
C
C
      M = M + 1
      CALL DRIVE(N,TO,HO,YO,TOUT,EPS,MF,INDEX)
      C = ABS(YO(1) - YO(3))*ECHG
      IF (YO(4).EQ.0.0) GO TO 50
      NP = YO(3)/MU/YO(4)
      DRIFT = W(YO(4)/NO)
      MUE = DRIFT/YO(4)
      DIFF = DL(YO(4)/NO)
      DMU = DIFF/MUE
      GO TO 60
   50 DRIFT = 0.0
      MUE = 0.0
      DIFF = 0.0
      DMU = 1.0
   60 CONTINUE
      WRITE(3,1008) M,ALPHA,MUE,DRIFT,DIFF,DMU
 1008 FORMAT (12X,I3,9X,7(1PE9.1,6X))
      WRITE(3,1002) TOUT,YO(1),YO(3),C,YO(2),NP,YO(4),YO(5),NQUSED
 1002 FORMAT(8(1PE12.4,3X),I4)
      IF (INDEX.EQ.0) GO TO 100
      WRITE (3,1003) INDEX
 1003 FORMAT(//26H ERROR RETURN WITH INDEX =,I3//)
      GO TO 200
  100 IF(K.EQ.1) GO TO 350
      IF (K.EQ.4) GO TO 385
  350 CONTINUE
      T(M) = TOUT
      JE(M) = YO(1)
      NE(M) = YO(2)
      NI(M) = NP
      JP(M) = YO(3)
      E(M) = YO(4)
      V(M) = YO(5)
C     FIND MINIMUM IN POTENTIAL
      VMIN = AMIN1(VMIN,V(M))
      IF (YO(2).LT.0.0) GO TO 400
      IF (TSTEP.LT.1.E-6*D) GO TO 400
      IF ((2.*YO(2)-YO2).LT.0.3) TSTEP = TSTEP/10.
      YO1 = YO(1)
      YO2 = YO(2)
      YO3 = YO(3)
      YO4 = YO(4)
      YO5 = YO(5)
      TOUT = TOUT + TSTEP
      GO TO 40
  385 CONTINUE
      T(M) = TOUT
      JE(M) = YO(1)
      NE(M) = YO(2)
```

```
  600 DELD = DD - D
      Y0(2) = Y020 - STEPNE
      GO TO 20
  700 STEPNE = ABS(STEPNE/2.)
      NEGFLG = 1
      IF (DELD*(DD-D).LT.0.0) SGN = -SGN
      DELD = DD - D
      Y0(2) = Y020 - STEPNE*SGN
      IF (ABS(DD-D).LE.1.E-3*D) GO TO 900
      IF (ABS(STEPNE).LT.ABS(.005*Y0(2))) GO TO 900
      GO TO 20
  900 CONTINUE
      IF (DPLT.EQ.1.0) CALL PLOT(MK)
 1004 FORMAT(//21H PROBLEM COMPLETED IN,I5,6H STEPS/
     C          21X,I5,14H F EVALUATIONS/
     C          21X,I5,14H J EVALUATIONS///)
  200 WRITE (3,1004) NSTEP,NFE,NJE
  300 CONTINUE
      CALL EXIT
      END
```

```
      SUBROUTINE DIFFUN(N,T,Y,YDOT)
      DIMENSION Y(N),YDOT(N)
      EXTERNAL W,DL
      COMMON/CONST/S,NO,EPSI,ALPHA,GAMMA,ECHG,MU,MUE,K,EFLD,NP
      REAL MU,NO,MUE
C     CHECK ON MAGNITUDE OF EXPONENT TO PREVENT UNDERFLOW OF RESULT
      IF (1.48E-15*NO/ABS(Y(4)).GT.250.*K) GO TO 10
      ALPHA = NO*2.9E-17*EXP(-1.48E-15*NO/ABS(Y(4)))
      GO TO 20
   10 ALPHA = 0.0
   20 CONTINUE
C
C     SIGN CONVENTION IS THAT THE DRIFT VELOCITY, W, IS POSITIVE
C     WHEN THE ELECTRIC FIELD, E, IS NEGATIVE
      SGN =-1.0
      IF (Y(4).LT.0.0) SGN =1.0
      YDOT(1) = S * (ALPHA*ABS(W(Y(4)/NO))-GAMMA*Y(3)/Y(4)/MU)*Y(2)
      YDOT(2) = (Y(2)*W(Y(4)/NO)/SGN - Y(1))/DL(Y(4)/NO)
      YDOT(3) = S * (ALPHA*ABS(W(Y(4)/NO))-GAMMA*Y(3)/Y(4)/MU)*Y(2)
      YDOT(4) = (ECHG/EPSI)*(Y(3)/Y(4)/MU - Y(2))
      YDOT(5) = -Y(4)
      IF((T.EQ.0.0).AND.(ABS(Y(2)-Y(3)/Y(4)/MU).GT.1.E-6*Y(2)))GO TO 90
C
C     THIS IF CHECK PREVENTS ROUNDOFF ERROR FROM MAKING DJE/DX AND
C     DJ+/DX POSITIVE WHEN STARTING INTEGRATION
      IF ((T.EQ.0.0).AND.(K.EQ.1)) GO TO 30
      GO TO 40
   30 YDOT(1) = +1.E4
      YDOT(2) = +1.E2
      YDOT(3) = YDOT(1)
      YDOT(4) = +1.
      YDOT(5) = 0.0
   40 CONTINUE
      IF ((T.EQ.0.0).AND.(K.EQ.2)) GO TO 50
      GO TO 60
   50 YDOT(1) = -1.E-4*SQRT(S/GAMMA)*W(EFLD/NO)/EFLD
      YDOT(2) = 0.0
      YDOT(3) = YDOT(1)
      YDOT(4) = 1.E-4
      YDOT(5) = -EFLD
   60 CONTINUE
      IF ((T.EQ.0.0).AND.(K.EQ.4)) GO TO 70
      GO TO 90
   70 CONTINUE
      YDOT(1) = +1.E4
      YDOT(2) = -1.E2
      YDOT(3) = YDOT(1)
      YDOT(4) = +1.
      YDOT(5) = 0.0
   90 CONTINUE
C
C     DIFF EQNS ARE NEGATED TO ALLOW FOR INTEGRATION FROM
C     SHEATH BACK TO CATHODE
      YDOT(1) = YDOT(1)*(-1.)**K
      YDOT(2) = YDOT(2)*(-1.)**K
      YDOT(3) = YDOT(3)*(-1.)**K
      YDOT(4) = YDOT(4)*(-1.)**K
```

```
      YDOT(5) = YDOT(5)*(-1.)**K
      RETURN
      END
```

```
      FUNCTION FLD(WE)
      DIMENSION WI(33),XI(33)
      COMMON/CONST/S,NO,EPSI,ALPHA,GAMMA,ECHG,MU,MUE,K,EFLD,NP
      REAL NO,MU,MUE,NP
      DATA WI/3169.2,4894.3,7657.9,13002.,22293.,30209.,53691.,53691.,
     C72756.,90267.,104566.,113097.,118391.,133171.,148334.,173524.,
     C195821.,222439.,250207.,291743.,343518.,390211.,450547.,544565.,
     C698072.,1029840.,1350700.,1731450.,2323430.,3037390.,3970640.,
     C5614230.,6524840./
      DATA XI/5.3765E-21,9.1264E-21,1.409E-20,2.1543E-20,3.0262E-20,
     C3.3814E-20,4.2638E-20,4.2638E-20,4.8117E-20,6.0674E-20,8.4372E-20
     C1.2126E-19,1.7595E-19,2.6122E-19,4.3053E-19,8.6616E-19,1.4605E-18
     C2.4791E-18,4.4056E-18,8.2471E-18,1.6482E-17,2.9868E-17,4.8428E-17
     C6.1674E-17,7.7518E-17,1.139E-16,1.5592E-16,2.0249E-16,2.8907E-16,
     C3.9555E-16,5.5182E-16,8.4372E-16,9.9357E-16/
      IF (WE.EQ.0.0) GO TO 10
      SGN =1.0
      IF (WE.GT.0.0) SGN = -1.0
      WE = ABS(WE)
      CALL INTRP(WI,XI,33,2,WE,XOUT)
      FLD = ABS(XOUT*NO)*SGN
      GO TO 20
   10 FLD = 0.0
   20 CONTINUE
      RETURN
      END
```

```
      FUNCTION DL(XIN)
C     THIS FUNCTION CALCULATES THE LONGITUDINAL DIFFUSION COEFFICIENT
C     FOR PARTICULAR VALUES OF E/N  (GRID VALUES FOR DLMU ARE
C     FROM LOWKE AND PARKER)
      DIMENSION DLMU(38),XI(38)
      COMMON/CONST/S,NO,EPSI,ALPHA,GAMMA,ECHG,MU,MUE,K,EFLD,NP
      EXTERNAL W,INTRP
      REAL NO,MU,MUE,NP
C     DATA FROM LOWKE AND PARKER,PHYS REV,181,P 307 AND LOWKE AND DAVIE
C     ,J APPL PHYS,48(12),DEC 77, P4995
      DATA DLMU/.0069242,.0069242,.007865,.008751,.015234,.03107,
     C.061224,.12401,.207139,.246053,.19269,.111456,.08299,.080085,
     C.084912,.111456,.171403,.267249,.36183,.48485,.57389,.647463,
     C.725177,.867117,.901086,
     C1.20595,1.58018,1.95908,2.31774,2.75962,3.1288,3.4653,3.5777,
     C3.6314,3.70162,3.93726,4.24172,4.6186/
      DATA XI/3.26437E-21,6.04227E-21,1.11096E-20,1.42495E-20,
     C1.87932E-20,2.20343E-20,2.53922E-20,2.91608E-20,3.24638E-20,
     C3.71535E-20,4.46272E-20,5.90609E-20,7.84332E-20,9.58738E-20,
     C1.61065E-19,3.20627E-19,8.5055E-19,2.19432E-18,4.11908E-18,
     C7.91954E-18,1.02353E-17,1.5021E-17,1.65348E-17,2.2636E-17,
     C2.93833E-17,
     C3.2961E-17,3.8566E-17,4.2521E-17,4.6979E-17,5.4853E-17,6.5418E-17
     C8.8044E-17,1.1529E-16,4.0926E-16,6.0214E-16,9.5433E-16,1.5816E-15
     C2.8471E-15/
      IF (XIN.EQ.0.0) GO TO 10
      XIN = ABS(XIN)
      CALL INTRP(XI,DLMU,38,2,XIN,YOUT)
      DL = ABS(YOUT*W(XIN)/(XIN*NO))
      GO TO 20
   10 DL = 0.0
   20 CONTINUE
      RETURN
      END
```

```
      FUNCTION W(XIN)
C     THIS FUNCTION CALCULATES ELECTRON DRIFT VELOCITY (CM/SEC) FOR
C     PARTICULAR VALUES OF E/N  (GRID VALUES FOR DRIFT VELOCITY ARE
C     FROM ENGELHART AND PHELPS)
      DIMENSION WI(33),XI(33)
      COMMON/CONST/S,NO,EPSI,ALPHA,GAMMA,ECHG,MU,MUE,K,EFLD,NP
      REAL NO,MU,MUE,NP
C     DATA FROM ENGELHARDT AND PHELPS,PHYS REV,(133),JAN 64,PA377
      DATA WI/3169.2,4894.3,7657.9,13002.,22293.,30209.,53691.,53691.,
     C72756.,90267.,104566.,113097.,118391.,133171.,148334.,173524.,
     C195821.,222439.,250207.,291743.,343518.,390211.,450547.,544565.,
     C698072.,1029840.,1350700.,1731450.,2323430.,3037390.,3970640.,
     C5614230.,6524840./
      DATA XI/5.3765E-21,9.1264E-21,1.409E-20,2.1543E-20,3.0262E-20,
     C3.3814E-20,4.2638E-20,4.2638E-20,4.8117E-20,6.0674E-20,8.4372E-20
     C1.2126E-19,1.7595E-19,2.6122E-19,4.3053E-19,8.6616E-19,1.4605E-18
     C2.4791E-18,4.4056E-18,8.2471E-18,1.6482E-17,2.9868E-17,4.8428E-17
     C6.1674E-17,7.7518E-17,1.139E-16,1.5592E-16,2.0249E-16,2.8907E-16,
     C3.9555E-16,5.5182E-16,8.4372E-16,9.9357E-16/
      IF (XIN.EQ.0.0) GO TO 10
      XIN = ABS(XIN)
      CALL INTRP(XI,WI,33,2,XIN,YOUT)
      W = YOUT
      GO TO 20
   10 W = 0.0
   20 CONTINUE
      RETURN
      END
```

```
      SUBROUTINE PEDERV(N,T,Y,PD,NOO)
      DIMENSION PD(NOO,NOO),Y(N)
      EXTERNAL DL,W
      COMMON/CONST/S,NO,EPSI,ALPHA,GAMMA,ECHG,MU,MUE,K,EFLD,NP
      REAL NO,MU,MUE,NP
C
C     SIGN CONVENTION IS THAT THE DRIFT VELOCITY, W, IS POSITIVE
C     WHEN THE ELECTRIC FIELD, E, IS NEGATIVE
      SGN =-1.0
      IF (Y(4).LT.0.0) SGN =1.0
      IF (Y(4).EQ.0.0) Y(4) = -1.E-10
C
      MUE = W(Y(4)/NO)/Y(4)
C     CHECK ON MAGNITUDE OF EXPONENT TO PREVENT UNDERFLOW OF RESULT
      IF (1.48E-15*NO/ABS(Y(4)).GT.250.*K) GO TO 10
      ALPHA = NO*2.9E-17*EXP(-1.48E-15*NO/ABS(Y(4)))
      GO TO 20
   10 ALPHA = 0.0
   20 CONTINUE
      PD(1,1) = 0.
      PD(1,2) = ALPHA*ABS(W(Y(4)/NO)) - GAMMA*Y(3)/Y(4)/MU
      PD(1,3) = -GAMMA*Y(2)/Y(4)/MU
      PD(1,4) = GAMMA*Y(2)*Y(3)/MU/Y(4)**2 + Y(2)*ALPHA*MUE
      PD(1,5) = 0.0
      PD(2,1) = -1./DL(Y(4)/NO)
      PD(2,2) = SGN*W(Y(4)/NO)/DL(Y(4)/NO)
      PD(2,3) = 0.0
      PD(2,4) = Y(2)*MUE/DL(Y(4)/NO)
      PD(2,5) = 0.0
      PD(3,1) = 0.0
      PD(3,2) = ALPHA*ABS(W(Y(4)/NO)) - GAMMA*Y(3)/Y(4)/MU
      PD(3,3) = - GAMMA*Y(2)/Y(4)/MU
      PD(3,4) = GAMMA*Y(2)*Y(3)/MU/Y(4)**2 + Y(2)*ALPHA*MUE
      PD(3,5) = 0.0
      PD(4,1) = 0.0
      PD(4,2) = -ECHG/EPSI
      PD(4,3) = ECHG/EPSI/Y(4)/MU
      PD(4,4) = PD(4,2)*Y(3)/MU/Y(4)**2
      PD(4,5) = 0.0
      PD(5,1) = 0.0
      PD(5,2) = 0.0
      PD(5,3) = 0.0
      PD(5,4) = -1.
      PD(5,5) = 0.0
C     PARTIAL DERIVATIVES ARE NEGATED TO ALLOW FOR INTEGRATION
C     FROM SHEATH BOUNDARY BACK TO CATHODE
      PD(1,2) = PD(1,2)*(-1.)**K
      PD(1,3) = PD(1,3)*(-1.)**K
      PD(1,4) = PD(1,4)*(-1.)**K
      PD(2,1) = PD(2,1)*(-1.)**K
      PD(2,2) = PD(2,2)*(-1.)**K
      PD(2,2) = PD(2,2)*(-1.)**K
      PD(3,2) = PD(3,2)*(-1.)**K
      PD(3,3) = PD(3,3)*(-1.)**K
      PD(3,4) = PD(3,4)*(-1.)**K
      PD(4,2) = PD(4,2)*(-1.)**K
      PD(4,3) = PD(4,3)*(-1.)**K
```

```
      PD(4,4) = PD(4,4)*(-1.)**K
      PD(5,4) = PD(5,4)*(-1.)**K
      RETURN
      END
```

```
      SUBROUTINE PED(N,T,Y,PW,NC,CON,IER)
      RETURN
      END
```

```
      SUBROUTINE TRIMAT(A,N,ND,PW,SAVE1)
      RETURN
      END
```

```
      SUBROUTINE PLOT(MK)
      DIMENSION T(200),JE(200),NE(200),NI(200),JP(200),E(200),V(200),
     CPT(200),PJE(200),PNE(200),PJP(200),PE(200),PNI(200),PV(200),
     CIPAK(150),X(2),Y(2)
      COMMON/CONST/S,NO,EPSI,ALPHA,GAMMA,ECHG,MU,MUE,K,EFLD,NP
      COMMON/PLT/T,JE,NE,NI,JP,E,V,VMIN,DKSHTH,DASHTH,MA,MAS,D
      REAL JE,JP,NE,NI,NP
      M = MA
      CALL COMPRS
      CALL BGNPL(MK)
      CALL BASALF(6HL/CSTD)
      CALL MIXALF(8HSTANDARD)
      CALL TITLE(" $"
     C,-100,
     C"(D)ISTANCE - CM$",100,"(N)E,(N)+ - 1/CM3$",100,8.0,6.0)
      CALL CROSS
      CALL GRAF(0.0,.1,.33,-8.E8,2.E8,8.E8)
      X(1) = .3
      X(2) = .33
      Y(1) = 0.0
      Y(2) = 0.0
      CALL CURVE(X,Y,2,0)
      CALL MESSAG("(C)ATHODE$",100,-.5,-.5)
      CALL MESSAG("(A)NODE$",100,7.7,-.5)
      CALL BLNK1(2.4,5.65,0.05,1.20)
      CALL LINES("(N)E E- NUMBER DENSITY$",IPAK,1)
      CALL LINES("(N)+ ION NUMBER DENSITY$",IPAK,2)
      CALL LINES("(J)E ELECTRON FLUX$",IPAK,3)
      CALL LINES("(J)+ ION FLUX$",IPAK,4)
      CALL LINES ("(V) VOLTAGE$",IPAK,5)
      CALL LINES ("(E) ELECTRIC FIELD$",IPAK,6)
      DO 350 MM = 1,MK
C     REVERSE POSITIONS OF BOUNDARY AND CATHODE, SHIFT ZERO IN
C     POTENTIAL FROM BOUNDARY TO CATHODE, AND CHANGE E FIELD
C     DIMENSION FROM V/CM TO KV/CM
      MMM = MK+1 - MM
      PT(MM) = DKSHTH - T(MMM)
      PJE(MM) = JE(MMM)
      PNE(MM) = NE(MMM)
      PNI(MM) = NI(MMM)
      PJP(MM) = JP(MMM)
      PE(MM) = E(MMM)
      PV(MM) = V(MMM) - VMIN
  350 CONTINUE
      MK1 = MK + 1
      DO 450 MM = MK1,MA
      PT(MM) = T(MM) + D - DASHTH
      PJE(MM) = JE(MM)
      PNE(MM) = NE(MM)
      PNI(MM) = NI(MM)
      PJP(MM) = JP(MM)
      PE(MM) = E(MM)
C     POTENTIAL AT ANODE SHEATH BOUNDARY IS SHIFTED BY CATHODE
C     FALL (VMIN) AND BY THE VOLTAGE DROP ACROSS THE POSITIVE
C     COLUMN (WHICH IS LINEAR IN X)
      PV(MM) = V(MM) - VMIN
  450 CONTINUE
```

```
      WRITE(3,10) MK
      WRITE(3,10) MAS
      WRITE(3,10) MA
   10 FORMAT(1X,I5,7(1PE13.5,2X))
      DO 20 MM = 1,MA
      WRITE(3,10)MM,PT(MM),PJE(MM),PNE(MM),PNI(MM),PJP(MM),PE(MM),PV(M
   20 CONTINUE
      CALL SPLINE
      CALL CURVE(PT,PNE,M,10)
      CALL CURVE(PT,PNI,M,10)
      CALL YGRAXS(-8.0E11,2.E11,+8.0E11,6.0,"(J)E,(J)+ - 1/CM2/SEC$",
     C-100,8.0,0.0)
      CALL DASH
      CALL SPLINE
      CALL CURVE(PT,PJE,M,10)
      CALL CURVE(PT,PJP,M,10)
      CALL YGRAXS(-8.0,2.,8.0,6.0,"(V)OLTAGE - (V)$",-100,8.7,0.0)
      CALL CHNDOT
      CALL SPLINE
      CALL CURVE(PT,PV,M,10)
      CALL YGRAXS(-160.,40.,160.,6.,"(E)·(F)IELD - (V)/CM$",100,-.7,0.)
      CALL CHNDSH
      CALL SPLINE
      CALL CURVE(PT,PE,M,10)
      CALL RESET("BLNK1")
      CALL LEGEND(IPAK,6,2.5,0.20)
      CALL ENDPL(MK)
      CALL DONEPL
      RETURN
      END
```

```
      PROGRAM CASEIII(INPUT,OUTPUT,TAPE3 = OUTPUT)
      DIMENSION YO(5),T(450),JE(450),NE(450),NI(450),JP(450),
     2E(450),V(450)
      COMMON/CONST/S,NO,EPSI,ALPHA,GAMMA,ECHG,MU,MUE,K,EFLD
      COMMON/PLT/T,JE,NE,NI,JP,E,V,VMIN,DKSHTH,DASHTH,MA,MAS,D
      COMMON/GEAR9/ HUSED,NQUSED,NSTEP,NFE,NJE
      EXTERNAL DIFFUN,PEDERV,M,FLD
      REAL ME,NO,NP,MU,MUE,MG,JE,NE,NI,JP
C
C     DISSPLA PLOT OPTION (1-YES  0-NO)
      DPLT = 1.0
C
C
C                 SET CONSTANTS FOR GEAR PROGRAM
C
C     NUMBER OF DIFF EQUNS IN SYSTEM
      N = 5
C     LOCAL ERROR TOLERANCE PARAMETER
      EPS = .001
C     STEP SIZE IN GEAR
      H0 = .00001
C     GEAR METHOD
      MF = 22
C
      EKICKB = 0.0
      EKICK = 0.0
      EKICKU = 50.
C
C                 SET PHYSICAL CONSTANTS FOR PROBLEM
C
C     ELECTRONIC CHARGE (COULOMB)
      ECHG = 1.6E-19
C     PERMITIVITY OF GAS (COULOMB/VOLT/CM)
      EPSI = 8.85E-14
C     ELECTRON MASS
      ME = .911E-27
C     BOLTZMANN CONSTANT
      BK = 1.38E-16
C
C
C                 SET PARAMETERS FOR DISCHARGE
C
C     SET INITIAL VALUE FOR JE + GAM2*JP
      GJPJE1 = 1.0
C     SECONDARY EMISSION COEFFICIENT (#ELECTRONS PER INCIDENT ION)
      GAM2 = .02
C     DISTANCE BETWEEN ELECTRODES (CM)
      D = .3
      T0 = 0.0
C     INITIAL DISTANCE STEP SIZE
      TSTEP = 1.E-3
C     INDEX FOR FIRST CALL TO GEAR
      INDEX = 1
C     GAS PRESSURE (DYNE/CM2)
      PRES = 240.*(1.013E6/760.)
C     GAS TEMPERATURE (K)
      TG = 273.
```

```
C     ELECTRON TEMPERATURE (K)
      TE = 11605.
C     NUMBER DENSITY OF GAS
      NO = PRES/BK/TG
C     MOLECULAR WEIGHT OF GAS (GM)
      MG = 40.*1.67E-27
C     POSITIVE ION MOBILITY (CM2/SEC/V)
      MU = 4.9E19/NO
C     RECOMBINATION COEFFICIENT (CM3/SEC)
      GAMMA = 8.81E-7
C     IONIZATION SOURCE (ION PAIRS/CM3/SEC)
      S = 3.6E16
C     NET CURRENT IN DISCHARGE (AMPS/CM2/SEC)
      C = 48.E-3
      CC = C
C     ELECTRON NUMBER DENSITY AT START (1/CM3)
      YO(2) = SQRT(S/GAMMA)
C     POSITIVE ION NUMBER DENSITY AT START (1/CM3)
      NP = YO(2)
C     ESTIMATE OF ELECTRON CURRENT DENSITY
      YO(1) = C/ECHG
      DO 12 JJ = 1,20
      CE = CC/ECHG + MU*NP*FLD(YO(1)/YO(2))
      IF (ABS(YO(1) - CE).LT.1.E-20*YO(1)) GO TO 15
        YO(1) = CE
      WRITE (3,999) YO(1),YO(2),EFLD,GAMMA
  999 FORMAT (10X,5(1PE20.12))
   12 CONTINUE
   15 CONTINUE
      YO(1) = CE
C     FROM JE AND NE, DETERMINE WE
      WRITE (3,1002) YO(1),YO(2)
      WE = YO(1)/YO(2)
C     THUS, ESTIMATE E FIELD
      EFLD = FLD(WE)
      MUE = WE/EFLD
C     ION CURRENT DENSITY AT START (1/CM2/SEC)
      YO(3) = MU*EFLD*NP
C     PERTURB E FIELD TO BEGIN INTEGRATION TOWARD CATHODE
      YO(4) = EFLD + .01*EFLD
C     POTENTIAL (VOLTS) AT START SET ARBITRARILY TO ZERO
      YO(5) = 0.0
      WRITE (3,999) YO(1),YO(2),YO(3),YO(4),YO(5)
      WRITE (3,999) NP,MUE,MU,WE,EFLD
C     FIRST OUTPUT POINT DESIRED
      TOUT = TO + 1.E-4
      WRITE (3,1000)
      WRITE (3,1001)
      WRITE (3,1009)
 1009 FORMAT (13X"M"12X"ALPHA"11X"MUE"13X"N"14X"DL"10X"DL/MUE"/)
      WRITE (3,1005)
      WRITE (3,1002) TO,YO(1),YO(3),C,YO(2),NP,YO(4),YO(5)
C     STORE PARAMETER VALUES AT BOUNDARY
  355 YO10 = YO(1)
      YO20 = YO(2)
      YO30 = YO(3)
      YO40 = YO(4)
```

```
      YO50 = YO(5)
C     M IS THE NUMBER OF THE INTEGRATION POINT
      M = 1
      T(M) = TO
      JE(M) = YO(1)
      NE(M) = YO(2)
      NI(M) = YO(3)/MU/EFLD
      JP(M) = YO(3)
      E(M) = EFLD
      V(M) = YO(5)
C     SET INITIAL VALUES OF NE AND J+
      YO3 = +1.0
      YO2 = +1.0
C     SET COMPARISON VALUE FOR VOLTAGE
      VMIN = 1000.
C
C     NOW, WITH K EQ 1, INTEGRATE TO CATHODE - THEN, WITH K EQ 2,
C     INTEGRATE TO ANODE SHEATH BOUNDARY - LATER, WITH K EQ 4,
C     INTEGRATE FROM ANODE SHEATH BOUNDARY TO ANODE
C     (K EQ ODD NUMBER NEGATES DIFFERENTIAL EQUATIONS AND PARTIAL
C     DERIVATIVES TO ALLOW INTEGRATION BACK TO CATHODE)
      K = 1
   30 CONTINUE
C
C     SGN USED LATER TO FIND POSITION AT WHICH NE GOES TO ZERO
      SGN = 1.0
C
 1000 FORMAT(1H1,3X"DISTANCE"10X"JE"13X"J+"7X"CURRENT DENSITY"6X,
     C"NE"13X"N+"11X"E FIELD"8X"VOLTAGE"4X"ORDER")
 1001 FORMAT(6X"CM"10X"1/CM2/SEC"6X"1/CM2/SEC"6X"AMPS/CM2"9X,
     C"1/CM3"10X"1/CM3"8X"VOLTS/CM"9X"VOLTS"///)
 1005 FORMAT (1X"CATHODE SHEATH BOUNDARY")
C
   40 CONTINUE
C
C               BEGIN LOOP TO SOLVE DE SYSTEM AT VARIOUS POINTS
C               BETWEEN ANODE AND CATHODE
C
C
      M = M + 1
      CALL DRIVE(N,TO,HO,YO,TOUT,EPS,MF,INDEX)
      C = ABS(YO(1) - YO(3))*ECHG
      NP = YO(3)/MU/YO(4)
      DRIFT = W(YO(4)/NO)
      MUE = DRIFT/YO(4)
      DIFF = DL(YO(4)/NO)
      DMU = DIFF/MUE
      WRITE(3,1008) M,ALPHA,MUE,DRIFT,DIFF,DMU
 1008 FORMAT (12X,I3,9X,7(1PE9.1,6X))
      WRITE(3,1002) TOUT,YO(1),YO(3),C,YO(2),NP,YO(4),YO(5),NOUSED
 1002 FORMAT(8(1PE12.4,3X),I4)
      IF (INDEX.EQ.0) GO TO 100
      WRITE (3,1003) INDEX
 1003 FORMAT(//26H ERROR RETURN WITH INDEX =,I3//)
      IF ((K.EQ.1).OR.(K.EQ.2)) GO TO 200
   98 EKICKU = EKICK
   99 CONTINUE
```

```
      EKICK = (EKICKU + EKICKB)/2.0
      M = PCM
      GO TO 410
  100 IF(K.EQ.1) GO TO 350
      IF(K.EQ.2) GO TO 375
      IF (K.EQ.4) GO TO 385
  350 CONTINUE
      T(M) = TOUT
      JE(M) = YO(1)
      NE(M) = YO(2)
      NI(M) = NP
      JP(M) = YO(3)
      E(M) = YO(4)
      V(M) = YO(5)
C     FIND MINIMUM IN POTENTIAL
      VMIN = AMIN1(VMIN,V(M))
      GJPJE = GAM2*YO(3) + YO(1)
      IF (GJPJE.LT.0.0) GO TO 400
      IF (TSTEP.LT.1.E-6*D) GO TO 400
      IF((2.*GJPJE-GJPJE1).LT.0.0) TSTEP = TSTEP/10.
      GJPJE1 = GJPJE
      GO TO 374
      IF (YO(2).LT.0.0) GO TO 400
      IF (TSTEP.LT.1.E-6*D) GO TO 400
      IF ((2.*YO(2)-YO2).LT.0.0) TSTEP = TSTEP/5.
  374 CONTINUE
      YO1 = YO(1)
      YO2 = YO(2)
      YO3 = YO(3)
      YO4 = YO(4)
      YO5 = YO(5)
      TOUT = TOUT + TSTEP
      GO TO 40
  375 CONTINUE
C     FILL PRINT ARRAYS AS STEP TOWARD ANODE
      PCM = M
      T(M) = TOUT
      JE(M) = YO(1)
      NE(M) = YO(2)
      NI(M) = NP
      JP(M) = YO(3)
      E(M) = YO(4)
      V(M) = YO(5)
C     INTEGRATE ONLY PART WAY THROUGH POSITIVE COLUMN, THEN
C     SKIP TO ANODE SHEATH BOUNDARY
      IF (TOUT.GE.(.8*D-DKSHTN)) GO TO 410
      TOUT = TOUT + TSTEP
      GO TO 40
  385 CONTINUE
      T(M) = TOUT
      JE(M) = YO(1)
      NE(M) = YO(2)
      NI(M) = NP
      JP(M) = YO(3)
      E(M) = YO(4)
      V(M) = YO(5)
      VMIN = AMIN1(VMIN,V(M))
```

```
      IF (YO(2).LT.0.0) GO TO 390
      IF (T(M).LT.5.*TSTEP) GO TO 389
      IF (YO(2).GT.YO2) GO TO 388
      IF (YO(3)/MU/YO(4).GT.YO3/MU/YO4) GO TO 98
      IF (YO(2).GT.1.E30) GO TO 388
      GO TO 389
  388 EKICK8 = EKICK
      GO TO 99
  389 CONTINUE
      IF (YO(2).LT.0.0) GO TO 390
      IF ((2.*YO(2)-YO2).LT.0.0) TSTEP = TSTEP/10.
      IF (TSTEP.LT.1.E-8*D) GO TO 390
      YO1 = YO(1)
      YO2 = YO(2)
      YO3 = YO(3)
      YO4 = YO(4)
      YO5 = YO(5)
      TOUT = TOUT + TSTEP
      GO TO 40
  390 CONTINUE
      MA = M
      DASHTH = TOUT
      GO TO 500
  400 CONTINUE
      DKSHTH = TOUT
C     MK IS THE INDEX NUMBER OF THE CATHODE
      MK = M
      WRITE (3,1006)
 1006 FORMAT (1X"CATHODE")
C     SET K = 2 FOR INTEGRATION TOWARD ANODE SHEATH BOUNDARY
      K = 2
C     RECALL PARAMETERS AT PLASMA/SHEATH BOUNDARY
      YO(1) = YO10
      YO(2) = YO20
      YO(3) = YO30
      YO(4) = EFLD + 1.E-8
      YO(5) = YO50
      NP = YO(3)/MU/EFLD
      C = CC
      HO = .00001
      EPS = .001
      TSTEP = .05*D
      TO = 0.0
C     FIRST OUTPUT POINT DESIRED
      TOUT = 0.0 + 1.E-4
      INDEX = 1
      WRITE (3,1000)
      WRITE (3,1001)
      WRITE (3,1009)
      WRITE (3,1005)
      WRITE (3,1002) TO,YO(1),YO(3),C,YO(2),NP,YO(4),YO(5)
      GO TO 30
  410 CONTINUE
      M = M + 1
C     INDEX NUMBER OF ANODE SHEATH
      MAS = M
      K = 4
```

```
      C = CC
      NE(M) = YO(2) = SQRT(S/GAMMA)
      NI(M) = NP = YO(2)
      E(M) = YO(4) = EFLD + EKICK
      JP(M) = YO(3) = MU*YO(4)*NP
      JE(M) = YO(1) = C/ECHG + YO(3)
      V(M) = YO(5) = 0.0
      WE = W(YO(4)/NO)
      B = YO(2)*WE
      WRITE (3,1012) YO(1),YO(2),YO(3),YO(4),YO(5),WE,B
 1012 FORMAT (1X,7(1PE15.7))
C     T(M) ASSIGNED A VALUE OF ZERO AT MAS SINCE ACTUAL POSITION OF
C     START OF ANODE SHEATH WILL BE CALCULATED ONCE DA'S.TH IS KNOWN
      T(M) = TO = 0.0
      TOUT = 0.0 + 1.E-4
      TSTEP = 1.E-3
      HO = .00001
      EPS = .001
      INDEX = 1
      WRITE (3,1000)
      WRITE (3,1001)
      WRITE (3,1011)
 1011 FORMAT (1X"ANODE SHEATH BOUNDARY")
      WRITE (3,1002) TO,YO(1),YO(3),C,YO(2),NP,YO(4),YO(5)
      GO TO 30
  500 WRITE (3,1007)
 1007 FORMAT (1X"ANODE")
      IF (OPLT.EQ.1.0) CALL PLOT(MK)
 1004 FORMAT(//21H PROBLEM COMPLETED IN,I5,6H STEPS/
     C          21X,I5,14H F EVALUATIONS/
     C          21X,I5,14H J EVALUATIONS///)
  200 WRITE (3,1004) NSTEP,NFE,NJE
  300 CONTINUE
      CALL EXIT
      END
```

```
      SUBROUTINE DIFFUN(N,T,Y,YDOT)
      DIMENSION Y(N),YDOT(N)
      EXTERNAL W,OL
      COMMON/CONST/S,NO,EPSI,ALPHA,GAMMA,ECHG,MU,MUE,K,EFLD
      REAL MU,NO,MUE
C     CHECK ON MAGNITUDE OF EXPONENT TO PREVENT UNDERFLOW OF RESULT
      IF (1.48E-15*NO/ABS(Y(4)).GT.400.) GO TO 10
      ALPHA = NO*2.9E-17*EXP(-1.48E-15*NO/ABS(Y(4)))
      GO TO 20
   10 ALPHA = 0.0
   20 CONTINUE
      MUE = W(Y(4)/NO)/Y(4)
C
C     SIGN CONVENTION IS THAT THE DRIFT VELOCITY, W, IS POSITIVE
C     WHEN THE ELECTRIC FIELD, E, IS NEGATIVE
      SGN =-1.0
      IF (Y(4).LT.0.0) SGN =1.0
      YDOT(1) = S + (ALPHA*ABS(W(Y(4)/NO))-GAMMA*Y(3)/Y(4)/MU)*Y(2)
      YDOT(2) = (Y(2)*W(Y(4)/NO)/SGN - Y(1))/OL(Y(4)/NO)
      YDOT(3) = S + (ALPHA*ABS(W(Y(4)/NO))-GAMMA*Y(3)/Y(4)/MU)*Y(2)
      YDOT(4) = (ECHG/EPSI)*(Y(3)/Y(4)/MU - Y(2))
      YDOT(5) = -Y(4)
C
C     THIS IF CHECK PREVENTS ROUNDOFF ERROR FROM MAKING DJE/DX AND
C     DJ+/DX POSITIVE WHEN STARTING INTEGRATION
      IF ((T.EQ.0.0).AND.(K.EQ.1)) GO TO 30
      GO TO 40
   30 YDOT(1) = 0.0
      YDOT(2) = 0.0
      YDOT(3) = 0.0
      YDOT(4) = 5.E2
      YDOT(5) = -EFLD
   40 CONTINUE
      IF (K.EQ.2) GO TO 50
      GO TO 60
C     SPATIAL DERIVATIVES OF JE, NE, J+, AND E SET TO ZERO IN
C     POSITIVE COLUMN TO PREVENT PLOTTING PROBLEMS
   50 YDOT(1) = YDOT(2) = YDOT(3) = YDOT(4) = 0.0
      YDOT(5) = -EFLD
   60 CONTINUE
      IF ((T.EQ.0.0).AND.(K.EQ.4)) GO TO 70
      GO TO 80
   70 CONTINUE
      YDOT(1) = +1.E8
      YDOT(2) = -1.E8
      YDOT(3) = YDOT(1)
      YDOT(4) = +1.E3
      YDOT(5) = -EFLD
   80 CONTINUE
C
C     DIFF EQNS ARE NEGATED TO ALLOW FOR INTEGRATION FROM
C     SHEATH BACK TO CATHODE.
      YDOT(1) = YDOT(1)*(-1.)**K
      YDOT(2) = YDOT(2)*(-1.)**K
      YDOT(3) = YDOT(3)*(-1.)**K
      YDOT(4) = YDOT(4)*(-1.)**K
      YDOT(5) = YDOT(5)*(-1.)**K
```

```
      RETURN
      END


      FUNCTION W(XIN)
C     THIS FUNCTION CALCULATES ELECTRON DRIFT VELOCITY (CM/SEC) FOR
C     PARTICULAR VALUES OF E/N  (GRID VALUES FOR DRIFT VELOCITY ARE
C     FROM ENGELHART AND PHELPS)
      DIMENSION WI(33),XI(33)
      COMMON/CONST/ S,NO,EPSI,ALPHA,GAMMA,ECHG,MU,MUE,K,EFLD
      REAL NO,MU,MUE
C     DATA FROM ENGELHARDT AND PHELPS,PHYS REV,(133),JAN 64,PA377
      DATA WI/3169.2,4894.3,7657.9,13002.,22293.,30209.,53691.,53691.,
     C72756.,90267.,104566.,113097.,118391.,133171.,148334.,173524.,
     C195821.,222439.,250207.,291743.,343518.,390211.,450547.,544565.,
     C698072.,1029840.,1350700.,1731450.,2323430.,3037390.,3970640.,
     C5614230.,6524840./
      DATA XI/5.3765E-21,9.1264E-21,1.409E-20,2.1543E-20,3.0262E-20,
     C3.3814E-20,4.2638E-20,4.2638E-20,4.8117E-20,6.0674E-20,8.4372E-20,
     C1.2126E-19,1.7595E-19,2.6122E-19,4.3053E-19,8.6616E-19,1.4605E-18,
     C2.4791E-18,4.4056E-18,8.2471E-18,1.6482E-17,2.9868E-17,4.8428E-17,
     C6.1674E-17,7.7518E-17,1.139E-15,1.5592E-16,2.0249E-16,2.8907E-16,
     C3.9555E-16,5.5182E-16,8.4372E-16,9.9357E-16/
      XIN = ABS(XIN)
      CALL INTRP(XI,WI,33,2,XIN,YOUT)
      W = YOUT
      RETURN
      END


      FUNCTION FLD(WE)
      DIMENSION WI(33),XI(33)
      COMMON/CONST/ S,NO,EPSI,ALPHA,GAMMA,ECHG,MU,MUE,K,EFLD
      REAL NO,MU,MUE
      DATA WI/3169.2,4894.3,7657.9,13002.,22293.,30209.,53691.,53691.,
     C72756.,90267.,104566.,113097.,118391.,133171.,148334.,173524.,
     C195821.,222439.,250207.,291743.,343518.,390211.,450547.,544565.,
     C698072.,1029840.,1350700.,1731450.,2323430.,3037390.,3970640.,
     C5614230.,6524840./
      DATA XI/5.3765E-21,9.1264E-21,1.409E-20,2.1543E-20,3.0262E-20,
     C3.3814E-20,4.2638E-20,4.2638E-20,4.8117E-20,6.0674E-20,8.4372E-20,
     C1.2126E-19,1.7595E-19,2.6122E-19,4.3053E-19,8.6616E-19,1.4605E-18,
     C2.4791E-18,4.4056E-18,8.2471E-18,1.6482E-17,2.9868E-17,4.8428E-17,
     C6.1674E-17,7.7518E-17,1.139E-15,1.5592E-16,2.0249E-16,2.8907E-16,
     C3.9555E-16,5.5182E-16,8.4372E-16,9.9357E-16/
      SGN =1.0
      IF (WE.GT.0.0) SGN = -1.0
      WE = ABS(WE)
      CALL INTRP(WI,XI,33,2,WE,XOUT)
      FLD = ABS(XOUT*NO)*SGN
      RETURN
      END
```

```
      FUNCTION DL(XIN)
C     THIS FUNCTION CALCULATES THE LONGITUDINAL DIFFUSION COEFFICIENT
C     FOR PARTICULAR VALUES OF E/N  (GRID VALUES FOR DLMU ARE
C     FROM LOWKE AND PARKER)
      DIMENSION DLMU(38),XI(38)
      COMMON/CONST/S,NO,EPSI,ALPHA,GAMMA,ECHG,MU,MUE,K,EFLD
      EXTERNAL W,INTRP
      REAL NO,MU,MUE
C     DATA FROM LOWKE AND PARKER,PHYS REV,181,P 307 AND LOWKE AND DAVIS
C     ,J APPL PHYS,48(12),DEC 77, P4995
      DATA DLMU/.0069242,.0069242,.007865,.008751,.015234,.03107,
     C.061224,.12401,.207139,.246053,.19269,.111456,.08289,.080095,
     C.084912,.111456,.171403,.267249,.35183,.48485,.571389,.647463,
     C.725177,.867117,.901086,
     C1.20595,1.58018,1.95908,2.31774,2.75962,3.1288,3.4653,3.5777,
     C3.6314,3.70162,3.93726,4.24172,4.6136/
      DATA XI/3.26437E-21,6.04227E-21,1.11096E-20,1.42495E-20,
     C1.87932E-20,2.20343E-20,2.53922E-20,2.91608E-20,3.24638E-20,
     C3.71535E-20,4.46272E-20,5.90609E-20,7.84332E-20,9.58738E-20,
     C1.61065E-19,3.20627E-19,8.5055E-19,2.19432E-18,4.11908E-18,
     C7.91954E-18,1.02353E-17,1.5021E-17,1.65348E-17,2.2636E-17,
     C2.93833E-17,
     C3.2961E-17,3.8566E-17,4.2521E-17,4.6979E-17,5.4853E-17,6.5418E-17
     C8.8044E-17,1.1529E-16,4.0926E-16,6.0214E-16,9.5433E-16,1.5816E-15
     C2.8471E-15/
      XIN = ABS(XIN)
      CALL INTRP(XI,DLMU,38,2,XIN,YOUT)
      DL = ABS(YOUT*W(XIN)/(XIN*NO))
      RETURN
      END
```

```
      SUBROUTINE PEDERV(N,T,Y,PD,NOO)
      DIMENSION PD(NOO,NOO),Y(N)
      EXTERNAL DL,W
      COMMON/CONST/S,NO,EPSI,ALPHA,GAMMA,ECHG,MU,MUE,K,EFLD
      REAL MU,NO,MUE
C
C     SIGN CONVENTION IS THAT THE DRIFT VELOCITY, W, IS POSITIVE
C     WHEN THE ELECTRIC FIELD, E, IS NEGATIVE
      SGN =-1.0
      IF (Y(4).LT.0.0) SGN =1.0
C
      MUE = W(Y(4)/NO)/Y(4)
C     CHECK ON MAGNITUDE OF EXPONENT TO PREVENT UNDERFLOW OF RESULT
      IF (1.48E-15*NO/ABS(Y(4)).GT.250.*K) GO TO 10
      ALPHA = NO*2.9E-17*EXP(-1.48E-15*NO/ABS(Y(4)))
      GO TO 20
   10 ALPHA = 0.0
   20 CONTINUE
      PD(1,1) = 0.
      PD(1,2) = ALPHA*ABS(W(Y(4)/NO)) - GAMMA*Y(3)/Y(4)/MU
      PD(1,3) = -GAMMA*Y(2)/Y(4)/MU
      PD(1,4) = GAMMA*Y(2)*Y(3)/MU/Y(4)**2 + Y(2)*ALPHA*MUE
      PD(1,5) = 0.0
      PD(2,1) = -1./DL(Y(4)/NO)
      PD(2,2) = SGN*W(Y(4)/NO)/DL(Y(4)/NO)
      PD(2,3) = 0.0
      PD(2,4) = Y(2)*MUE/DL(Y(4)/NO)
      PD(2,5) = 0.0
      PD(3,1) = 0.0
      PD(3,2) = ALPHA*ABS(W(Y(4)/NO)) - GAMMA*Y(3)/Y(4)/MU
      PD(3,3) = - GAMMA*Y(2)/Y(4)/MU
      PD(3,4) = GAMMA*Y(2)*Y(3)/MU/Y(4)**2 + Y(2)*ALPHA*MUE
      PD(3,5) = 0.0
      PD(4,1) = 0.0
      PD(4,2) = -ECHG/EPSI
      PD(4,3) = ECHG/EPSI/Y(4)/MU
      PD(4,4) = PD(4,2)*Y(3)/MU/Y(4)**2
      PD(4,5) = 0.0
      PD(5,1) = 0.0
      PD(5,2) = 0.0
      PD(5,3) = 0.0
      PD(5,4) = -1.
      PD(5,5) = 0.0
C     PARTIAL DERIVATIVES ARE NEGATED TO ALLOW FOR INTEGRATION
C     FROM SHEATH BOUNDARY BACK TO CATHODE
      PD(1,2) = PD(1,2)*(-1.)**K
      PD(1,3) = PD(1,3)*(-1.)**K
      PD(1,4) = PD(1,4)*(-1.)**K
      PD(2,1) = PD(2,1)*(-1.)**K
      PD(2,2) = PD(2,2)*(-1.)**K
      PD(3,2) = PD(3,2)*(-1.)**K
      PD(3,3) = PD(3,3)*(-1.)**K
      PD(3,4) = PD(3,4)*(-1.)**K
      PD(4,2) = PD(4,2)*(-1.)**K
      PD(4,3) = PD(4,3)*(-1.)**K
      PD(4,4) = PD(4,4)*(-1.)**K
      PD(5,4) = PD(5,4)*(-1.)**K
      RETURN
      END
```

```
      SUBROUTINE PLOT(MK)
      DIMENSION T(450),JE(450),NE(450),NI(450),JP(450),E(450),V(450),
     CPT(450),PJE(450),PNE(450),PJP(450),PE(450),PNI(450),PV(450),
     CIPAK(150)
      COMMON/CONST/S,NO,EPSI,ALPHA,GAMMA,ECHG,MU,MUE,K,EFLD
      COMMON/PLT/T,JE,NE,NI,JP,E,V,VMIN,DKSHTH,DASHTH,MA,MAS,D
      REAL JE,JP,NE,NI
      M = MA
      CALL COMPKS
      EKCK = EKICK
      CALL BGNPL(MK)
      CALL PAGE(11.00,8.5)
      CALL PHYSOR(1.5,1.5)
      CALL BASALF(6HL/CSTD)
      CALL MIXALF(8HSTANDARD)
      CALL TITLE(" ",0,
     C"(D)ISTANCE - CM$",100,"(N)E,(N)+ - 1/CM3$",100,8.0,6.0)
      CALL CROSS
      CALL GRAF(0.0,.1,.3,-15.0E11,5.0E11,+15.0E11)
      CALL MESSAG("(C)ATHODE$",100,-.5,-.5)
      CALL MESSAG("(A)NODE$",100,7.7,-.5)
      CALL BLNK1(2.4,5.65,0.05,1.20)
      CALL LINES("(N)E E- NUMBER DENSITY$",IPAK,1)
      CALL LINES("(N)I ION NUMBER DENSITY$",IPAK,2)
      CALL LINES("(J)E ELECTRON FLUX$",IPAK,3)
      CALL LINES("(J)I ION FLUX$",IPAK,4)
      CALL LINES ("(V) VOLTAGE$",IPAK,5)
      CALL LINES ("(E) ELECTRIC FIELD$",IPAK,6)
      CALL NOCHEK
      A = -1.35
      B = -.75
      Y = 6.75
      Z = 9.35
      CALL STRTPT(A,B)
      CALL CONNPT(A,Y)
      CALL CONNPT(Z,Y)
      CALL CONNPT(Z,B)
      CALL CONNPT(A,B)
      CALL MESSAG("(F)IG 3.  (L)OW (C)URRENT (D)ENSITY (P)LASMAS",
     C100,+1.0,-1.0)
      DO 350 MM = 1,MK
C     REVERSE POSITIONS OF BOUNDARY AND CATHODE, SHIFT ZERO IN
C     POTENTIAL FROM BOUNDARY TO CATHODE, AND CHANGE E FIELD
C     DIMENSION FROM V/CM TO KV/CM
      MMM = MK+1 - MM
      PT(MM) = DKSHTH - T(MMM)
      PJE(MM) = JE(MMM)
      PNE(MM) = NE(MMM)
      PNI(MM) = NI(MMM)
      PJP(MM) = JP(MMM)
      PE(MM) = E(MMM)/1000.
      PV(MM) = (V(MMM) - VMIN)
      PV(MM) = PV(MM)/1000.
  350 CONTINUE
      MK1 = MK + 1
      MAS1 = MAS - 1
      DO 400 MM = MK1 , MAS1
```

```
C       FILL REMAINDER OF PRINT ARRAYS WITHOUT INVERTING ANY POSITIONS,
C       BUT SHIFTING THE POTENTIAL ZERO AND CHANGING V/CM TO KV/CM
        PT(MM) = T(MM) + DKSHTH
        PJE(MM) = JE(MM)
        PNE(MM) = NE(MM)
        PNI(MM) = NI(MM)
        PJP(MM) = JP(MM)
        PE(MM) = E(MM)/1000.
        PV(MM) = (V(MM) - VMIN)
        PV(MM) = PV(MM)/1000.
  400 CONTINUE
        DO 450 MM = MAS , MA
        PT(MM) = T(MM) + D - DASHTH
        PJE(MM) = JE(MM)
        PNE(MM) = NE(MM)
        PNI(MM) = NI(MM)
        PJP(MM) = JP(MM)
        PE(MM) = E(MM)/1000.
C       POTENTIAL AT ANODE SHEATH BOUNDARY IS SHIFTED BY CATHODE
C       FALL (VMIN) AND BY THE VOLTAGE DROP ACROSS THE POSITIVE
C       COLUMN (WHICH IS LINEAR IN X)
        PV(MM) =(V(MM) - VMIN - EFLD*(D - DASHTH - DKSHTH))
        PV(MM) = PV(MM)/1000.
  450 CONTINUE
        WRITE (3,10) MK
        WRITE (3,10) MAS
        WRITE (3,10) MA
        DO 20 MM = 1,MA
        WRITE(3,10)MM,PT(MM),PJE(MM),PNE(MM),PNI(MM),PJP(MM),PE(MM),PV(M
   10 FORMAT (1X,I5,7(1PE13.5,2X))
   20 CONTINUE
        CALL CURVE (PT,PNE,M,0)
        CALL DASH
        CALL CURVE (PT,PNI,M,0)
        CALL YGRAXS(-3.0E17,1.E17,+3.0E17,6.0,"(J)E,(J)+ - 1/CM2/SECS",
     C-100,8.0,0.0)
        CALL DASH
        CALL SPLINE
        CALL CURVE (PT,PJP,M,0)
        CALL RESET("DASH")
        CALL CURVE (PT,PJE,M,0)
        CALL YGRAXS(-3.00,1.00,3.00,6.,"(V)OLTAGE - K(V)S",-100,8.7,0.0)
        CALL CHNDOT
        CALL SPLINE
        CALL CURVE (PT,PV,M,0)
        CALL YGRAXS(-100.,25.,100.,6.,"(E) (F)IELD - K(V)/CMS",100,-.7,0.
        CALL CHNDSH
        CALL SPLINE
        CALL CURVE (PT,PE,M,0)
        CALL ENDPL(MK)
        CALL DONEPL
        RETURN
        END
```

```
      PROGRAM CASEIII(INPUT,OUTPUT,TAPE3 = OUTPUT)
      DIMENSION Y(7),T(600),JE(600),NE(600),NI(600),JP(600),
     GE(600),N(600),NII(600),JI(600)
      COMMON/CONST/S,N0,EPSI,ALPHA,GAMMA,ECHG,MU,MUE,K,EFLD,NOX,NEX,PG
      COMMON/PLOT/T,JE,NE,NI,JP,E,V,VMIN,OKSMTH,EASHTH,MA,MAS,D,NII,JI,
     CEKICK
      COMMON/GEAR3/ HUSED,NQUSED,NSTEP,NFE,NJE
      EXTERNAL DIFFUN,PEDERV,W,FLD
      REAL ME,N0,NP,MU,MUE,MG,JE,NE,NI,JP,JI,NII,MUN,NN,NOX,NEX
C
C     DISSPLA PLOT OPTION (1-YES  0-NO)
      IPLT = 1.0
C
C
C                 SET CONSTANTS FOR GEAR PROGRAM
C
C     NUMBER OF DIFF EQUNS IN SYSTEM
      N = 6
C     LOCAL ERROR TOLERANCE PARAMETER
      EPS = .001
C     STEP SIZE IN GEAR
      H0 = .00001
C     GEAR METHOD
      MF = 22
C
C
C                 SET PHYSICAL CONSTANTS FOR PROBLEM
C
C     ELECTRONIC CHARGE (COULOMB)
      ECHG = 1.6E-19
C     PERMITIVITY OF GAS (COULOMB/VOLT/CM)
      EPSI = 8.85E-14
C     ELECTRON MASS
      ME = .911E-27
C     BOLTZMANN CONSTANT
      BK = 1.38E-16
C
C
C                 SET PARAMETERS FOR DISCHARGE
C
C     SET INITIAL VALUE FOR JE + GAM2*JP
      GJPJE1 = 1.0
C     SECONDARY EMISSION COEFFICIENT (#ELECTRONS PER INCIDENT ION)
      GAM2 = .02
C     DISTANCE BETWEEN ELECTRODES (CM)
      D = .3
      T0 = 1.0
C     INITIAL DISTANCE STEP SIZE
      TSTEP = 1.E-4
      TSTEP = 5.E-6
      TSTEP = 5.E-4
C     INDEX FOR FIRST CALL TO GEAR
      INDEX = 1
C     GAS PRESSURE (DYNE/CM2)
      PRES = 760.*(1.013E6/760.)
      PGAS = 760.
C     GAS TEMPERATURE (K)
```

```
      TG = 273.
C     ELECTRON TEMPERATURE (EV)
      TE = .04
C     NUMBER DENSITY OF GAS
      NO = PRES/BK/TG
C     NUMBER DENSITY OF ATTACHING GAS
      NOX = 1.*(1. 13E6/760.)/BK/TG
      NOX = 1.E-2*NOX
C     MOLECULAR WEIGHT OF GAS (GM)
      MG = 40.*1.67E-27
C     POSITIVE ION MOBILITY (CM2/SEC/V)
      MU = 4.9E3/NO
C     NEGATIVE ION MOBILITY
      MUN = - MU
C     RECOMBINATION COEFFICIENT (CM3/SEC)
      GAMMA = 1.01E-7
C     IONIZATION SOURCE (ION PAIRS/CM3/SEC)
      S = 3.6E16
C     NET CURRENT IN DISCHARGE (AMPS/CM2/SEC)
      C = 2.E-3
      CC = C
C     ELECTRON NUMBER DENSITY AT START (1/CM3)
      WRITE (3,999) PGAS,TG,NOX,NO,S,GAMMA
      E = 1.
      Y0(2) = SQRT(S/GAMMA/(1.+B))
      Y0(1) = C/ECHG
      EF = FLD(Y0(2)/Y0(1))
      RA = DATCH(EF/NO)
      CNJ = 1.E-9*NOX
      RD = 3.E-10
      AN = 5.E-2*NOX
      DO 12 JJ = 1,20
      EF = FLD(Y0(1)/Y0(2))
      GM = GAMA(EF/NO)
      RA = DATCH(EF/NO)
      B = NOX*RA/(RD*DND + Y0(2)*RA)
      Y0(2) = SQRT(S/GM/(1.+B))
      AN = 5.E-2*NOX - B*Y0(2)
      IF (AN.LT.0.0) AN = 0.0
      EF = FLD(Y0(1)/Y0(2))
      Y0(1) = C/ECHG + MU*EF*Y0(2) + 2.*B*Y0(2)*MU*EF
      WRITE (3,999) Y0(1),Y0(2),GM,EF,B,RA,AN
   12 CONTINUE
   15 CONTINUE
  999 FORMAT (1X,7(1PE17.9))
C     POSITIVE ION NUMBER DENSITY AT START (1/CM3)
      NP = Y0(2)*(1.+B)
C     NEGATIVE ION NUMBER DENSITY (1/CM3)
      NN = B*Y0(2)
      NE = Y0(1)/Y0(2)
C     THUS, ESTIMATE E FIELD
      EFLD = FLD(NE)
C     PERTURB E FIELD TO BEGIN INTEGRATION TOWARD CATHODE
      Y0(4) = EFLD + .01*EFLD
      NUE = NE/EFLD
C     POSITIVE ION CURRENT DENSITY IN POSITIVE COLUMN (1/CM2/SEC)
      Y0(3) = MU*EFLD*NP
```

```
C       NEGATIVE ION CURRENT DENSITY IN POSITIVE COLUMN (1/CM2/SEC)
        YJ(5) = NN*MUN*EFLD
C       TOTAL FLUX
        C = (YJ(1) + YJ(6) - YJ(3))*ECHG
C       DETERMINE ELECTRON TEMPERATURE FOR THIS FIELD
        TE = TEMP(EFLD/ND)
C       RATE OF IONIZATION OF METASTABLES
        SIM = 5.E-8*SQRT(TE)*EXP(-4.15/TE)
C       NUMBER DENSITY OF METASTABLES
        NEX = (1.E-8*ND - YJ(3)/MU/YJ(4))*1.E+EXP(-11.65/TE)
C       POTENTIAL (VOLTS) AT START, SET ARBITRARILY TO ZERO
        YJ(5) = 0.
        WRITE (3,999) YJ(1),YJ(2),YJ(3),YJ(4),YJ(6),NN,NP
        WRITE (3,999) MUE,WE,EFLD,TE,REX,RIM,NEX
C       FIRST OUTPUT POINT DESIRED
        TOUT = T0 + 1.E-6
        WRITE (3,1000)
        WRITE (3,1001)
        WRITE (3,1009)
 1009 FORMAT (13X"X"12X"ALPHA"11X"MUE"13X"W"14X"DL"10X"DL/MUE"/)
        WRITE (3,1005)
        WRITE (3,1002) T0,YJ(1),YJ(3),YJ(6),C,YJ(2),NP,NN,YJ(4),YJ(5)
C       STORE PARAMETER VALUES AT BOUNDARY
  355 Y010 = YJ(1)
        Y02J = YJ(2)
        Y03J = YJ(3)
        Y04J = YJ(4)
        YC5C = YJ(5)
        Y06J = YJ(6)
        Y07J = NN
C       P IS THE NUMBER OF THE INTEGRATION POINT
        P = 0
C       SET INITIAL VALUES OF NE AND J+
        Y03 = +1.J
        Y02 = +1.0
C       SET COMPARISON VALUE FOR VOLTAGE
        VMIN = 10J0.
C
C       NOW,  WITH K EQ 1, INTEGRATE TO CATHODE - THEN, WITH K EQ 2,
C       INTEGRATE TO ANODE SHEATH BOUNDARY - LATER, WITH K EQ 4,
C       INTEGRATE  FROM ANODE SHEATH BOUNDARY TO ANODE
C       (K EQ ODD NUMBER NEGATES DIFFERENTIAL EQUATIONS AND PARTIAL
C       DERIVATIVES TO ALLOW INTEGRATION BACK TO CATHODE)
        K = 1
   30 CONTINUE
C
C       SGN USED LATER TO FIND POSITION AT WHICH NE GOES TO ZERO
        SGN = 1.0
C
 1000 FORMAT(1H1,3X"DISTANCE"8X"JE"11X"J+"11X"J-"5X"CURRENT DENSITY"4X,
     C"NE"11X"N+"11X"N-"9X"E FIELD"6X"VOLTAGE")
 1001 FORMAT(6X"CM"8X"1/CM2/SEC"4X"1/CM2/SEC"4X"1/CM2/SEC"4X"AMPS/CM2"
     C"1/CM3"8X"1/CM3"8X"1/CM3"6X"VOLTS/CM"7X"VOLTS"///)
 1005 FORMAT (1X"CATHODE SHEATH BOUNDARY")
C
   40 CONTINUE
C
```

```
C                BEGIN LOOP TO SOLVE DE SYSTEM AT VARIOUS POINTS
C                BETWEEN ANODE AND CATHODE
C
C
      M = M + 1
      CALL DRIVE(N,T,H0,Y0,TOUT,EPS,MF,INDEX)
      C = (Y0(1) + Y0(6) - Y0(3))*ELMG
      NN = -Y0(6)/MU/Y0(4)
      NP = Y0(3)/MU/Y0(4)
      DRIFT = ABS(Y0(4)/N0)
      MUE = DRIFT/Y0(4)
      DIFF = DL(Y0(4)/N0)
      CMU = DIFF/MUE
      TE = TEMP(Y0(4)/N0)
      REX = 6.7E7*SQRT(TE)*7.E-16*(2.*TE+11.65)*EXP(-11.65/TE)
      RDX = 3.31E-11*SQRT(TE)*(11.65+2.*TE)
      RIM = 5.05E-8*SQRT(TE)*EXP(-4.15/TE)
      NEX = (1.E14*N0 - Y0(3)/MU/Y0(4))*1.*EXP(-11.65/TE)
      WRITE (3,1008) M,ALPHA,MUE,DRIFT,DIFF,TE,NEX,RIM
 1008 FORMAT (12X,I2,9X,7(1PE9.1,6X))
      WRITE (3,1002) TOUT,Y0(1),Y0(3),Y0(6),C,Y0(2),NP,NN,Y0(4),Y0(5)
 1002 FORMAT(9(1PE12.4,1X),1PE12.4)
      IF (INDEX.EQ.0) GO TO 100
      WRITE (3,1003) INDEX
 1003 FORMAT(//26H ERROR RETURN WITH INDEX =,I3//)
      GO TO 205
  100 IF(K.EQ.1) GO TO 350
      IF(K.EQ.2) GO TO 375
      IF (K.EQ.4) GO TO 385
  350 CONTINUE
      T(M) = TOUT
      JE(M) = Y0(1)
      NE(M) = Y0(2)
      NI(M) = NP
      JP(M) = Y0(3)
      E(M) = Y0(4)
      V(M) = Y0(5)
      JI(M) = Y0(6)
      NII(M) = NN
C     FIND MINIMUM IN POTENTIAL
      VMIN = AMIN1(VMIN,V(M))
      GJPJE = GAM2*Y0(3) + Y0(1)
      IF (GJPJE.LT.0.0) GO TO 400
      IF (TSTEP.LT.1.E-6*D) GO TO 400
      IF((2.*GJPJE-GJPJE1).LT.0.0) TSTEP = TSTEP/10.
      GJPJE1 = GJPJE
      GO TO 374
      IF (Y0(2).LT.0.0) GO TO 420
      IF (TSTEP.LT.1.E-6*D) GO TO 400
      IF ((2.*Y0(2)-Y02).LT.0.0) TSTEP = TSTEP/5.
  374 CONTINUE
      Y01 = Y0(1)
      Y02 = Y0(2)
      Y03 = Y0(3)
      Y04 = Y0(4)
      Y05 = Y0(5)
      TOUT = TOUT + TSTEP
```

```
      GO TO 4)
  375 CONTINUE
C     FILL PRINT ARRAYS AS STEP TOWARD ANODE
      T(M) = TOUT
      JE(M) = YO(1)
      NE(M) = YO(2)
      NI(M) = NF
      JP(M) = YO(3)
      E(M) = YO(4)
      V(M) = YO(5)
      JI(M) = YO(6)
      NII(M) = NN
C     INTEGRATE ONLY PART WAY THROUGH POSITIVE COLUMN, THEN
C     SKIP TO ANODE SHEATH BOUNDARY
      IF (TOUT.GE.(.3) GO TO 410
      IF (TOUT.GE.(.9*D-DKSHTH)) GO TO 410
      TOUT = TOUT + TSTEP
      GO TO 40
  385 CONTINUE
      T(M) = TOUT
      JE(M) = YO(1)
      NE(M) = YO(2)
      NI(M) = NF
      JP(M) = YO(3)
      E(M) = YO(4)
      V(M) = YO(5)
      VMIN = AMIN1(VMIN,V(M))
      IF (YO(2).LT.0.0) GO TO 390
      IF ((2.*YO(2)-Y02).LT.0.0) TSTEP = TSTEP/10.
      IF (TSTEP.LT.1.E-8*D) GO TO 390
      Y01 = YO(1)
      Y02 = YO(2)
      Y03 = YO(3)
      Y04 = YO(4)
      Y05 = YO(5)
      TOUT = TOUT + TSTEP
      GO TO 40
  390 CONTINUE
      PA = M
      DASHTH = TOUT
      GO TO 50
  400 CONTINUE
      DKSHTH = TOUT
C     MK IS THE INDEX NUMBER OF THE CATHODE
      MK = M
      WRITE (3,1006)
 1006 FORMAT (1X"CATHODE")
C     SET K = 2 FOR INTEGRATION TOWARD ANODE SHEATH BOUNDARY
      K = 2
C     RECALL PARAMETERS AT PLASMA/SHEATH BOUNDARY
      YO(1) = YO10
      YO(2) = YO20
      YO(3) = YO30
C     PERTURB E FIELD SLIGHTLY TO BEGIN INTEGRATION THRU POS COLUMN
      YO(4) = EFLD
      YO(5) = YO50
      YO(6) = YO60
```

```
      NN = Y[illegible]
      NP = Y[illegible](3)/MU/EFLD
      C = CC
      H0 = .0001
      EPS = .01
      TSTEP = 1.E-4
      T0 = 0.0
C     FIRST OUTPUT POINT DESIRED
      TOUT = 0.0 + 1.E-6
      INDEX = 1
      WRITE (3,1000)
      WRITE (3,1001)
      WRITE (3,1009)
      WRITE (3,1005)
      WRITE (3,1002) T0,Y0(1),Y0(3),Y0(6),C,Y0(2),NP,NN,Y0(4),Y0(5)
      GO TO 30
  410 CONTINUE
      M = M + 1
C     INDEX NUMBER OF ANODE SHEATH
      MAS = M
      K = 4
      C = CC
      E(M) = Y0(4) = +.1
      RA = DATCH(Y0(4)/N0)
      GM = GAMA(Y0(4)/N0)
      Y0(2) = Y020
      AN = 5.E-2*NOX
      B = NOX*RA/(PO*DNO + Y0(2)*RA)
      Y0(2) = SQRT(S/GM/(1.+B))
      B = NOX*RA/(RO*DNO + Y0(2)*RA)
      Y0(2) = SQRT(S/GM/(1.+B))
      B = NOX*RA/(RO*DNO + Y0(2)*RA)
      NE(M) = Y0(2) = SQRT(S/GM/(1.+E))
      JE(M) = Y0(1) = C/ECHG + Y0(2)*MU*Y0(4)*(1.+2.*B)
      NI(M) = NP = Y0(2)*(1.+B)
      JP(M) = Y0(3) = MU*Y0(4)*NP
      NII(M) = NN = E*Y0(2)
      JI(M) = Y0(6) = NN*MUN*Y0(4)
      V(M) = Y0(5) = 0.0
      WE = W(Y0(4)/N0)
      C = (Y0(1) + Y0(6) - Y0(3))*ECHG
      WRITE (3,1012) Y0(1),Y0(2),Y0(3),Y0(4),Y0(5),Y0(6),NN
 1012 FORMAT (1X,7(1PE15.7))
C     T(M) ASSIGNED A VALUE OF ZERO AT MAS SINCE ACTUAL POSITION OF
C     START OF ANODE SHEATH WILL BE CALCULATED ONCE DASHTH IS KNOWN
      T(M) = T0 = 0.0
      TOUT = 1.E-6
      TSTEP = 5.E-6
      TSTEP = 1.E-4
      TSTEP = 5.E-4
      H0 = .00001
      EPS = .001
      INDEX = 1
      WRITE (3,1000)
      WRITE (3,1001)
      WRITE (3,1011)
 1011 FORMAT (1X"ANODE SHEATH BOUNDARY")
```

```
      WRITE (3,1002) T*,YJ(1),YJ(3),YJ(6),C,YJ(2),NP,NN,YJ(4),YJ(5)
      GO TO 32
  500 WRITE (3,1007)
 1007 FORMAT (1X"ANGLE")
      IF (IPLT.EQ.1.2) CALL PLOT(PK)
 1004 FORMAT(//21H PROBLEM COMPLETED IN,I5,6H STEPS/
     C          21X,I5,14H F EVALUATIONS/
     C          21X,I5,14H J EVALUATIONS///)
  200 WRITE (3,1004) NSTEP,NFE,NJE
  300 CONTINUE
      CALL EXIT
      END
```

```
      SUBROUTINE DIFFUN(N,T,Y,YDOT)
      DIMENSION Y(N),YDOT(N)
      EXTERNAL W,DL
      COMMON/CONST/S,NO,EPSI,ALPHA,GAMMA,ECHG,MU,MUE,K,EFLD,NOX,NEX,BO
      REAL NO,MU,MUE,NN,NOX,NEX
C     CHECK ON MAGNITUDE OF EXPONENT TO PREVENT UNDERFLOW OF RESULT
      IF (1.48E-15*NO/ABS(Y(4)).GT.4.6) GO TO 10
      ALPHA = NO*2.9E-17*EXP(-1.48E-15*NO/ABS(Y(4)))
      GO TO 20
   10 ALPHA = 0.0
   20 CONTINUE
      MUE = W(Y(4)/NO)/Y(4)
      AN = 5.E-2*NOX - ABS(Y(6)/MU/Y(4))
      IF (AN.LT.0.0) AN = 0.0
      ETA = DATCH(Y(4)/NO)*AN/ABS(W(Y(4)/NO))
      GAMMA = GAMMA(Y(4)/NO)
      DNO = 1.E-3*NOX
      BO = 3.E-10
      NN = -Y(6)/MU/Y(4)
      TE = TEMP(Y(4)/NO)
      RIM = 5.0E-8*SQRT(TE)*EXP(-4.15/TE)
      REX = 6.7E7*SQRT(TE)*7.E-18*(2.*TE+11.65)*EXP(-11.65/TE)
      ROX = 3.91E-11*SQRT(TE)*(11.65+2.*TE)
      NEX = (1.E6*NO - Y(3)/MU/Y(4))*1.*EXP(-11.65/TE)
C
C     SIGN CONVENTION IS THAT THE DRIFT VELOCITY, W, IS POSITIVE
C     WHEN THE ELECTRIC FIELD, E, IS NEGATIVE
      SGN =-1.0
      IF (Y(4).LT.0.0) SGN =1.0
      YDOT(1) = S*Y(2)*((ALPHA-ETA)*ABS(W(Y(4)/NO))-GAMMA*Y(3)/MU/Y(4)
     C+RC*NN*DNO +RIM*Y(2)*NEX
      YDOT(2) = (Y(2)*W(Y(4)/NO)/SGN - Y(1))/DL(Y(4)/NO)
      YDOT(3) = S*Y(2)*((ALPHA)*ABS(W(Y(4)/NO))-GAMMA*Y(3)/MU/Y(4))
     C + RIM*Y(2)*NEX
      YDOT(4) = (ECHG/EPSI)*(Y(3)/MU/Y(4)-Y(2)-NN)
      YDOT(5) = -Y(4)
      YDOT(6) = Y(2)*DATCH(Y(4)/NO)*AN + BO*Y(6)/MU/Y(4)*DNO
C
C     THIS IF CHECK PREVENTS ROUNDOFF ERROR FROM MAKING DJE/DX AND
C     DJ+/DX POSITIVE WHEN STARTING INTEGRATION
      IF ((T.EQ.0.0).AND.(K.EQ.1)) GO TO 30
      GO TO 40
   30 YDOT(1) = 0.0
      YDOT(2) = 0.0
      YDOT(3) = 0.0
      YDOT(4) = 5.E2
      YDOT(5) = -EFLD
      YDOT(6) = 0.0
   40 CONTINUE
      IF (K.EQ.2) GO TO 50
      GO TO 60
C     SPATIAL DERIVATIVES OF JE, NE, J+, AND E SET TO ZERO IN
C     POSITIVE COLUMN TO PREVENT PLOTTING PROBLEMS
   50 YDOT(1) = YDOT(2) = YDOT(3) = YDOT(4) = 0.0
      YDOT(5) = -EFLD
      YDOT(6) = 0.0
   60 CONTINUE
```

```
      IF ((T.EQ.3.E).AND.(K.EQ.4)) GO TO 7&
      GO TO 8J
   7& CONTINUE
      YDOT(1) = +1.E8
      YDOT(2) = -1.E8
      YDOT(3) = YDOT(1)
      YDOT(4) = +1.E3
      YDOT(5) = -EFLC
      YDOT(6) = 3.E
   8J CONTINUE
C
C     DIFF EQNS ARE NEGATED TO ALLOW FOR INTEGRATION FROM
C     SHEATH BACK TO CATHODE
      YDOT(1) = YDOT(1)*(-1.)**K
      YDOT(2) = YDOT(2)*(-1.)**K
      YDOT(3) = YDOT(3)*(-1.)**K
      YDOT(4) = YDOT(4)*(-1.)**K
      YDOT(5) = YDOT(5)*(-1.)**K
      YDOT(6) = YDOT(6)*(-1.)**K
      RETURN
      END


      FUNCTION GAMA(XIN)
      GAMA = 8.81E-7
      RETURN
      END


      FUNCTION DLN(XIN)
       DLN = .13655
      RETURN
      END


      FUNCTION RECOMB(XIN)
      RECOMB = 1.E-9
      RETURN
      END
```

```
      FUNCTION CATCH(YIN)
C     ATTACHMENT RATE IN CM3/SEC
C
      DIMENSION YI(23),AT(23)
      DATA YI/.001,.01,.1,.5,2.,5.,8.778,11.531,13.889,15.664,
     C20.476,27.213,36.233,42.065,48.519,58. 3,66.899,76.222,
     C87.526,9[illegible].962,3[illegible].,600.,1[illegible]0./
      DATA AT/1.E-18,1.E-17,1.E-16,1.E-15,
     C1.E-14,1.E-13,1.[illegible]95E-12,2.1091E-12,3.39E-12,
     C4.9386E-12,9.279E-12,1.5[illegible]52E-11,2.1483E-11,2.4751E-11,
     C2.7752E-11,3.1261E-11,3.4[illegible]1E-11,3.672E-11,3.8[illegible]3E-11,3.9792E-11,
     C5.2E-11,7.E-11,1.E-10/
      YIN = ABS(YIN/1.E-17)
      CALL INTRP(YI,AT,23,2,YIN,ATOUT)
      CATCH = ATOUT
      RETURN
      END


      FUNCTION TEMP(XNIN)
      DIMENSION XN(16),T(16)
      DATA XN/.001,.01,.1,1.,2.,3.,4.,5.,10.,20.,30.,40.,50.,
     C60.,100.,1000./
      DATA T/.026,.06,.31,2.425,3.373,4.113,4.661,4.959,5.327,
     C5.608,5.841,6.046,6.229,6.395,6.5,6.9/
      XNIN = ABS(XNIN/1.E-17)
      CALL INTRP(XN,T,16,2,XNIN,TOUT)
      IF (XNIN.LT..01) TOUT = .04
      TEMP = .04
      TEMP = TOUT
      RETURN
      END
```

```
      FUNCTION W(XIN)
C     THIS FUNCTION CALCULATES ELECTRON DRIFT VELOCITY (CM/SEC) FOR
C     PARTICULAR VALUES OF E/N  (GRID VALUES FOR DRIFT VELOCITY ARE
C     FROM ENGELHART AND PHELPS)
      DIMENSION WI(33),XI(33)
      COMMON/CONST/S,NO,EPSI,ALPHA,GAMMA,ECHG,MU,MUE,K,EFLD,NOX,NEX,PS
      REAL NO,MU,MUE
C     DATA FROM ENGELHARDT AND PHELPS,PHYS REV,(133),JAN 64,PA377
      DATA WI/3169.2,4894.3,7657.9,13062.,22293.,30209.,53691.,53691.,
     C72756.,91267.,104566.,113097.,118391.,133171.,148334.,173524.,
     C195821.,222439.,250287.,291743.,343518.,390211.,450547.,544565.,
     C698072.,1029840.,1359700.,1731450.,2323430.,3037390.,3970640.,
     C5614230.,6524840./
      DATA XI/5.3765E-21,9.1264E-21,1.409E-20,2.1543E-20,3.0262E-20,
     C3.3814E-20,4.2638E-20,4.2638E-20,4.8117E-20,6.0674E-20,5.4372E-2
     C1.2126E-19,1.7595E-19,2.6122E-19,4.3053E-19,8.6616E-19,1.4605E-1
     C2.4791E-18,4.4056E-18,8.2471E-18,1.6482E-17,2.9868E-17,4.8428E-1
     C6.1674E-17,7.7518E-17,1.139E-16,1.5592E-16,2.0249E-16,2.3907E-16,
     C3.9555E-16,5.5182E-16,8.4372E-16,9.9357E-16/
      XIN = ABS(XIN)
      CALL INTRP(XI,WI,33,2,XIN,YOUT)
      W = YOUT
      RETURN
      END
```

```
      FUNCTION FLD(WE)
      DIMENSION WI(33),XI(33)
      COMMON/CONST/S,NO,EPSI,ALPHA,GAMMA,ECHG,MU,MUE,K,EFLD,NOX,NEX,PS
      REAL NO,MU,MUE
      DATA WI/3169.2,4894.3,7657.9,13062.,22293.,30209.,53691.,53691.,
     C72756.,91267.,104566.,113097.,118391.,133171.,148334.,173524.,
     C195821.,222439.,250287.,291743.,343518.,390211.,450547.,544565.,
     C698072.,1029840.,1359700.,1731450.,2323430.,3037390.,3970640.,
     C5614230.,6524840./
      DATA XI/5.3765E-21,9.1264E-21,1.409E-20,2.1543E-20,3.0262E-20,
     C3.3814E-20,4.2638E-20,4.2638E-20,4.8117E-20,6.0674E-20,5.4372E-2
     C1.2126E-19,1.7595E-19,2.6122E-19,4.3053E-19,8.6616E-19,1.4605E-1
     C2.4791E-18,4.4056E-18,8.2471E-18,1.6482E-17,2.9868E-17,4.8428E-17
     C6.1674E-17,7.7518E-17,1.139E-16,1.5592E-16,2.0249E-16,2.3907E-16,
     C3.9555E-16,5.5182E-16,8.4372E-16,9.9357E-16/
      SGN =1.0
      IF (WE.GT.0.0) SGN = -1.0
      WE = ABS(WE)
      CALL INTRP(WI,XI,33,2,WE,XOUT)
      FLD = ABS(XOUT*NO)*SGN
      RETURN
      END
```

```
      FUNCTION DL(XIN)
C     THIS FUNCTION CALCULATES THE LONGITUDINAL DIFFUSION COEFFICIENT
C     FOR PARTICULAR VALUES OF E/N  (GRID VALUES FOR DLMU ARE
C     FROM LOWKE AND PARKER)
      DIMENSION DLMU(38),XI(38)
      COMMON/CONST/S,NO,EPSI,ALPHA,GAMMA,ECHG,MU,MUE,K,EFLD,NOX,NEX,PS
      EXTERNAL W,INTRP
      REAL NO,MU,MUE
C     DATA FROM LOWKE AND PARKER,PHYS REV,181,P 337 AND LOWKE AND DAVI
C     ,J APPL PHYS,48(12),DEC 77, P4935
      DATA DLMU/.369242,.369242,.7865,.8751,.015234,.03177,
     C.061224,.124 1,.207139,.246853,.19269,.111456,.06289,.038065,
     C.064912,.111456,.171433,.267249,.36183,.43485,.571369,.647463,
     C.725177,.867117,.931486,
     C1.20595,1.58 18,1.9559 8,2.31774,2.75962,3.1288,3.4653,3.5777,
     C3.6314,3.7 182,3.93726,4.24172,4.61566/
      DATA XI/3.26437E-21,6.34227E-21,1.11.96E-20,1.42495E-20,
     C1.87932E-20,2.20343E-20,2.53922E-20,2.91608E-20,3.24638E-20,
     C3.71535E-20,4.40272E-20,5.96609E-20,7.84332E-20,9.58738E-20,
     C1.61165E-19,3.21627E-19,8.5055E-19,2.19432E-18,4.11908E-18,
     C7.91954E-18,1.12353E-17,1.5021E-17,1.65348E-17,2.2636E-17,
     C2.83833E-17,
     C3.2961E-17,3.8563E-17,4.2521E-17,4.6979E-17,5.4853E-17,6.5418E-1
     C6.6144E-17,1.1529E-16,4.0926E-16,6.6214E-16,9.5433E-16,1.5816E-1
     C2.6471E-15/
      XIN = ABS(XIN)
      CALL INTRP(XI,DLMU,38,2,XIN,YOUT)
      DL = ABS(YOUT*W(XIN)/(XIN*NO))
      RETURN
      END
```

```
      SUBROUTINE FEDERV(N,T,Y,PD,NDD)
      DIMENSION PD(NDD,NDD),Y(N)
      EXTERNAL DL,W
      COMMON/CONST/S,ND,EPSI,ALPHA,GAMMA,ECHG,MU,MUE,K,EFLD,NOX,NEX,P
      REAL MU,ND,MUE
C
C     SIGN CONVENTION IS THAT THE DRIFT VELOCITY, W, IS POSITIVE
C     WHEN THE ELECTRIC FIELD, E, IS NEGATIVE
      SGN =-1.
      IF (Y(4).LT.0.) SGN =1.
C
      MUE = W(Y(4)/ND)/Y(4)
C     CHECK ON MAGNITUDE OF EXPONENT TO PREVENT UNDERFLOW OF RESULT
      IF (1.46E-15*ND/ABS(Y(4)).GT.250.*K) GO TO 10
      ALPHA = ND*2.9E-17*EXP(-1.43E-15*ND/ABS(Y(4)))
      GO TO 20
   10 ALPHA = 0.0
   20 CONTINUE
      PD(1,1) = 0.
      PD(1,2) = ALPHA*ABS(W(Y(4)/ND)) - GAMMA*Y(3)/Y(4)/MU
      PD(1,3) = -GAMMA*Y(2)/Y(4)/MU
      PD(1,4) = GAMMA*Y(2)*Y(3)/MU/Y(4)**2 + Y(2)*ALPHA*MUE
      PD(1,5) = 0.0
      PD(2,1) = -1./DL(Y(4)/ND)
      PD(2,2) = SGN*W(Y(4)/ND)/DL(Y(4)/ND)
      PD(2,3) = 0.0
      PD(2,4) = Y(2)*MUE/DL(Y(4)/ND)
      PD(2,5) = 0.0
      PD(3,1) = 0.0
      PD(3,2) = ALPHA*ABS(W(Y(4)/ND)) - GAMMA*Y(3)/Y(4)/MU
      PD(3,3) = - GAMMA*Y(2)/Y(4)/MU
      PD(3,4) = GAMMA*Y(2)*Y(3)/MU/Y(4)**2 + Y(2)*ALPHA*MUE
      PD(3,5) = 0.0
      PD(4,1) = 0.0
      PD(4,2) = -ECHG/EPSI
      PD(4,3) = ECHG/EPSI/Y(4)/MU
      PD(4,4) = PD(4,2)*Y(3)/MU/Y(4)**2
      PD(4,5) = 0.0
      PD(5,1) = 0.0
      PD(5,2) = 0.0
      PD(5,3) = 0.0
      PD(5,4) = -1.
      PD(5,5) = 0.0
C     PARTIAL DERIVATIVES ARE NEGATED TO ALLOW FOR INTEGRATION
C     FROM SHEATH BOUNDARY BACK TO CATHODE
      PD(1,2) = PD(1,2)*(-1.)**K
      PD(1,3) = PD(1,3)*(-1.)**K
      PD(1,4) = PD(1,4)*(-1.)**K
      PD(2,1) = PD(2,1)*(-1.)**K
      PD(2,2) = PD(2,2)*(-1.)**K
      PD(3,2) = PD(3,2)*(-1.)**K
      PD(3,3) = PD(3,3)*(-1.)**K
      PD(3,4) = PD(3,4)*(-1.)**K
      PD(4,2) = PD(4,2)*(-1.)**K
      PD(4,3) = PD(4,3)*(-1.)**K
      PD(4,4) = PD(4,4)*(-1.)**K
      PD(5,4) = PD(5,4)*(-1.)**K
      RETURN
      END
```

```
      SUBROUTINE PLOT(MK)
      DIMENSION T(600),JE(600),NE(600),NI(600),JP(600),E(600),V(600),
     CFT(600),PJE(600),PNE(600),PJP(600),PE(600),PNI(600),PV(600),
     CIPAK(15),JI(600),PJI(600),NII(600),PNII(600)
      COMMON/CONST/S,N1,EPSI,ALPHA,GAMMA,ECHG,MU,MUE,K,EFLD,NOX,NEX,P,
      COMMON/PLT/T,JE,NE,NI,JP,E,V,VMIN,DKSHTH,CASHTH,MA,MAS,D,NII,JI,
     CEKICK
      REAL JE,JP,JI,NE,NI,NII
      M = MA
      EKCK = EFLD -.1
      CALL COMPRS
      CALL PGNPL(MK)
      CALL PAGE(11.00,8.5)
      CALL PHYSOP(1.5,1.5)
      CALL BASALF(EHL/OSTD)
      CALL MIXALF(&HSTANDARD)
      CALL TITLE(" ",0,
     C"(D)ISTANCE - CM$",100,"(N)E,(N)-,(N)+ - 1/CM3$",100,8.0,6.0)
      CALL CROSS
      CALL GRAF(0.0,.1,.3,-6.0E11,2.0E11,+6.0E11)
      CALL MESSAG("(C)ATHODE$",100,-.5,-.5)
      CALL MESSAG("(A)NODE$",100,7.7,-.5)
      CALL BLNK1(2.4,5.65,0.5,1.75)
      CALL LINES("(N)E NUMBER DENSITY (X)1E8$",IPAK,1)
      CALL LINES("(N)+ NUMBER DENSITY$",IPAK,2)
      CALL LINES("(N)- NUMBER DENSITY (X)1E8$",IPAK,3)
      CALL LINES("(J)E ELECTRON FLUX$",IPAK,4)
      CALL LINES("(J)+ POS ION FLUX$",IPAK,5)
      CALL LINES ("(J)- NEG ION FLUX (X)1E8$",IPAK,6)
      CALL LINES ("(V) VOLTAGE$",IPAK,7)
      CALL LINES ("(E) ELECTRIC FIELD$",IPAK,8)
      CALL NOCHEK
      A = -1.35
      B = -.75
      Y = 6.75
      Z = 9.75
      CALL STRTPT(A,B)
      CALL CONNPT(A,Y)
      CALL CONNPT(Z,Y)
      CALL CONNPT(Z,B)
      CALL CONNPT(A,B)
      CALL MESSAG("(F)IG 3.  (L)OW (C)URRENT (D)ENSITY (P)LASMA$",
     C100,+1.0,-1.0)
      DO 35 MM = 1,MK
C     REVERSE POSITIONS OF BOUNDARY AND CATHODE, SHIFT ZERO IN
C     POTENTIAL FROM BOUNDARY TO CATHODE, AND CHANGE E FIELD
C     DIMENSION FROM V/CM TO KV/CM
      MMM = MK+1 - MM
      FT(MM) = DKSHTH - T(MMM)
      PJE(MM) = JE(MMM)
      PNE(MM) = NE(MMM)
      PNI(MM) = NI(MMM)
      PJP(MM) = JP(MMM)
      PE(MM) = E(MMM)/1000.
      PJI(MM) = JI(MMM)*1000.
      PNII(MM) = NII(MMM)*100.
      PV(MM) = (V(MMM) - VMIN)
```

```
      WRITE(3,10) MM,PT(MM),PJE(MM),PNE(MM),PNI(MM),PJP(MM),PE(MM),PV(M
  45  CONTINUE
      MK1 = MK + 1
      MAS1 = MAS - 1
      DO 460 MM = MK1 , MAS1
C     FILL REMAINDER OF PRINT ARRAYS WITHOUT INVERTING ANY POSITIONS,
C     BUT SHIFTING THE POTENTIAL ZERO AND CHANGING V/CM TO KV/CM
      PT(MM) = T(MM) + DKSHTH
      PJE(MM) = JE(MM)
      PNE(MM) = NE(MM)
      PNI(MM) = NI(MM)
      PJP(MM) = JP(MM)
      PE(MM) = E(MM)/1000.
      PJI(MM) = JI(MM)*1000.
      PNII(MM) = NII(MM)*100.
      PV(MM) = (V(MM) - VMIN)
      WRITE(3,10) MM,PT(MM),PJE(MM),PNE(MM),PNI(MM),PJP(MM),PE(MM),PV(M
  460 CONTINUE
      DO 450 MM = MAS , MA
      WRITE(3,10) MM,PT(MM),PJE(MM),PNE(MM),PNI(MM),PJP(MM),PE(MM),PV(M
      PT(MM) = T(MM) + D - DASHTH
      PJE(MM) = JE(MM)
      PNE(MM) = NE(MM)
      PNI(MM) = NI(MM)
      PJP(MM) = JP(MM)
      PE(MM) = E(MM)/1000.
      PJI(MM) = JI(MM)*1.0E0.
      PNII(MM) = NII(MM)*100.
C     POTENTIAL AT ANODE SHEATH BOUNDARY IS SHIFTED BY CATHODE
C     FALL (VMIN) AND BY THE VOLTAGE DROP ACROSS THE POSITIVE
C     COLUMN (WHICH IS LINEAR IN X)
      PV(MM) =(V(MM) - VMIN - EFLD*(G - DASHTH - DKSHTH))
     C + (EKCK)*(D-DASHTH - DKSHTH)/2.
  450 CONTINUE
      WRITE (3,11) MK
      WRITE (3,11) MAS
      WRITE (3,11) MA
      DO 20 MM = 1,MA
      WRITE(3,10) MM,PT(MM),PJE(MM),PNE(MM),PNI(MM),PJP(MM),PE(MM),PV(MM
   10 FORMAT (1X,I5,7(1PE13.5,2X))
   20 CONTINUE
      CALL CURVE(PT,PNII,M,10)
      CALL CURVE (PT,PNE,M,1)
      CALL DASH
      CALL CURVE (PT,PNI,M,1)
      CALL YGRAXS(-2.1E15,.5E15,+2.0E15,6.0,"(J)E,(J)+ - 1/CM2/SEC$",
     C-100,8.0,0.0)
      CALL DASH
      CALL SPLINE
      CALL CURVE(PT,PJI,M,10)
      CALL CURVE (PT,PJP,M,0)
      CALL RESET("DASH")
      CALL CURVE (PT,PJE,M,0)
      CALL YGRAXS(-3.3,10.0,30.0,6.,"(V)OLTAGE - (V)$",-100,8.7,0.0)
      CALL CHNDOT
      CALL SPLINE
      CALL CURVE (PT,PV,M,1)
```

```
      CALL YGRIXS(-4.0,2.,4.0,6.,"(E)  (F)IELD - K(V)/CM$",100.,-.7,0.)
      CALL GUNOSH
      CALL SPLINE
      CALL CURVE (ET,PE,M,1)
      CALL ENDPL(MK)
      CALL DONEPL
      RETURN
      END
```

VITA

Marc R. Hallada was born on 9 February 1953 in Crystal Falls, Michigan. After graduating from high school in Crystal Falls in 1971, he entered the United States Air Force Academy. Upon graduation from the Academy in 1975, he received a bachelor of science degree in physics and mathematics and a regular commission in the United States Air Force. He was assigned to the Applied Physics Division of the Nuclear Technology Office at the Air Force Weapons Laboratory from October 1975 to April 1980. He entered the School of Engineering of the Air Force Institute of Technology in June of 1980.

Permanent address: 120 Iron Street
Crystal Falls, Michigan 49920

Unclassified
SECURITY CLASSIFICATION OF THIS PAGE (When Data Entered)

REPORT DOCUMENTATION PAGE	READ INSTRUCTIONS BEFORE COMPLETING FORM
1. REPORT NUMBER: AFIT/GEP/PH/81D-4	2. GOVT ACCESSION NO.: AD A115 513
3. RECIPIENT'S CATALOG NUMBER	
4. TITLE (and Subtitle): CATHODE SHEATH EFFECTS IN EXTERNALLY-IONIZED GAS DISCHARGES	5. TYPE OF REPORT & PERIOD COVERED: MS Thesis
	6. PERFORMING ORG. REPORT NUMBER
7. AUTHOR(s): Marc R. Hallada, Captain, USAF	8. CONTRACT OR GRANT NUMBER(s)
9. PERFORMING ORGANIZATION NAME AND ADDRESS: Air Force Institute of Technology (AFIT-EN), Wright-Patterson AFB, Ohio 45433	10. PROGRAM ELEMENT, PROJECT, TASK AREA & WORK UNIT NUMBERS: 2301S288
11. CONTROLLING OFFICE NAME AND ADDRESS: Aerospace Power Division/POOC-3, Air Force Aero Propulsion Laboratory, Wright-Patterson AFB, Ohio 45433	12. REPORT DATE: December 1981
	13. NUMBER OF PAGES: 153
14. MONITORING AGENCY NAME & ADDRESS(if different from Controlling Office)	15. SECURITY CLASS. (of this report): Unclassified
	15a. DECLASSIFICATION/DOWNGRADING SCHEDULE

16. DISTRIBUTION STATEMENT (of this Report)
Approved for public release; distribution unlimited.

15 APR 1982

17. DISTRIBUTION STATEMENT (of the abstract entered in Block 20, if different from Report)

Dean for Research and Professional Development
Air Force Institute of Technology (ATC)
Wright-Patterson AFB, OH 45433

18. SUPPLEMENTARY NOTES
Approved for public release; IAW AFR 190-17

JERRAL F. GUESS, Captain, USAF
Director of Information

19. KEY WORDS (Continue on reverse side if necessary and identify by block number)
Plasma Switch
Gas Discharge
Externally-Sustained

20. ABSTRACT (Continue on reverse side if necessary and identify by block number)
Lowke's theoretical investigation of gas discharges sustained by an external ionization source was extended. In addition to the processes of electron diffusion, electron-ion recombination, and ionization of the ground state considered by Lowke, electron-impact ionization of metastable states and secondary and secondary emission from the cathode were included in the present analysis. Current-voltage (I-V) characteristics were obtained for discharges in argon and methane. At current densities of $1A/cm^2$, Townsend ionization in the cathode sheath resulted in positive-ion number densities which significantly

DD FORM 1 JAN 73 1473 EDITION OF 1 NOV 65 IS OBSOLETE

Unclassified
SECURITY CLASSIFICATION OF THIS PAGE (When Data Entered)

exceeded those in the positive column. I-V characteristics obtained revealed a sharp rise in the current at an "ignition" voltage. The slope of the high-current region of the characteristic increased for an increase in secondary emission. With the addition of metastable ionization, the ignition voltage and the entire I-V characteristic shifted to lower discharge voltages. Below the ignition voltage and at low external ionization source strengths, an unstable region of negative differential conductivity was observed.

[1]J. J. Lowke, D. K. Davies, J. Apply. Phys., 48(12), 499 (1977).